DETERMINATION OF GEOTECHNICAL PROPERTIES OF CLAYEY SOIL FROM

RESISTIVITY IMAGING (RI)

by

GOLAM KIBRIA

Presented to the Faculty of the Graduate School of

The University of Texas at Arlington in Partial Fulfillment

of the Requirements

for the Degree of

MASTER OF SCIENCE IN CIVIL ENGINEERING

THE UNIVERSITY OF TEXAS AT ARLINGTON

August 2011

ACKNOWLEDGEMENTS

ABSTRACT

DETERMINATION OF GEOTECHNICAL PROPERTIES OF CLAYEY SOILS FROM

RESISTIVITY IMAGING (RI)

Golam Kibria

The University of Texas at Arlington, 2011

Supervising Professor: Sahadat Hossain

The use of resistivity imaging (RI) in the subsurface investigation has increased in recent years. RI is a non destructive method and provides a continuous image of the subsurface. Based on the electrical conduction phenomenon of soil, spatial and temporal moisture variation and heterogeneity of subsurface can be evaluated from RI. However, only qualitative evaluation of subsurface can be obtained from RI. The correlation between RI results and geotechnical engineering properties of soils has become an important issue for rigorous use of this method in site investigation.

The current study attempts to develop the relationship and correlations between geotechnical parameters with electrical resistivity of soil. These correlations can be used for determining geotechnical properties from RI. Soil samples collected for the current study mostly consisted of medium to high plasticity clay with plasticity index more than 30. High energy X-Ray fluorescence (XRF) and scanning electron microscope (SEM) image analysis showed that the dominant clay mineral in the soil samples might be montmorillonite.

The effects of moisture content, unit weight, degree of saturation, specific surface area, pore space, ion composition, compaction condition and fine fraction on soil resistivity were determined. Test results showed that soil resistivity decreased with the average rate of 13.8 Ohm-m for the increase of moisture from 10% to 20% at fixed unit weight. However, soil resistivity ranged from 2.1 to 2.42 ohm-m at 50% moisture content. Enhanced interaction between the clay particles and water and occurrence of ionic conduction reduced electrical resistivity with the increase of moisture content. Test results also indicated that soil resistivity decreased almost linearly with an average rate of 0.3 Ohm-m/pcf between moist unit weight 88.5 to 100 pcf at 18% moisture content. The average rate of reduction was 0.08 Ohm-m/pcf for further increase in moist unit weight in same moisture content. Reduction of interclod pores and better particle-to-particle contact might cause reduction in soil resistivity with the increase of unit weight. However, soil resistivity was more sensitive to moisture content than unit weight. In addition, average resistivity of the samples decreased from 6.7 to 3.2 Ohm-m with the increase of degree of saturation from 40% to 90% due to elimination of interclod macro pores, reorientation of clay particle and remolding of clay.

Soil resistivity increased from 4.3 to 14.2 Ohm-m with the increase of specific surface area from 69.6 to 107.1 m^2/gm at 18% moisture content and 75 pcf dry unit weight. Lack of formation of water film around the soil particle might restrict the current flow. Moreover, soil resistivity increased from 4.4 to 14.2 Ohm-m for the increase of pore space from 1.91% to 10.56% at 18% moisture content and 75 pcf dry unit weight and then decreased. Test results showed that soil resistivity increased from 4.3 to 14.2 Ohm-m with the increase of calcium ion from 8.3% to 13.9% at 18% moisture content and 75 pcf dry unit weight.

Observed soil resistivity was high when samples were compacted at dry of optimum because of less pronounce bridging between soil particles. However, soil resistivity decreased when samples were compacted at wet of optimum. Near saturated voids and better interparticle bridging might caused the reduction in resistivity. Correlation of resistivity with unconfined shear strength of soil showed that soil samples prepared with moisture content below optimum, resistivi-

ty was high and strength was low. However, both resistivity and strength was low at moisture condition above optimum condition. In addition, soil resistivity were in between 3.16 to 3.6 Ohm-m for the increase of fine fraction from 66% to 94.8%. Therefore, the observed variation in soil resistivity with the fine content was not significant. Based on the study, it can be summarized that geotechnical engineering properties can be determined from RI under certain site specific conditions and moisture is the most influencing factor in electrical conduction.

TABLE OF CONTENTS

APPENDIX

LIST OF ILLUSTRATIONS

xi

LIST OF TABLES

CHAPTER 1

INTRODUCTION

1.1 Background

The use of geophysical methods in site investigation is gaining notable recognition from the global engineering and construction community. During site investigation, several parameters are investigated by geologist and geotechnical engineers. However, they can only obtain information at certain key locations and interpolate soil conditions area wide. Geophysical methods have the possibility to give an "image" of the subsurface, as shown in Figure 1.1. Also, with the development of new software for the interpretation of resistivity measurements, 2D and 3D resistivity imaging (RI) is extensively used today in shallow geophysical investigation.
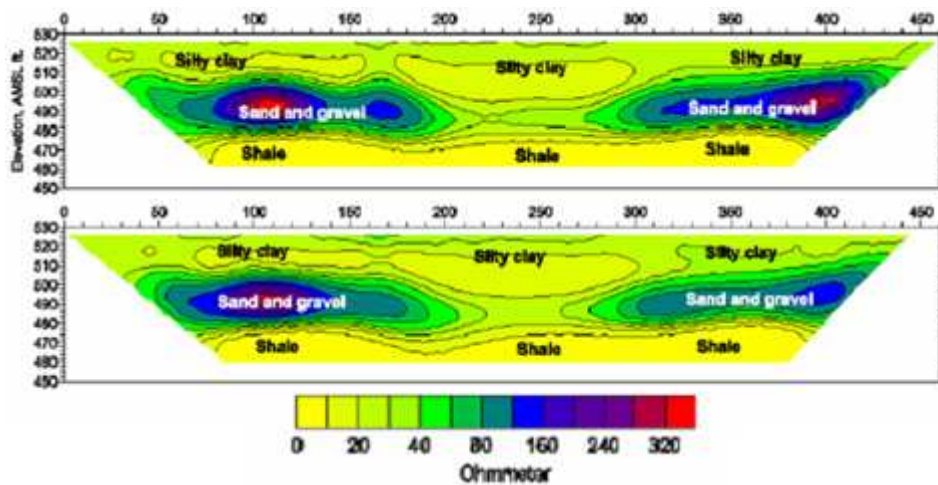
Figure 1.1: Mapping of Stratigraphy, Sand and Gravel Lenses in Clay and Shale Environment

Geologists have been using RI to study the properties of rock and subsurface materials successfully. It was documented that Gray and Wheeler used electrical resistivity in 1720 in the field of geology (Jakosky, 1950; Van Nostrand and Cook, 1966). The objective of their study was to determine the conductivity of rocks. In 1746, Watson ascertained that subsurface has the abili

1

ty to conduct electricity (Van Nostrand and Cook, 1966). Robert W. Fox conducted a study on the sulfide ore to determine the existence of conductivity. He indicated the existence of natural current within his sample by using copper electrode (Van Nostrand and Cook, 1966). The application of DC current to quantify resistivity was performed by Conard Schlumberger in 1912. It was reported as one of the most successful experimental approach of electrical resistivity survey (Aizebeokhai, 2010). In United States, the idea was developed by Frank Wenner in 1915 (Aizebeokhai, 2010). After that, the method has undergone by significant improvement in last three decades. To comprehend the heterogeneity and to provide accurate image of subsurface, different electrode combinations and inversion models are being utilized. With the advancement of modern techniques, it is now possible to obtain image of subsurface within a very short time.

RI is a non destructive method of site investigation. The method is less expensive and subsurface investigation of a large area can be conducted in a short time period. However, soil test borings are traditionally used for subsurface exploration. In addition, Standard Penetration Test (SPT), Cone Penetration Test (CPT), Vane Shear Test, Dilatometer Test and Pressuremeter Test are also widely used in geotechnical investigation. All of these methods provide information of a point at different subsoil depths. Besides, RI provides continuous information in vertical and horizontal direction of subsurface. Advantages of RI over conventional methods can be summarized below

- Provide continuous image of subsurface.
- Has the ability to cover a large area within a short time period.
- Less expensive.
- Has the ability to determine heterogeneity and high moisture zone.
- Data can be processed in a very short time.

Because of these benefits, the use of RI has increased significantly. It is one the most convenient available technique for preliminary subsurface investigation and geo-hazard studies. Therefore, RI can be considered as complimentary to soil boring for site investigation and geo-hazard study.

2

1.2 Problem Statement

The use of RI by geotechnical engineers have been increasing all over the world. It is a convenient method to evaluate spatial and temporal variation of moisture and heterogeneity of subsoil. The working principle of this method is based on the conduction phenomenon of soil. However, RI provides qualitative information of subsurface. Limited studies have been conducted to obtain geotechnical parameters using RI. Quantification of geotechnical properties has become an important issue for rigorous use of RI in engineering applications.

The correlation of different geotechnical properties with RI will close the gap that currently exists between geophysical engineering and geotechnical engineering. The geotechnical engineers will be able to interpret the geophysical data and utilize the information for their design. Therefore, the development of geotechnical parameters from RI will make this method more effective for subsurface investigation.

The presence of moisture changes consistency and strength of soil. Moisture is also important for conduction phenomenon of soil. Conductivity and resistivity also depend on the mineralogy of soil, particle size distribution, Index properties, unit weight, porosity, degree of saturation and other parameters. Proper understanding of the causes of variation of these parameters with resistivity can be helpful for development of correlations.

1.3 Objective of the Current Study

The study was conducted to determine the relationship of geotechnical properties of clay soil with the electrical resistivity. Soil samples were collected from Midlothian, Texas. It is important to determine the variation of resistivity with the change different parameters to obtain correlations. The specific objectives of the study is presented here:

- To determine the type of soil according Unified Soil Classification System (USCS).
- To determine the variation of soil resistivity with moisture content at different condition.
- To identify the relation between soil resistivity with pore space using scanning electron microscope (SEM) image.

- To identify the relationship between different ions of clay soil with electrical resistivity using high energy X-Ray fluorescence (XRF).
- To generate compaction curve to develop correlation of compaction condition with soil resistivity.
- To determine the correlation between soil strength and soil resistivity.
- To determine the variation of soil resistivity with particle sizes, Liquid limit and Plasticity Index and specific surface area.

1.4 Organization

A brief summary about the organization of the thesis is presented here

Chapter 1 presents the background of electrical resistivity measurement in soil, the statement of the problem, specific objectives of the study and thesis organization.

Chapter 2 introduces detailed literature about the conduction phenomenon of clay soil, clay mineralogy, application of electrical resistivity in soil, soil resistivity models, existing correlations and resistivity measurement.

Chapter 3 provides different methodologies that were followed in the study.

Chapter 4 presents results and discussions of conducted tests.

Chapter 5 is for summary and conclusions of the study.

CHAPTER 2

LITERATURE REVIEW

2.1 Resistivity

Electrical resistivity is a material property which indicates how well a material retards electrical conduction. Resistivity relates electrical potential and current to the geometrical dimension of the specified region. It is the reciprocal of conductivity. Electrical conduction takes place due to the movement of charges. Charges are displaced from the original equilibrium condition under the application of electric potential. However, charge density depends on the applied electric field and resistivity of the material. Resistivity can be defined by considering current flow through a cylindrical section. To define resistivity, assuming a cylindrical section with cross sectional area and length of A and L, if current flow is I through section resistance R and potential drop across the section is V, then resistivity can be expressed by the following equation

$$\rho = RA/L$$

where, ρ=Electrical Resistivity, R= Resistance of the material, V= Potential, I= Current , A= Cross sectional Area and L= Length. The schematics of cylindrical section and flow of current are presented in Figure 2.1.

(a)   (b)
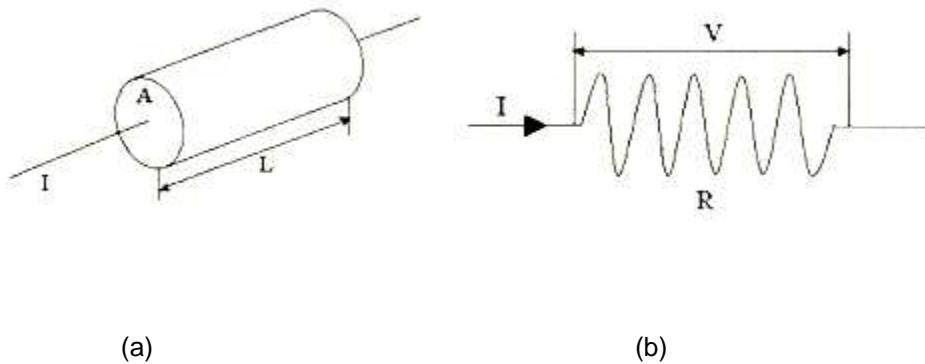
Figure 2.1: (a) Cylindrical Section (b) Flow of Current

5

2.2 Clay Minerals

Clay minerals are formed by chemical weathering of rock forming minerals. They are small colloidal size crystal and chemically known as hydrous aluminosilicates. Clay mineral consists of crystal sheet with repeated atomic structure. There are two fundamental crystal sheets such as tetrahedral or silica and octahedral or alumina. The tetrahedral sheet consists of four oxygen atoms at the corners surrounding a silicon atom. In an octahedral sheet, six oxygen atoms enclose aluminum, magnesium, iron or other atom. Schematics of single tetrahedron and octahedron are presented in Figure 2.2 and 2.3.
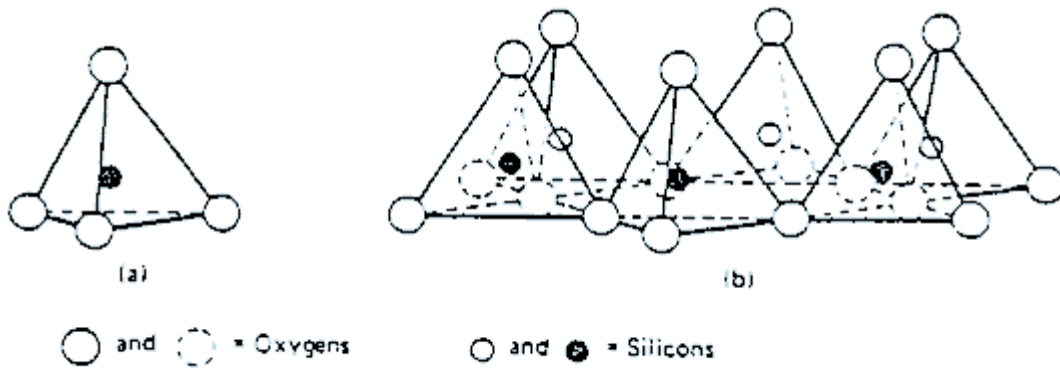
Figure 2.2: Single Unit of Tetrahedral Mineral (Holtz and Kovacs, 1981)
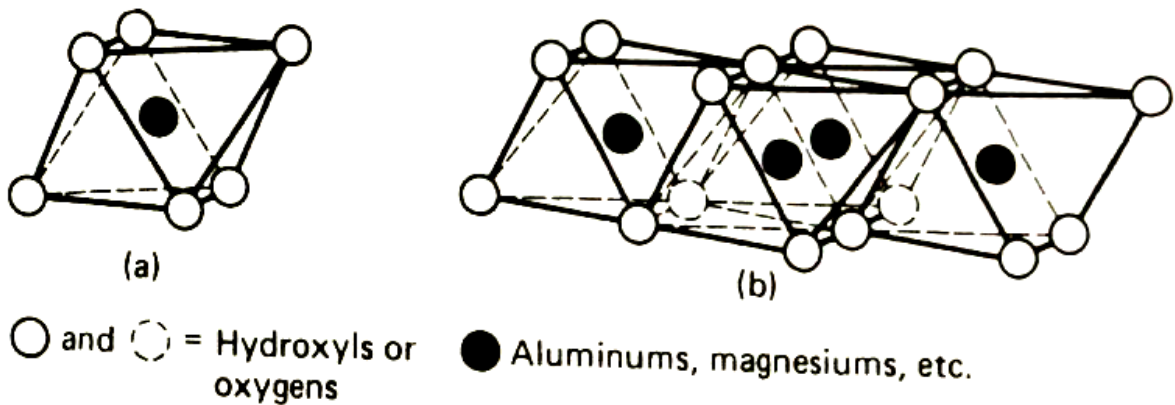
Figure 2.3: Single Unit of Octahedral Mineral (Holtz and Kovacs, 1981)

6

Depending on the variation of basic sheet structure, different clay minerals are identified. However, kaolinite, montmorillonite and illite are the most common minerals found in clay soils.

2.2.1 Kaolinite

Kaolinite consists of one tetrahedral and one octahedral sheet. It is also known as 1:1 clay mineral. Successive basic layers are bonded together by hydrogen bond between hydroxyls of the octahedral sheet and oxygen of the tetrahedral sheet. Due to this hydrogen bond, a large crystal of kaolinite is formed. Structure of kaolinite is presented in Figure 2.4.
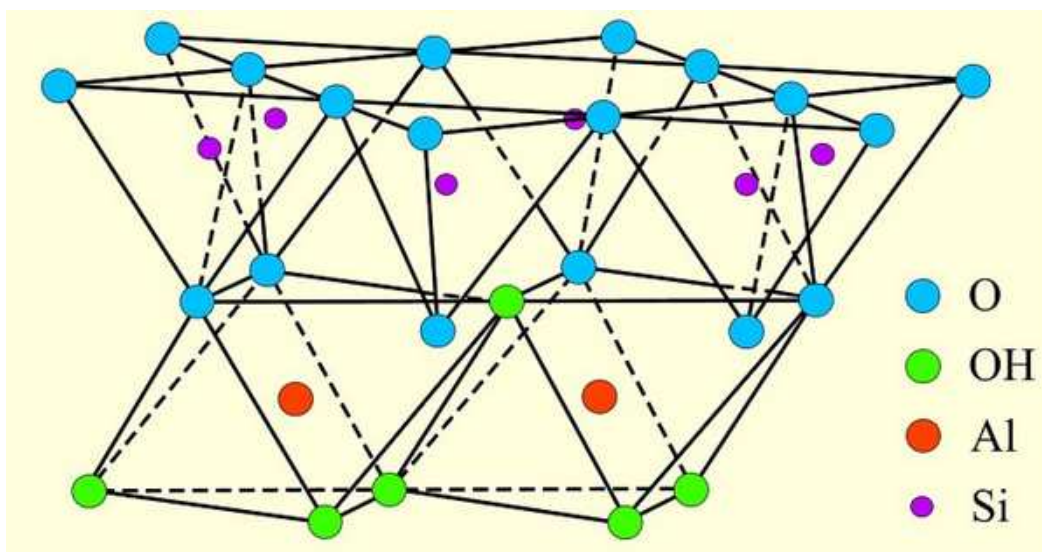
Figure 2.4: Structure of Kaolinite Crystal (http://pubs.usgs.gov)

2.2.2 Montmorillonite

Montmorillonite is also known as Smectite. There are two silica sheets and one alumina sheet in montromorillonite. They are called as 2:1 mineral. The top of the silica sheets are bonded by Van der Waals' force and there is a net negative charge deficiency in octahedral sheet. Thus, water and exchangeable ions can enter and break the layer. Structure of montromorillonite is presented in Figure 2.5.
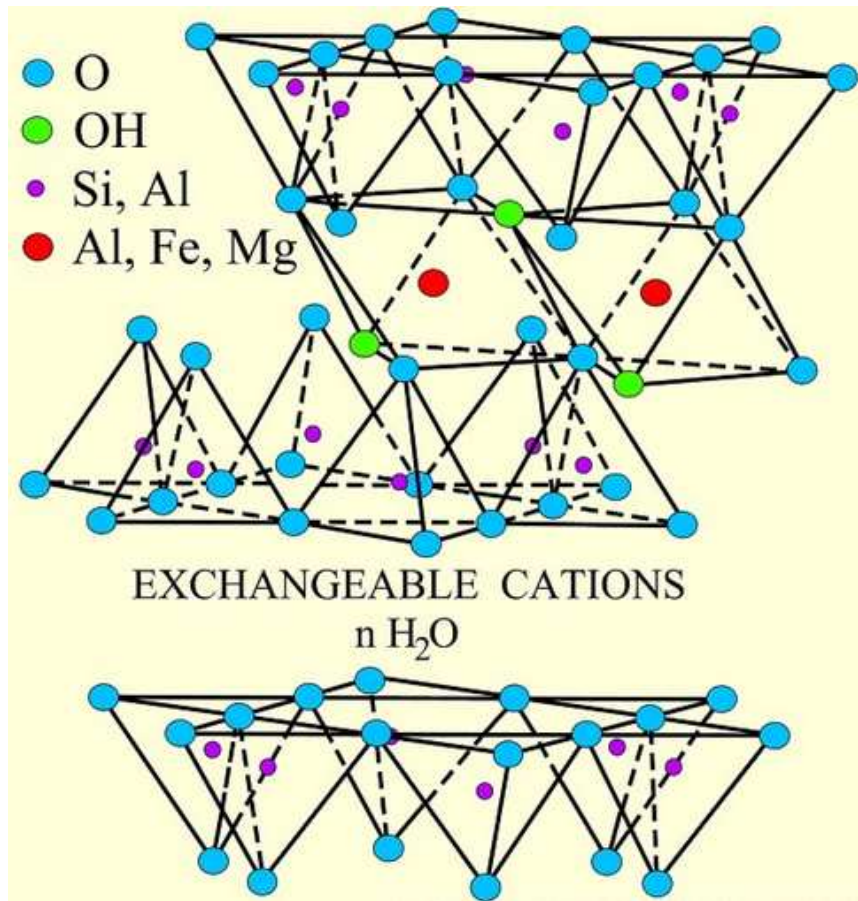
Figure 2.5: Structure of Montmorillonite Crystal (http://pubs.usgs.gov)

2.2.3 Illite

Professor R.E. Grim discovered illite in the University of Illinois in 1937 (Holtz and Kovacs, 1981). It is composed of two silica sheets and one alumina sheet, which is similar to montromorillonite. Thus, the structure is known as 2:1 mineral. In illite, the basic layers are bonded by potassium. The presence of potassium makes the bond between the layers very strong. The schematic of the structure of illite is presented in Figure 2.6.
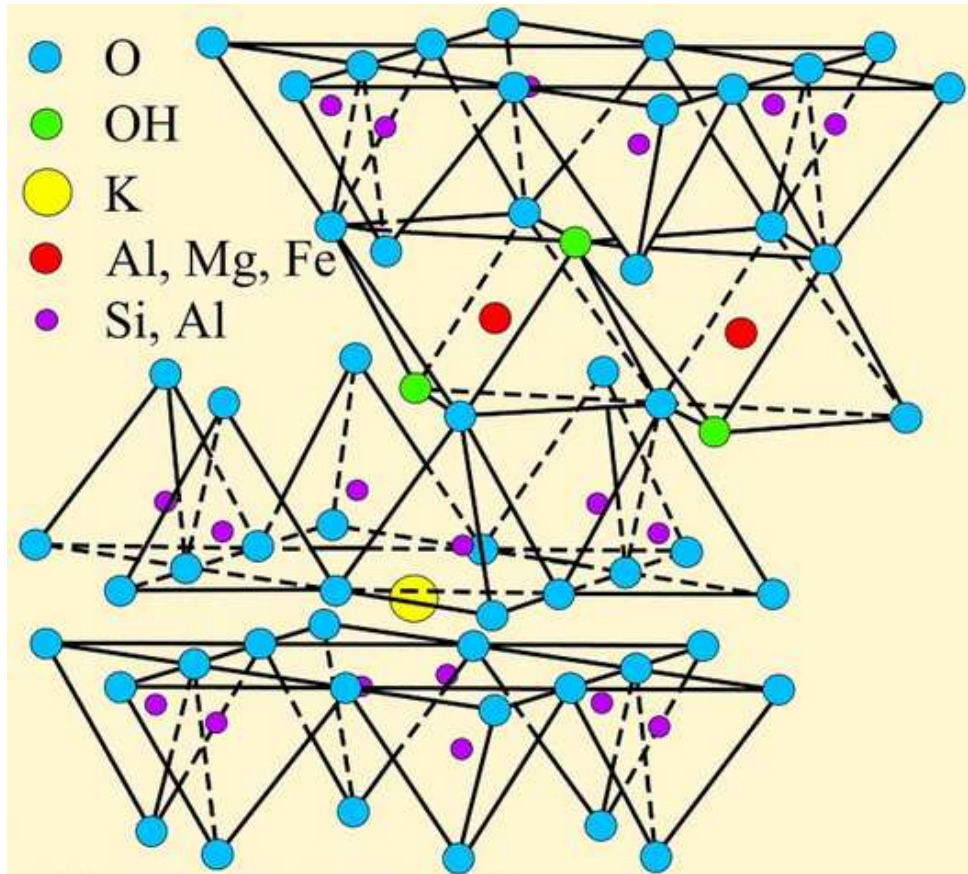
Figure 2.6: Structure of Illite Crystal (http://pubs.usgs.gov)

Clay mineral, layer type and typical chemical formula are presented in Table 2.1

Table 2.1: Clay Mineral, Layer Type and Typical Chemical Formula (Yang, 2002)

Clay Mineral	Layer type	Typical Chemical Formula
Kaolinite	1:1	$[Si_4]Al_4O_{10}(OH)_8 \cdot nH_2O$ (n= 0 or 4)
Montromorillonite	2:1	$M_x[Si_8]Al_{3\cdot2}Fe_{0\cdot2}Mg_{0\cdot6}O_{20}(OH)_4$
Illite	2:1	$M_x[Si_{6\cdot8}Al_{1\cdot2}]Al_3Fe_{0\cdot25}Mg_{0\cdot75}O_{20}(OH)_4$

2.3 Electrical Conduction in Clay Soil

Electrical conduction in porous media like soil generally occurs by the movement of ions through electrolytic pore water in the void and surface charge (Bryson, 2005). Surface charge is negligible in coarse grained soils. Ions can be displaced under the application of electrical poten-

9

tial through the pores with the presence of electrolytic water. However, electrical conductivity depends on pore fluid conductivity as well as surface charge in clay soils. Generally, clay particles possess net negative charge. Thus, cations are attracted by the clay particles. Immediately adjacent to the particle surface layer, there is an adsorbed layer of fixed ions. In dry clay, adsorbed cations are tightly held by the negative charge of the clay particles. After neutralizing the net negative charges of clay particles, excess cations are present as salt precipitates. Precipitated salts go in to the soil-water solution in the presence of water. It was documented in the literature that the cations produce high concentration around the solid particles. To equalize charge concentration, they try to diffuse throughout the structure. Negative electrical charge of the solid particles restricted the diffusion. Anions are also excluded from the negative force of the particles. Adjacent to the adsorbed layer, there are relatively mobile ions consist both positive and negative charges. The charged surface and distributed charge surface together is known as diffuse layer. When an electric potential is applied, ions in the double layer displaced along a plane called shear plane or z-potential plane and causes conduction. The location of z-potential plane is close to the stern plane. (Rinaldi and Cuestas. 2002). It is obvious that the presence of water enhances the conductivity due to interaction between water ions and present ions in clay structure. Charge distribution around clay surface is presented in Figure 2.7.
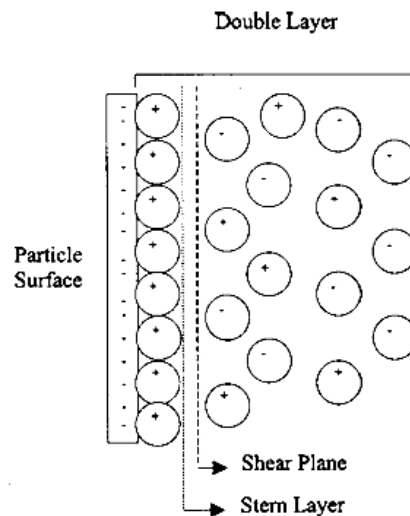
Figure 2.7: Charge Distribution in the double layer (Rinaldi and Cuestas, 2002)

10

2.4 Soil Resistivity Model

Resistivity of different component of porous media is related to the resistivity of conducting medium by electrical mixing model (Bryson, 2005). G.E. Archie developed an empirical formula to correlate bulk resistivity of saturated soil to the pore fluid resistivity and porosity in 1942. If the resistivity of soil is ρ, resistivity of pore fluid is ρ_w and porosity is n, then Archie's formula is

$$\rho = a.\rho_w.n^{-m}$$

where, a is a fitting parameter and m is cementation factor. The value of m depends on the inter-connectivity of pore network and tortuosity. In sand and gravel, m is ranged between 1.4 to 2.2. However, it was assumed that conduction occur due to the presence of pore fluid only. Moreover, with the change of degree of saturation, soil resistivity changes. Therefore, several modifications were done by the researchers to make Archie's law more versatile.

Shah and Singh (2005) described a generalized form of Archie's law. According to the authors, the effect of surface conductivity was included in the cementation factor. Hence, it is not necessary to incorporate conductivity of soil matrix in Archie's law. They described the relationship in terms of conductivity as stated below

$$\sigma_b = c.\,\sigma_w.\,\theta^m$$

where, σ_b= Bulk Conductivity of soil, σ_w= Pore water conductivity, θ= Volumetric moisture content

Authors also proposed empirical relationships between fitting and cementation parameters, "c" and "m" with clay percentage which can be expressed as

$$c = i.\ Clay^j \ and \ m = k.\ Clay^l$$

When clay content is more than 5% by volume, then the value of i= 0.6, j= 0.55, k= 0.92 and l= 0.2. However, at clay content more than 5%, c and m become constant. Authors proposed that the constant values were, c= 1.45 and m=1.25.

Keller and Frischknecht (1966) proposed a relationship, which correlated unsaturated (ρ) and saturated soil resistivity (ρ_{sat}) with degree of saturation. The expression was

$$\rho/\rho_{sat}=S^{-B}$$

where, S is the degree of saturation and B is the empirical factor.

In most of the geophysical application, relation between bulk soil resistivity and pore water resistivity is measured with the aid of formation factor (F). Formation factor can be given by the ratio of bulk resistivity (ρ) and pore water resistivity (ρ_w) such as

$$F=\rho/\rho_w$$

2.5 Factor Affecting Soil Resistivity

2.5.1 Moisture Content

The amount of water present in the soil is one of the most important parameters geotechnical engineer needs to know. It can be defined either weight basis or volume basis. Measurement of moisture content in the weight basis is known as gravimetric moisture content. In the weight basis, the ratio of amount of water present in the void to the amount of solids is known as moisture content. The equation to calculate gravimetric moisture content is expressed as

$$w = \frac{W_w}{W_s} \ x \ 100\%$$

where, Ww = Weight of water, Ws= Weight of solid soil

However, volumetric water content measures moisture content in terms of volume of water. It is calculated from the ratio of water volume present in soil and total volume. The equation can be written as

$$\theta = \frac{V_w}{V_t}$$

where, Vw= Volume of moisture, Vt= Total volume of soil mass.

Volumetric moisture content is related to gravimetric moisture content by the following expression

$$\Theta = w.(\gamma_d/\gamma_w)$$

where, γ_d= Dry unit weight of soil, γ_w= Unit weight of water.

Several studies showed that moisture content is the most dominating factor which influences electrical resistivity of soil. Electrical conductivity occurs mainly due to the displacement of ions in the pore water. When moisture content increases from air dry to full saturation, adsorbed ions in the solid particles are released. Thus, mobility of electrical charge increases with the increase of moisture. Free electrical charges cause decrease in electrical resistivity under the application of electric field. It is seen electrical resistivity of soil decreases rapidly with the increase of moisture content more than 15% (Samouelian et al., 2007). Voronin (1986) described the effect of moisture content on soil resistivity by a nonlinear curve as presented in Figure 2.8.
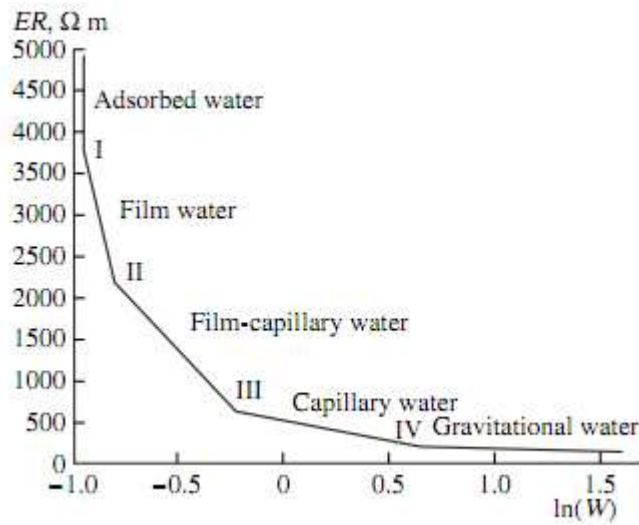
Figure 2.8: Soil Moisture and Electrical Resistivity Relationship (Voronin, 1986)

Moisture content and electrical resistivity curve was divided in to various zones based on the different moisture condition in soil. The segments of the curve correspond to the specific water content are adsorbed water, film water, film capillary water, capillary water and gravitational water. According to the author, electrical resistivity decreases rapidly in the adsorption water zone with the increase of moisture content. Ions of water molecules are immobile in the adsorbed water zone. However, the dipolar water ions create a conductive path for electrical current. Thus electrical resistivity decreases sharply with the increase of moisture in the adsorption zone. In the

film water zone Van der Waals' force increases. As a result electrical resistivity decreases less sharply in the film water zone. When maximum possible thickness of water film is achieved, water goes from film to fissure. In the film capillary water zone relative portion of film water decreases and capillary water increases. Molecular attraction force is higher than the capillary force in this zone. Therefore, electrical resistivity decreases less dramatically in the film capillary and capillary water zone. In the gravitational water zone mobility of electrical charges become independent of movement of water molecule ions. Thus, electrical resistivity is almost independent of water content in this zone.

2.5.2 Dielectric Permittivity of Soil

Electrical properties of the soil are controlled by dielectric permittivity of the soil. Dielectric permittivity is a measure of the material to store charge under applied electric field. Dielectric loss is opposite to dielectric permittivity. Dielectric loss can be defined as a measure of the proportion of the charge transferred to conduction. Saarenketo (1998) stated that the separation of electric charge can occur in four methods: electrical, molecular, orientational and interfacial polarization. Therefore, bonding of water molecules around the soil particles influences the dielectric permittivity of soil. It also depends on the frequency of current. The definition of dielectric permittivity can be given by the following equation

$$K^*(\omega) = K'(\omega) - iK''(\omega)$$

 where, K'= Real part of dielectric permittivity and K''= Imaginary part of dielectric permittivity.

The author indicated that real part of the expression of dielectric permittivity might vary with natural soil constituents.

2.5.3 Geologic Formation and Arrangement of Soil Solids

Generally, soil electrical resistivity exhibits a wide range of value. Soil resistivity is low for coastal soil and high for rocks. Study also demonstrated that soil resistivity is also affected by geological formation. Research conducted by Giao et al., (2002) showed that presence of diatom micro fossils substantially alter the geotechnical properties of clay. This kind of change in struc-

14

ture also affects electrical properties of clay. Robain et al., (1996) presented resistivity variation with the structure of the pedological materials. According to the authors, low and high resistivity values are related to the macro and meso porosity of soil.

Geometry of the pores determines the proportion of the water and air in the soil. Air is considered as dielectric material. If the pores of soil are filled with water then electrical conductivity may change. Usually clay soil is more conductive than sandy soil. However, saturated sandy soil may demonstrate low resistivity than dry compacted clay. Because of these factors, overlapping of resistivity values is observed for different type of soils. Typical range of electrical resistivity value of soil is presented in Figure 2.9.
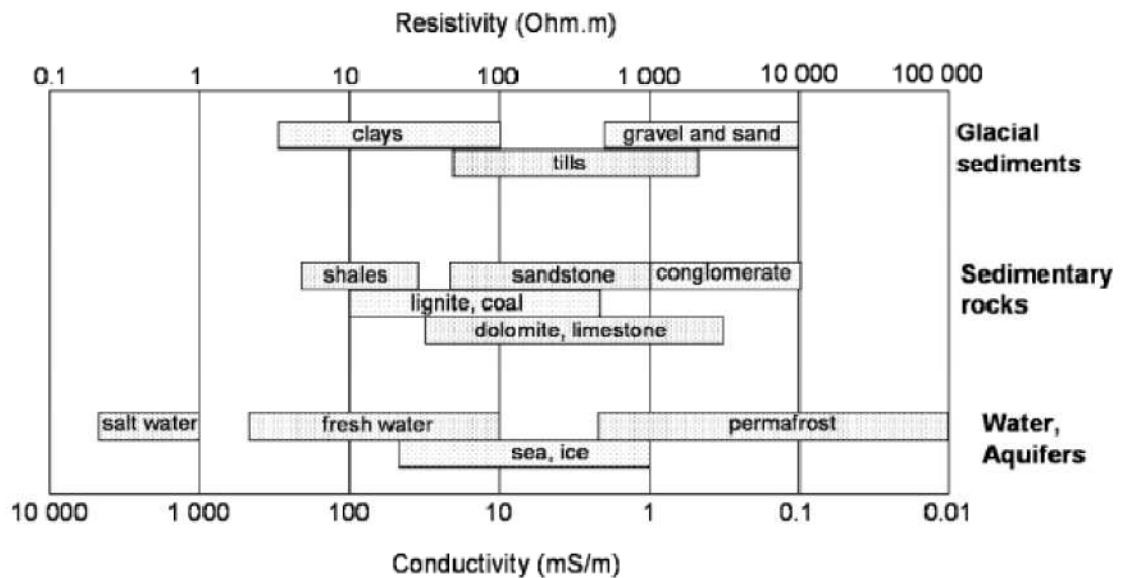
Figure 2.9: Typical range of Electrical Resistivity of Different Soils (Samouelian et al., 2005)

Research collaboration to measure soil resistivity of natural clays around the world was initiated by Korea and Japan. The objective of the research was to establish a database of clay soil resistivity. It was observed that resistivity of the investigated clay varied in a narrow range. Recorded data of electrical resistivity of clay soil is presented in the Figure 2.10.
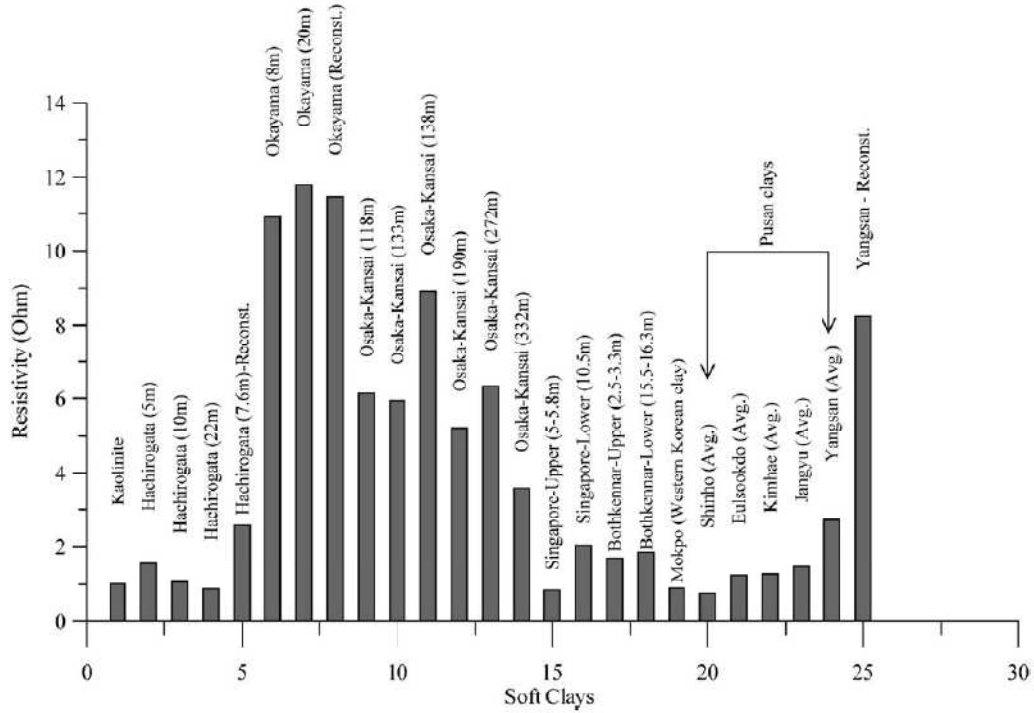
Figure 2.10: Electrical Resistivity of Different Clays in the World (Giao et al., 2003)

2.5.4 Composition of Pore Water in Soil

Soil with different pore water composition shows different electrical conductivity. Different ions such as H^+, OH^-, SO_4^{2-}, Na^+, Cl^- present in the soil. They do not affect the conductivity in the same way because of their difference in ion mobility. Kalinski and Kelly (1993) presented a study on the effect of pore water conductivity in soil resistivity. It was observed that increase of pore water conductivity increases soil conductivity at constant volumetric water content as shown in Figure 2.11.

16
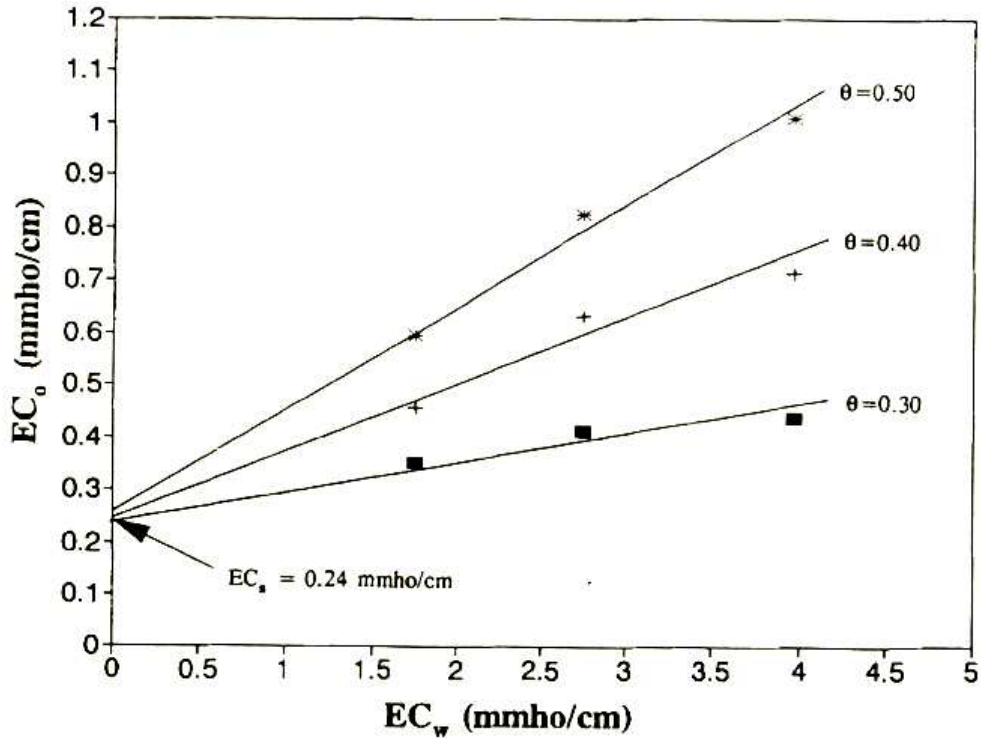
Figure 2.11: Relationship between Bulk soil and Pore water Conductivity (Kalinski and Kelly, 1993)

Kalinski and Kelly (1993) also presented an equation to estimate pore water conductivity. The relationship was expressed as

$$ECw = ECo - \frac{ECs}{\theta(a\theta + b)}$$

Where, ECw=Pore water electrical conductivity, ECs= Apparent Soil particle surface electrical conductivity, ECo= Bulk Soil electrical conductivity, Θ= Volumetric water content, a and b= Constant.

Rinaldi and Cuestas (2002) reported the influence of sodium chloride and other electrolytes on Argentine loess soil. Washed samples were prepared at constant density and electrolytes were added. Conductivity was measured at different concentration of various electrolytes. A linear relationship was observed between conductivity of soil and electrolyte as presented in Figure 2.12.
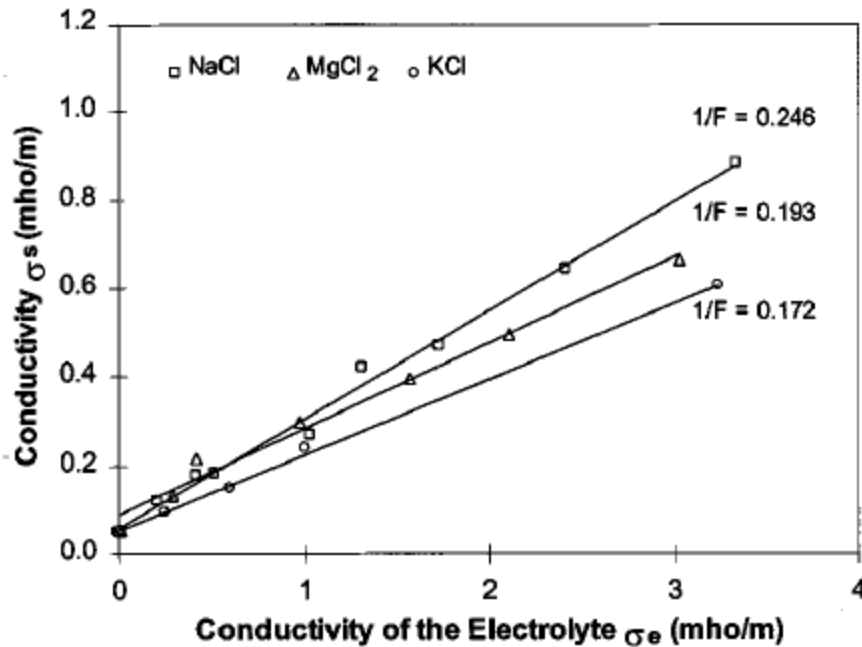
Figure 2.12: Relationship between Conductivity of Saturated sample at Different Electrolytes (Rinaldi and Cuestas, 2002)

According to the study, samples contain sodium showed highest conductivity, followed by magnesium and potassium. However, the difference in conductivity was not due to the ion mobility of different electrolytes only. Combined effects of ion mobility, adsorption and soil structure were responsible for different soil conductivity.

2.5.5 Organic Content

Organic soil generally composed of decayed materials. Decomposed materials are intermixed with soil minerals and formed a distinct texture in organic soil. It can retain higher proportion of water and electrolytes. Thus, the conductivity of organic soil is high. Ekwue and Bartholomew (2010) reported the effect of peat on conductivity of some soils in Trinidad. They observed that increase of peat content increased the conductivity at constant water content and bulk density as presented in Figure 2.13.

(a)   (b)
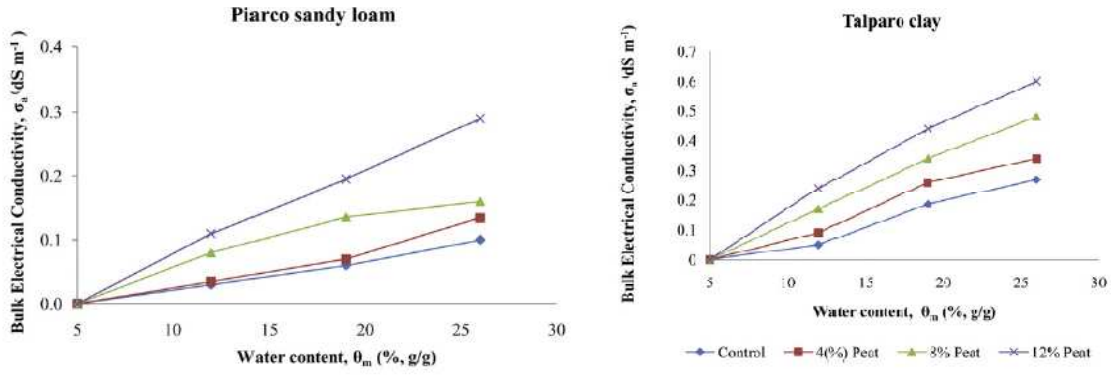
Figure 2.13: Apparent Electrical Conductivity at different peat content (a) Picaro Sandy Loam (b) Talparo Clay (Ekwue and Bartholomew, 2010)

2.5.6 Bulk Density and Degree of Saturation

Density is an important geotechnical property which relates volume with mass of soil. Bulk Density of soil can be defined as the ratio of weight of soil to the total volume. It can be defined by the phase diagram (Figure 2.14) of soil. The expression is

$$\gamma = \frac{W}{Vt}$$

where, W=Weight of soil mass and V_t= Total volume.

Bulk density is closely related to degree of saturation. It is defined by the ratio of volume of water to the volume of void. It can be given by

$$Sr = \frac{Vv}{Vw}$$

Where, Vw= Volume of water, Vv= Volume of void
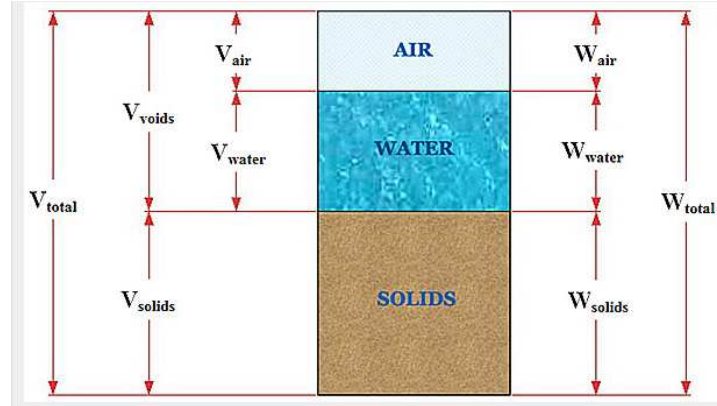
Figure 2.14: Phase Diagram of Soil

Research showed that soil resistivity is affected by the change in bulk density and degree of saturation. Increase of bulk density is associated with reduction of pore air in soil. Therefore, the degree of saturation increases. Dissolved ions from the pore water adsorb on the solid surface and affects the formation of double layer in fine grained soil Therefore, increase of degree of saturation cause proportional decrease of soil resistivity. However, this relationship is valid above a critical value of degree of saturation. Critical degree of saturation is corresponds to minimum amount of water required to maintain a continuous film of water in soil. An abrupt increase of soil resistivity occurs below critical degree of saturation (Bryson, 2005). Moreover, bulk density increases contact between individual particles. Reduction in pore space and closer contacts between the particles allow easy conduction of current. According to the study of Rinaldi and Cuestas (2002), relationship curve of conductivity and degree of saturation was concave upward. The effect of degree of saturation on conductivity at different electrolyte concentration is presented in Figure 2.15.
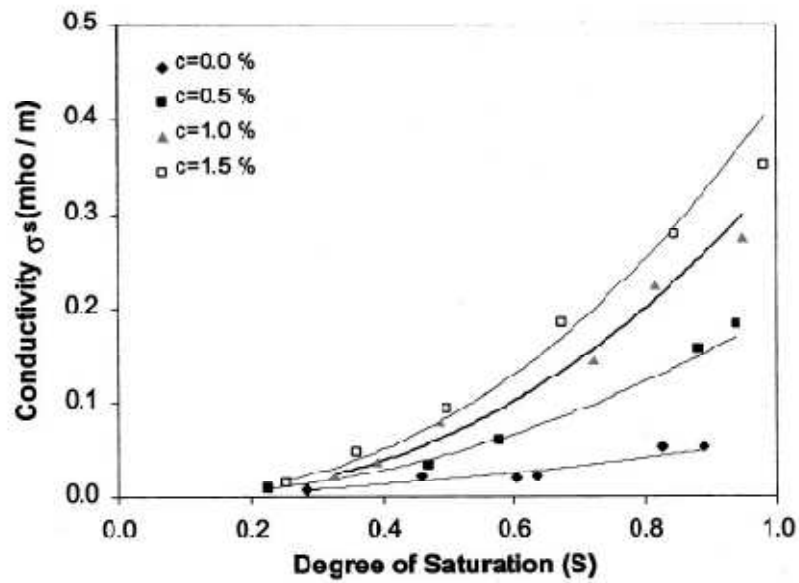
Figure 2.15: Influence of Degree of Saturation in Soil Conductivity (Rinaldi and Cuestas, 2002)

Abu Hassanein et al., (1996) conducted resistivity measurements of four different soils at different initial degree of saturation. It was observed that the electrical resistivity was inversely correlated with initial degree of saturation. It was also noted that initial degree of saturation and electrical resistivity was independent of compactive effort. The results of the study are presented in Figure 2.16.
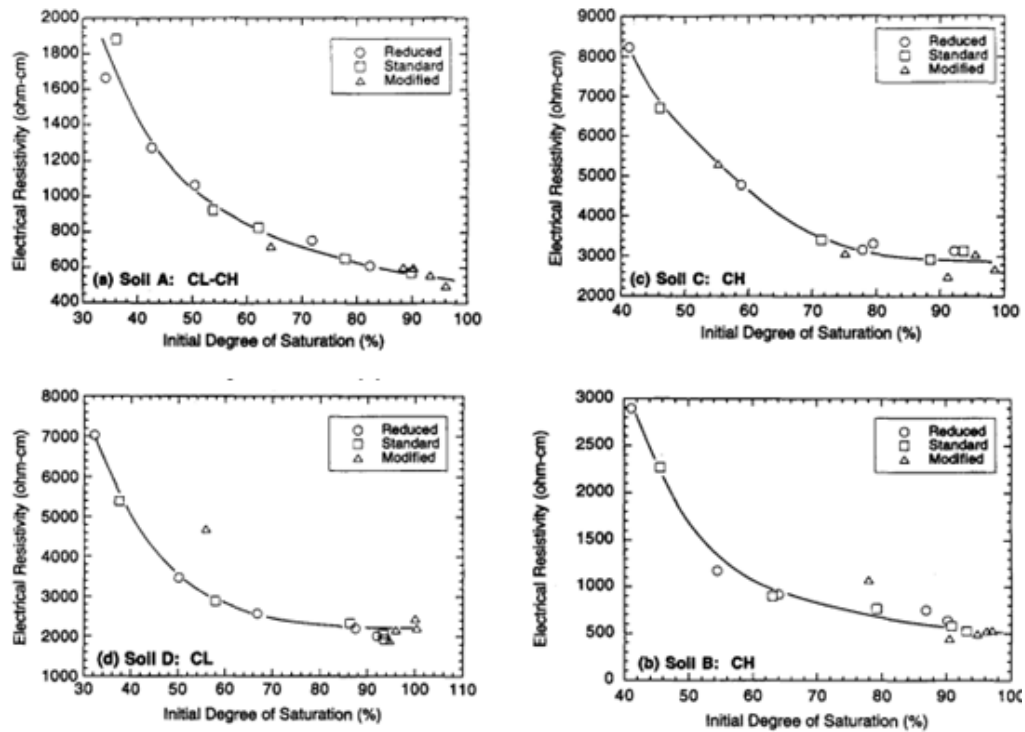
Figure 2.16: Variation of Electrical Resistivity with Initial Degree of Saturation for Different Soils
(Abu Hassanein et al., 1996)

2.5.7 Temperature and Operating Frequency

Electrical resistivity decreases with the increase of temperature because of the agitation of ions. It was observed that increase of temperature per degree celsius increases electrical conductivity by 2.02% (Campbell, 1948). In field scale, variation temperature during a year can be broadly classified in to two temporal scales: day and season. In most of the studies in the field scale an assumption was made that the temperature remained constant over the day. However, in annual scale (season) effect of temperature cannot be avoided. Abu Hassanein et al., (1996) presented a study on the effect of temperature on three different soils. It was observed that above $0^{\circ}C$ relationship between electrical resistivity and soil was approximately exponential as shown in Figure 2.17.

22
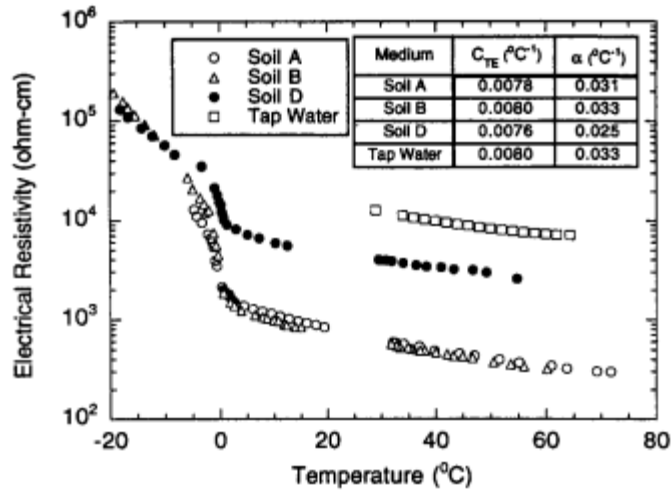
Figure 2.17: Variation of Electrical Resistivity with Temperature (Abu Hassanein et al., 1996)

Experiments showed that operating frequency affects soil resistivity. Application of electric field in clay soil causes ions to be released from double layer at high frequency. Thus, overall conductivity of the soil increases. This phenomenon is called double layer relaxation. In most soils frequencies below 100 kHz, conductivity becomes independent of frequency. However, at low frequency electrode polarization can also occur. When polarization occurs, ions in the electrode cannot exchange and accumulate near electrode. Accumulation of ions create double layer adjacent to electrode. Double layer at the electrode is considered as a low conductive thin film and reduces overall conductivity. This mechanism occurs at frequency below 2 or 3 kHz. The effect of polarization is significant for electrode made of gold, nickel and copper (Rinaldi and Cuestas, 2002). Typical curve of conductivity to be observed in clay soil at different frequency is presented in Figure 2.18.
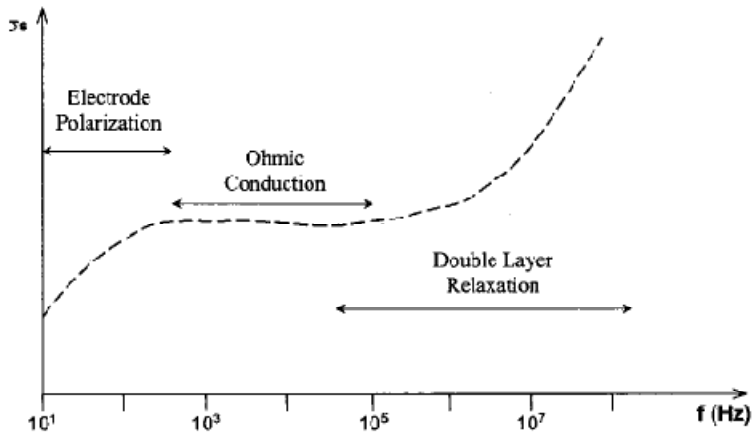
Figure 2.18: Typical Curve of Conductivity in Clay soil at Different Frequency (Rinaldi and Cuestas, 2002)

Research conducted on Argentine loess by Rinaldi and Cuestas (2002) showed that conductivity became straight line after 3 kHz frequency as presented in Figure 2.19. Below 3 kHz conductivity was non linear. Tests were conducted at constant moisture content, density and different electrolyte concentration. Authors indicated that such behavior was attributed due to the electrical polarization.
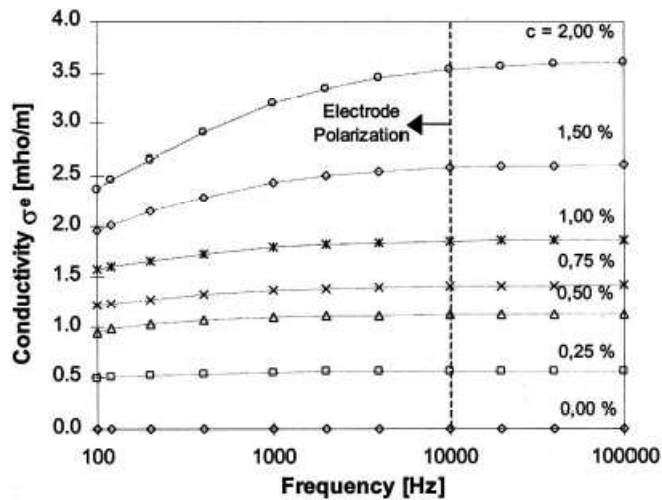
Figure 2.19: Variation of Conductivity at different Frequency (Rinaldi and Cuestas, 2002)

2.6.1 Atterberg Limits

Atterberg Limits are moisture content where the soil changes its states and behaviors. With the increase of water content, soil state changes from brittle solid to plastic solid and then to a viscous fluid. The Index properties are widely used by geotechnical engineers to identify the soil behavior in response to moisture. Research has been conducted to identify the relationship between Atterberg Limits and resistivity. Abu Hassanein et al., (1996) evaluated variation of electrical resistivity with Atterberg limits. Soil samples were compacted at optimum moisture content and dry unit weight using Standard Proctor method. It was observed that soil with higher LL and PI had lower resistivity as presented in Figure 2.20. Figure 2.20 also shows that decrease of resistivity with the increase of LL and PI tends to be a power function of electrical resistivity. Only exception was found for samples having high coarse fraction. Soils with 47% coarse fraction showed high resistivity. The trend of decreasing resistivity with increase of LL and PI was also consistent with the mineralogy of samples. Clay samples having greater quantity of smectite have higher LL and PI. These soils are more active and exhibit higher surface conductivity. LL and PI of non swelling clay are strongly influenced by the diffuse double layer. Surface conductivity of the clay depends largely on the diffuse double layer. Therefore, electrical resistivity depends on the Atterberg limits of the soils.
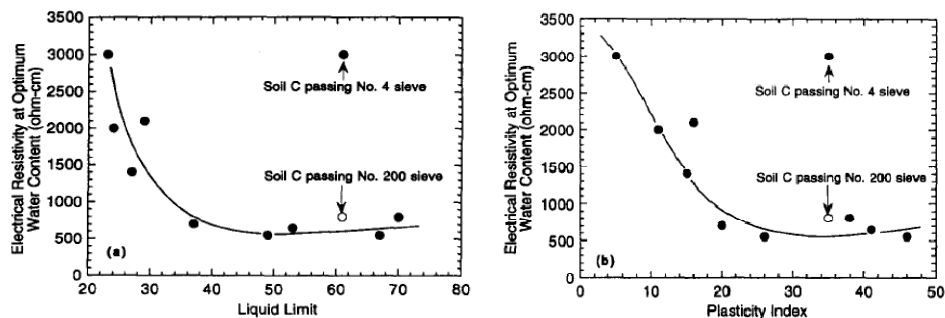
Figure 2.20: Relationship between Electrical Resistivity and Atterberg Limits at Optimum Water Content (Abu Hassanein et al., 1996)

2.6.2 Compaction

Compaction is the process of densification of soil by the application of mechanical energy. Generally, compaction is done at specific moisture content to achieve maximum densification of soil. Compaction condition can be determined by Standard Proctor and Reduced Proctor Test. However, different indirect approaches were initiated to observe compaction condition. Several researchers utilized electrical resistivity to evaluate compaction condition. Compaction is associated with the decrease of void ratio and increase of degree of saturation. Good correlations between electrical resistivity and compaction condition were observed in several studies. A laboratory scale test was performed by Rinaldi and Cuestas (2002) to evaluate relationship between electrical conductivity and compaction. Samples were sieved through No 40 sieve and compacted at 18% moisture content. Compaction was conducted using Standard Proctor method in a rectangular mixing pan. After compaction, conductivity was measured using four probe electrode device. Iso-conductivity contour obtained from the test is presented in Figure 2.21.
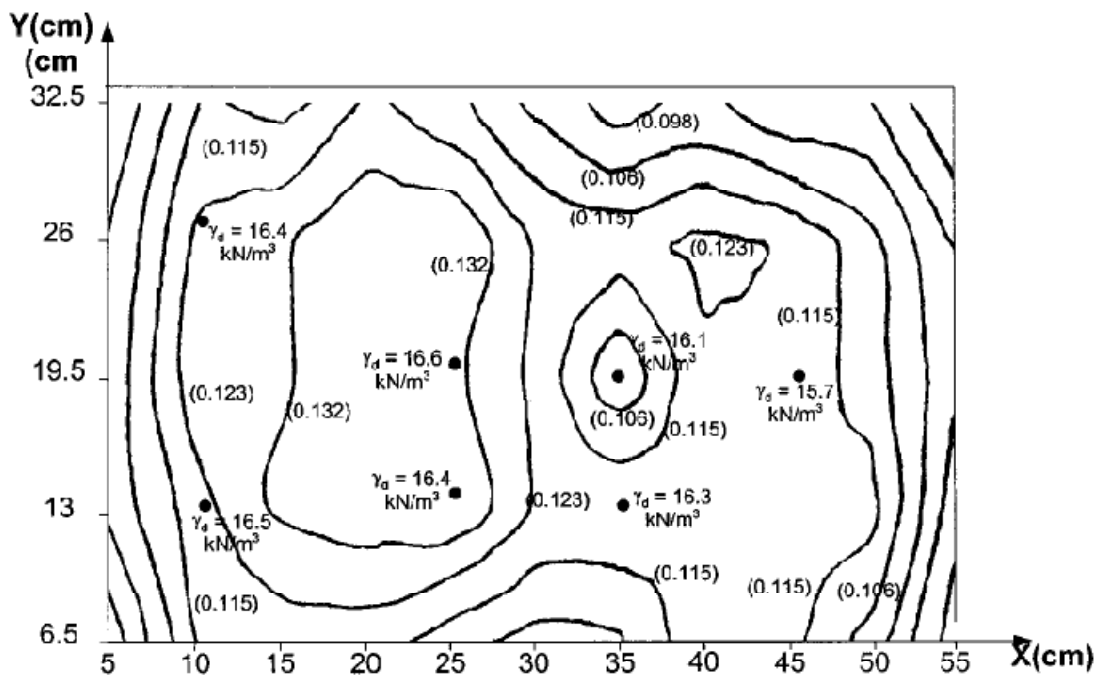
Figure 2.21: Iso Conductivity Contour of Compacted Sample, Parentheses showed electrical conductivity in mho/m (Rinaldi and Cuestas, 2002)

From the Figure 2.21, it is depicted that conductivity at central portion is greater than right hand side and border. Author indicated that variation of conductivity was attributed due to the variation of soil unit weight. Unit weight was higher at left hand side and decreased at right hand side and border due to the low stiffness of the wall of the mixing pan.

McCarter (1984) conducted a study on the effect of air void ratio in soil resistivity. He indicated that reduction in air void ratio in soil structure had significant effect on soil resistivity. Tests were conducted on Cheshire and London clay. With the increase of degree of compaction or degree of saturation decrease of soil resistivity was observed for both samples. Author concluded that only moisture content could not be a criterion in resistivity measurement. Compaction condition also played an important role in resistivity.

Abu Hassanein et al., (1996) performed a comprehensive study on the effect of molding water content and compactive effort in soil resistivity. Samples were compacted at three different compaction methods: Standard, Modified and Reduced Proctor. Observed test results on the study are presented in Figure 2.22.
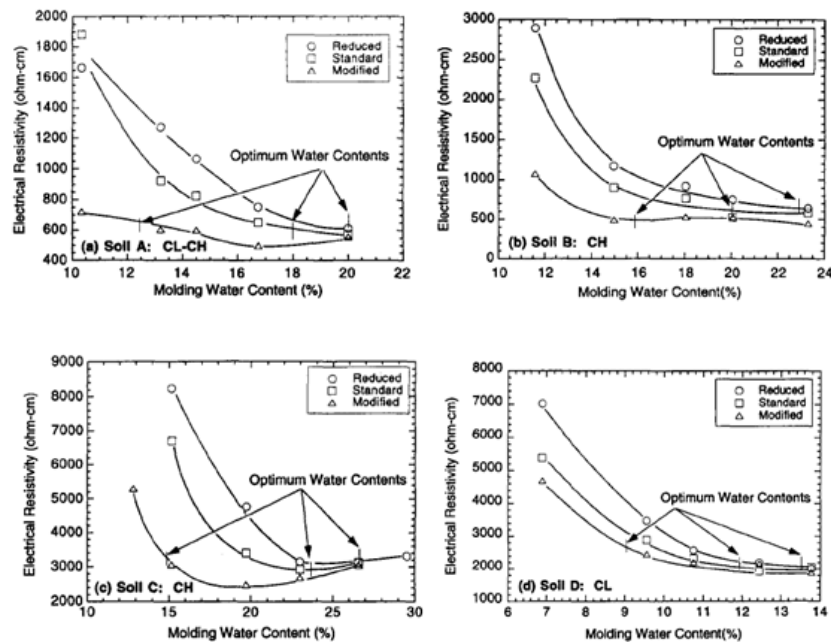
Figure 2.22: Relationship among Electrical Resistivity, Molding Water Content and Compactive Effort for Different Soils (Abu Hassanein et al., 1996)

27

Observed resistivity was high when soil was compacted at dry optimum and low when compacted at wet optimum. Resistivity was sensitive of molding water content when water content was below optimum. At wet optimum, resistivity had become almost independent of molding water content. Authors indicated that this relation could be used to evaluate compaction condition of soil. Relationship between resistivity and compaction was discussed in the light of structural change of soil during compaction. At low compactive effort and dry of optimum water content, clay clods are difficult to remold. Interclod pores are also relatively large in this condition. Many pores are filled with dielectric air and inter particle contacts are poor. Furthermore diffuse double layers are not fully developed. Therefore, soil shows high resistivity. In contrast, when soil is compacted at wet optimum and high compactive effort, clods of clay are easily remolded. At this condition, pores are nearly saturated and smaller in size compare to previous case. Better particle-to-particle contact and formation of bridge between particles improve conductivity. Thus, lower resistivity is attained when compacted at wet optimum water content and high compactive effort (Abu Hassanein et al., 1996). Moreover, study showed that change in compactive effort did not affect resistivity significantly when compacted at wet optimum.

2.6.3 Void Ratio

The ratio of volume of void to the volume of solid is known as void ratio. Void ratio is presented by the equation,

$$e = V_v/V_s$$

Where, Vv= Volume of void, Vs= Volume of solid (phase diagram Figure 2.14).

It was documented that soil resistivity is significantly affected by the void ratio. This relationship led many researches to determine the correlation between these two parameters. Kim et al., (2011) carried out a study to determine void ratio from resistivity in a sea shore soil. For the purpose of the study, electrical resistivity was measured using a newly designed Electrical Resistivity Cone Probe (ERCP). The research was conducted in two approaches: first laboratory tests were conducted to obtain well known Archie's law and then results are validated with field data.

Pore water was extracted from the soil using a miniature centrifuge to calibrate Archie's law for the specific soil samples in the laboratory. After calibration, porosity profile was obtained using coefficient of cementation (m parameter of Archie's law) ranged from 1.4 to 2.0. To validate the obtained results, two field tests were carried out in Incheon and Busan, Korea. In the field, ERCP was pushed at penetration rates of 1 mm/s and 3.3 mm/s in to the sites. Undisturbed samples were obtained using thin walled samplers to estimate volume based void ratio in the laboratory. Volume based void ratio matched well with resistivity based void ratio obtained from calibrated Archie's law. According to the authors, void ratio can be determined from resistivity when Archie's law is calibrated for specific soil sample.

2.6.4 Consolidation

Consolidation means dissipation of excess pore water pressure with time. The consequence of consolidation is settlement. With the settlement, pore water is dissipated and contact between soil particles increases. It was observed that reduction of water in consolidation affects soil resistivity. Various studies were conducted to determine the effect of consolidation in soil resistivity. McCarter and Desmazes (1997) investigated changes in electrical conductivity of clay soil in response to consolidation. Modified consolidation cell was utilized to conduct tests on soil samples having moisture content of 71%. Test results are presented in Figure 2.23.
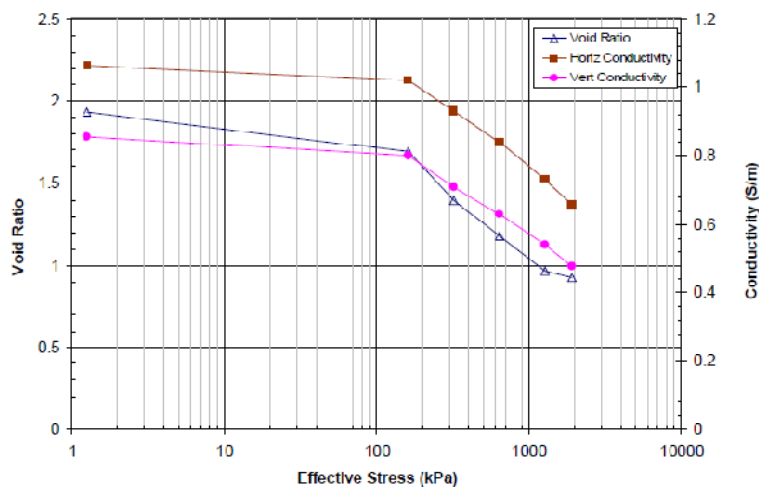
Figure 2.23: Relationship of conductivity with consolidation (McCarter and Desmazes, 1997)

Figure 2.23 indicates that the changes of void ratio and conductivity with effective stress are very similar. According to the authors, conduction in saturated soil occurred through continuous interstitial water. Thus, fractional volume of water and composition of pore fluid influenced electrical properties significantly. Conductivity of soil decreased with consolidation process due to the dissipation of pore water.

Bryson (2005) linked void ratio with conductivity from the curve obtained by McCarter and Desmazes (1997). Volumetric strain in one dimensional consolidation occurs due to the vertical strain. Reduction in sample height is associated with the change in void space in vertical direction. Thus, change in the vertical conductivity is related to the change in void space in vertical direction. According to the Figure 2.23, vertical conductivity is a function of void ratio.

One dimensional settlement in terms of conductivity can be expressed as

$$S = \frac{\Delta e}{(1+e)}H = \frac{\Delta\sigma}{1+\sigma v}(\xi)\ H,\ (Bryson, 2005)$$

Where, Δe= change in void ratio, e= initial void ratio, $\Delta\sigma$ = change in vertical conductivity, σ_v= Initial vertical conductivity, ξ= factor relating vertical conductivity and void ratio, H= sample height.

The compression index for one dimensional consolidation of normally consolidated clay can be written as

$$Cc = \xi\ (\Delta\sigma)/log(P/Po),\ (Bryson, 2005)$$

where, P= consolidating pressure and Po= initial pressure.

Bryson (2005) indicated that consolidation behavior can be determined from electrical conductivity of soil.

2.6.5 Soil Moisture Quantification

Quantification of moisture in soils is very important in geotechnical engineering. Conventionally, soil moisture is determined from laboratory test or installation of moisture sensor in the field. However, electrical resistivity can be utilized to determine moisture condition of subsurface.

Resistivity decreases with the increase of soil moisture. This phenomenon led to several studies to quantify moisture content of soil from resistivity in the laboratory and field scale.

Crony et al., (1950) described a methodology to determine soil moisture using electrical resistance method. The measurement was based on three relationships: the suction of the water in the absorbent and moisture content of the absorbent, moisture content of the absorbent and the resistance of the gauge, the suction of water in the soil and moisture content of the soil. Plaster of Paris and high alumina cement were used as absorbent materials. Electrodes were made of copper. It was observed that electrical resistance gauges could be used to determine the soil suction and soil moisture. However, their reliability as a soil moisture meter was doubtful because of the disturbance of the soil. The accuracy of electrical resistance gauges was adequate to use in civil engineering purposes compare to agricultural purposes. According to the study, calibration of electrical gauges was important to obtain precise results. Accurate assessment of suction and moisture content of the absorbent was identified as major problem in this method. Very small differences in mixing and curing of absorbent influenced the results significantly.

McCarter (1984) investigated response of resistivity of the soil samples at different moisture contents. It was observed that resistivity decreased sharply with the increase of moisture content. Author concluded that resistivity is a function of moisture content and degree of saturation.

Kalinski and Kelly (1993) conducted laboratory investigation to determine volumetric moisture content from electrical conductivity of soil. Resistivity was measured by four probe circular cell. Porous plate extracted water was collected for measurement of pore water conductivity (*ECw*). Results showed that with the increase of volumetric moisture content, *ECo/ECw* (ratio of soil conductivity and pore water conductivity) increased as shown in Figure 2.24.
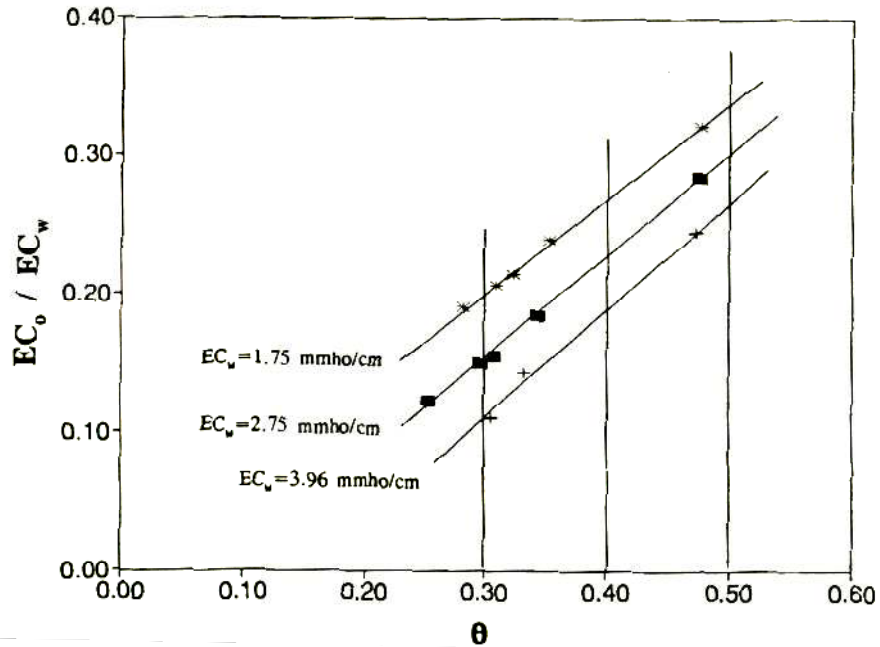
Figure 2.24: Relationship between Ratio of bulk soil and pore water conductivity with volumetric moisture content (Kalinski and Kelly, 1993)

Assuming surface conductivity ($ECs= 0.24$ mho/ cm), following regression equation was developed by the authors,

$$EC_o= EC_s+ EC_w\theta(1.04\theta-0.09)$$

It was observed that model predicted and measured volumetric moisture contents were in good agreement.

Ozcep et al., (2003) presented a study to determine relationship of soil resistivity and water content in Turkey. The study area was Istanbul and Golcuk. Electrical resistivity was measured using Vertical Electrical Sounding (VES) in 210 points of two sites. Soil test boring was conducted for collection of samples. Soil resistivity was ranged between 1 to 50 Ohm-m. Moisture content of the collected samples was in between 20% to 60%. The relationship between soil resistivity and water content was determined as an exponential function as presented in the Figure 2.25.
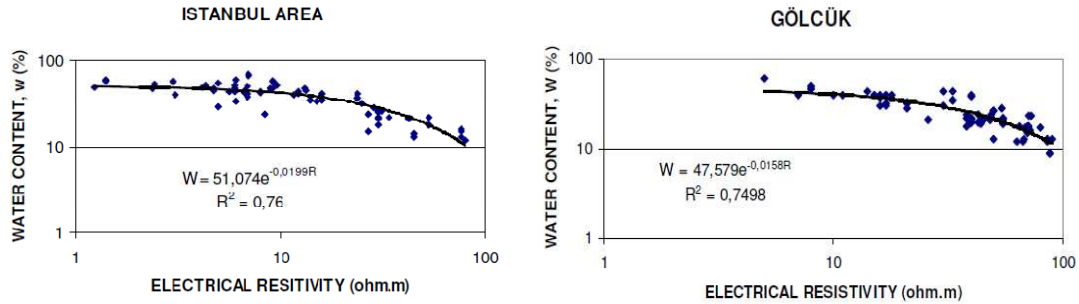
Figure 2.25: Relationship between Electrical Resistivity and Water content at two Sites in Turkey (Ozcep et al., 2003)

Schwartz et al., (2008) conducted a study to quantify field scale soil moisture content using electrical resistivity imaging method. The investigated site was located at Virginia Tech Kentland experimental farm, Mongomery County, Virginia. Electrical Resistivity Imaging (ERI) and Time Domain Reflectometry (TDR) were used simultaneously to obtain resistivity and moisture content. 2D ERI profiles were converted in to 2D soil moisture profile incorporating physical and chemical properties of soil. Archie's law was numerically optimized to determine moisture content from ERI at site specific condition. According to the authors, extractable cations can be used as a proxy for pore water resistivity to develop Archie's law. This methodology eliminated difficulties in measuring extracted pore water resistivity. Authors indicated that model (based on Archie's law) could be used to quantify 2D soil moisture content profile using 2D ERI profiles in a site specific condition. It was also observed that the model produced useful results to determine heterogeneities of moisture in meter scale. However, the model was not capable to resolve small scale heterogeneities in soil moisture. Moreover, depending on the site, different extractable cations might be required to calibrate Archie's law to get appropriate results.

Brunet et al. (2009) conducted research to obtain water deficit from Electrical Resistivity Tomography (ERT). The study area was Southern Cevennes, France. More than 10 ERT were conducted between February 2006 and December 2007. Time Domain Refletometry (TDR) measurements of water content were made along three vertical profiles at different depths as presented in Figure 2.26.

33
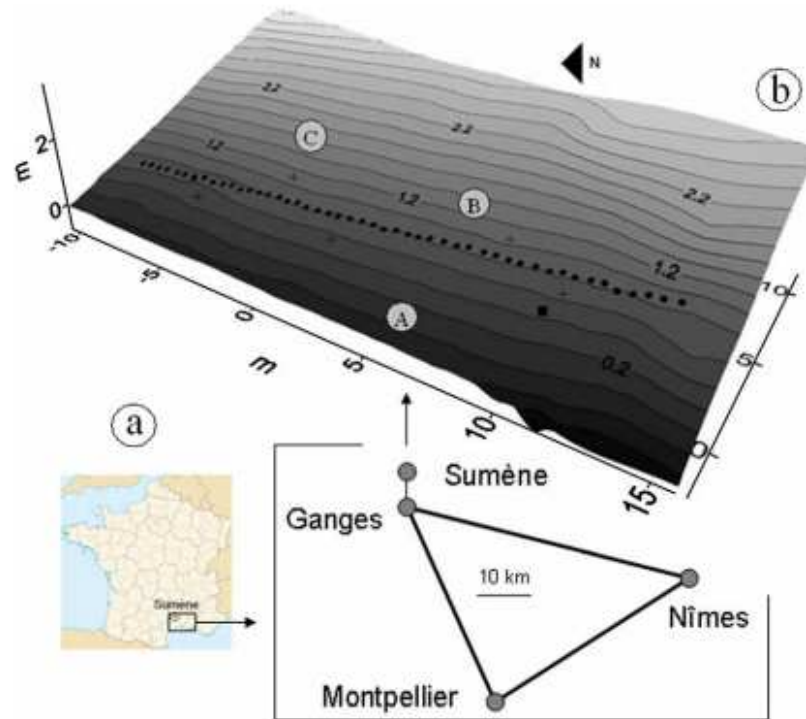
Figure 2.26: In the schematic-(a) Study area (b) Experimental field site, A.TDR tubes, ■ Rain gauge ● Electrode (Brunet et al., 2009)

TDR profiles were located within 5m of ERT profiles. Archie's law was calibrated in the laboratory using cementation coefficient (m) of 1.25 and coefficient of saturation (n) of 1.65. Constant porosity of 0.42 and resistivity of soil solution of 22 Ohm-m was also assumed in the calibration. In situ soil water content and water deficit were calculated from the calibrated Archie's law at 25^0C temperature. The variation of ERT and TDR measurements were within 15%. Authors indicated that interpretation of water content or water deficit was highly sensitive to the porosity.

2.6.6 Soil Strength

Determination of soil strength is required in most of the geotechnical engineering aspects. Traditionally Standard Penetration Test (SPT) and Cone Penetration Test (CPT) are widely used in the field for determination of soil strength. However, accurate assessment of strength may require laboratory testing. Several researchers have been trying to determine soil strength from resistivity.

Sudha et al., (2008) performed site characterization using Electrical Resistivity Tomography (ERT), Standard penetration test (SPT) and Dynamic Cone Penetration Test (DCPT). The study locations were Aligarh and Jhansi in Uttar Pradesh, India. Electrical Resistivity Imaging (ERI) was conducted by Schlumberger-Wenner method with electrode spacing of 5 m. ERI of the two sites are presented in Figure 2.27.
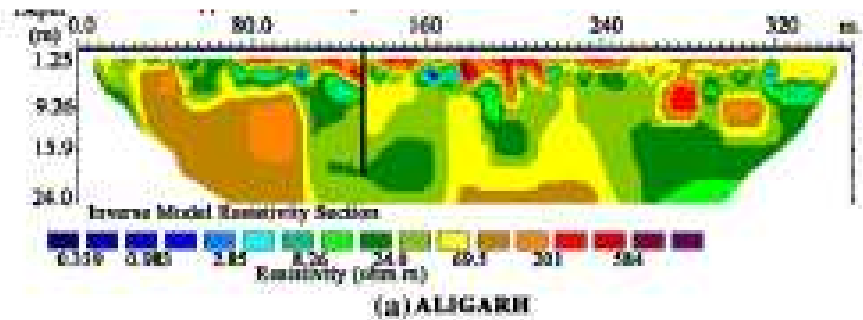
(a)
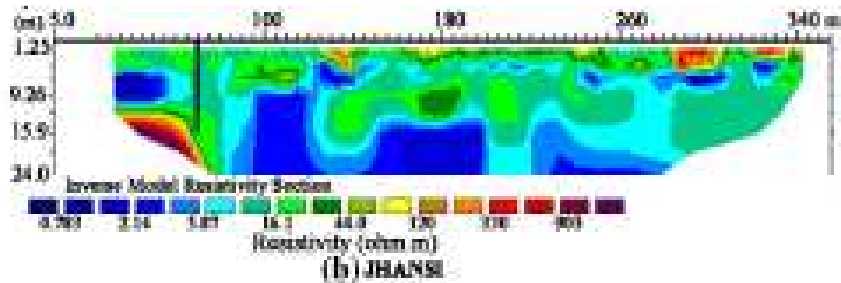
(b)

Figure 2.27: Resistivity Imaging of (a) Aligarh and (b) Jhansi (Sudha et al., 2008)

Resistivity image of Aligarh and Jhansi showed high resistivity near surface zone. High resistivity was characterized by presence of boulder near surface area. Low resistivity zone was reported due to existence of fine soils in Jhansi. Obtained SPT values were plotted with resistivity at the borehole location as shown in Figure 2.28.
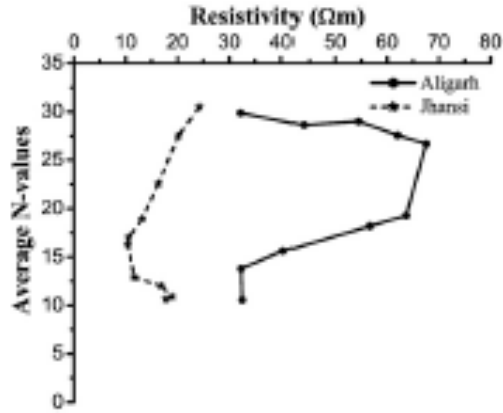
Figure 2.28: SPT value Vs Resistivity plot (Sudha et al., 2008)

Figure 2.28 showed no specific correlations between SPT and resistivity. However, linear correlation was observed when SPT values were plotted with transverse resistance as presented in Figure 2.29.

(a)   (b)
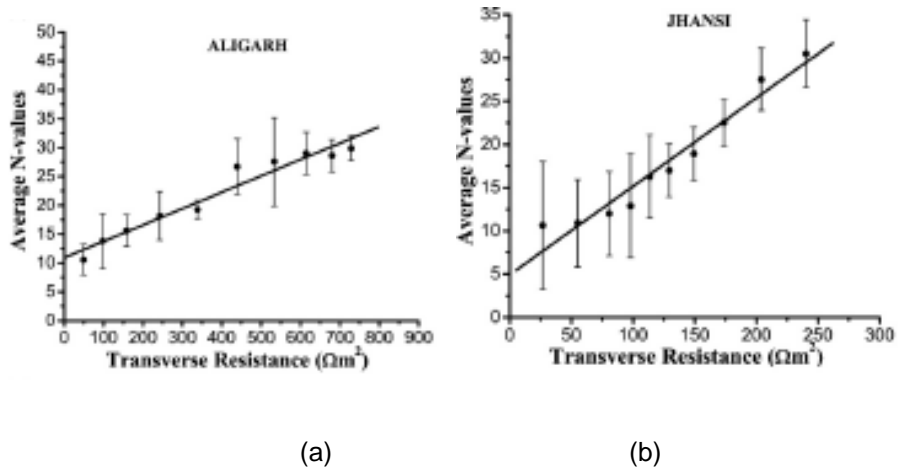
Figure 2.29: SPT Vs Transverse Resistivity of two Locations Aligarh
(b) Jhansi (Sudha et al., 2008)

The authors concluded that the correlation of SPT with transverse resistivity was site specific and solely dependent on the geologic environment of the study period.

Braga et al., (1999) conducted a study in the Rio Claro, Sao Paulo, Brazil. Total five sites were selected for Vertical Electrical Sounding (VES), DC resistivity and Standard Penetration

36

Tests (SPT). The local geology was characterized by Rio Claro formation, Corumbatai formation and intrusive basic rocks. The resistivity and chargeability values of the sites were varied significantly. Subsurface was divided into different layers such as low resistive clay, intermediate resistive silty clay and silty sand and high resistive sand. For upper two layers, SPT values varied from 3 to 8. Corresponding resistivity of the layers ranged from 336 to 26646 Ohm-m. SPT values were changed from 9 to 50 in the third layer. The resistivity of the third layer was in between 200 to 516 Ohm-m. SPT of Corumbatai residual soil was varied from 3 to 10 and corresponding resistivity ranged from 131 to 2900 Ohm-m. SPT and resistivity values were different in siltstone and siltstone fracture. For siltstone fracture, SPT ranged from 11 to 19 and resistivity varied from 79 to 219 Ohm. Siltstone was characterized by comparatively high SPT (N>19) and low resistivity (25 to 40 Ohm-m). According to the study, observed results could be used in the location having similar lithology for preliminary geotechnical investigation.

2.6.7 Hydraulic Conductivity

Hydraulic conductivity describes the ease of water flow through soil. It depends on porosity, structure, saturation and totuosity of soil. Electrical resistivity also depends on these parameters (Bryson, 2005). Several researches showed that hydraulic and electrical conductivity were correlated with each other.

Abu Hassainein et al., (1996) determined hydraulic conductivity from electrical resistivity. The objective was to evaluate the quality of compacted clay liner. Four soil samples were tested in three different compaction conditions. It was observed that hydraulic conductivity increased with the increase of resistivity. However, for soils C and D (CH and CL soil), hydraulic conductivity was independent of compactive effort. Test results are presented in Figure 2.30.
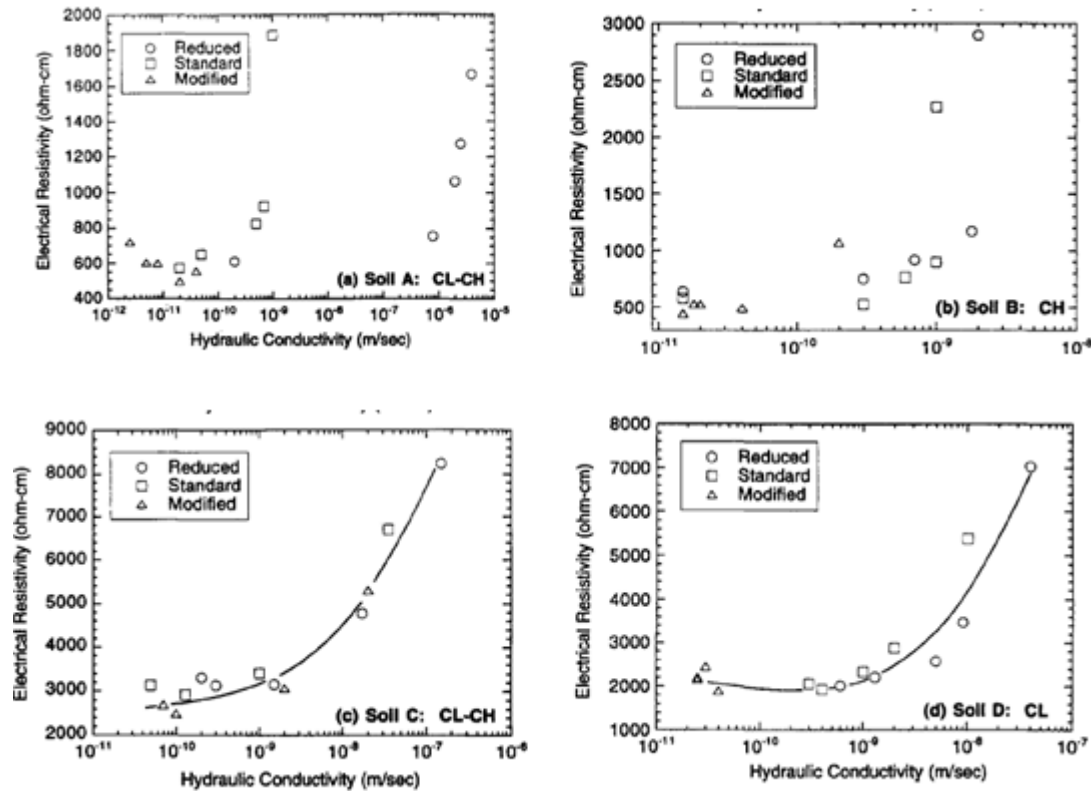
Figure 2.30: Relationship of Hydraulic Conductivity with Electrical resistivity in Different Soils (Abu Hassainein et al.,1996)

According to the authors, electrical resistivity measurement could not replace determination of hydraulic conductive of compacted clay.

2.7 Resistivity Measurement

Soil resistivity tests can be conducted either in the field or on the collected samples in laboratory. The resistivity test in laboratory is widely used in to identify corrosion potential and contamination of soil. However, field tests are conducted to investigate subsurface, environmental and hydrological condition. Resistivity imaging (RI) has the ability to provide a continuous image of subsurface.

2.7.1 Laboratory Measurement of Resistivity

In the laboratory, soil resistivity is conducted by measuring voltage drop across a known resistance which is in series connection with sample. The relationship between the resistance of

conductor having regular geometric shape and its resistivity is the basis of the laboratory mea-surement. In general case, two electrodes are placed in the end of cylinder and current (I) is measured under applied voltage (V). Sample resistance (R) is obtained from Ohm's law. Resis-tivity is determined incorporating the geometric factor such as length (L) of the sample and cross sectional area (A) by the following expression,

$$\rho = R.\frac{A}{L}$$

Here, current is carried predominantly by the movement of electrons in electrodes and ions in pore fluid of the sample. Therefore, charge is carried across interface by electrochemical reac-tion. If the contact resistance is higher than the resistance of the soil sample, then current cannot pass through the sample. Typical laboratory set up is presented in Figure 2.31.
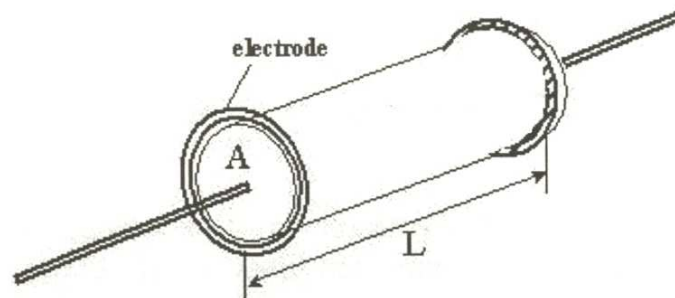
Figure 2.31: Laboratory Test Set up of Soil Resistivity

2.7.2 Field Measurement

Resistivity Imaging (RI) is conducted to get a continuous picture of complex subsurface. Spatial variation of subsoil over an area can be determined by RI. However, closely spaced grid points for electrodes are necessary for high resolution of the image. In field test, a number of electrodes are placed and cables are connected with the electrodes, measuring equipment and power source. Survey can be conducted by different arrays such as Shlumberger, Dipole Dipole, Pole Pole, Pole Dipole and Wenner array. The resolution of the image can be different for varied array method in a site. Observed variations are mainly due to geologic structure, heterogeneity of

subsurface and sensitivity of the method, electromagnetic coupling and noise (Aizebeokhal, 2010). Basic principles of different methods are presented in the following subsections.

2.7.2.1 Schlumberger Array

Schlumberger array was first used in 1920. The current electrodes are placed symmetrically with voltage electrodes in this method as shown in Figure 2.32.
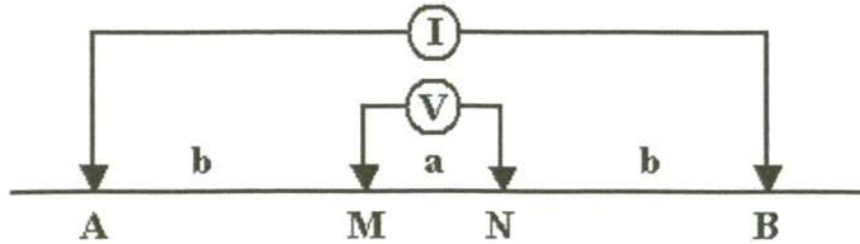
Figure 2.32: Electrodes Set up in Schlumberger Array

Here, voltage electrode spacing is kept small and current electrode spacing is changed. Apparent resistivity is calculated from the following equation

$$\rho = \frac{V \Pi b (b + a)}{I a}$$

2.7.2.2 Dipole Dipole

Dipole Dipole array is the most convenient method in the field condition. Moreover, this method provides good results when large spacing is required. Here, current and voltage electrodes are placed in same spacing "a". The spacing in between them is an integer multiple of "a". Electrode positions are presented in Figure 2.33.
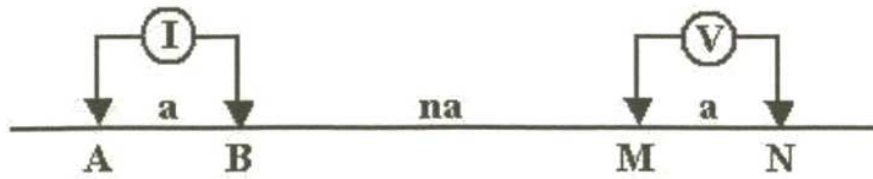
Figure 2.33: Electrodes Set up in Dipole Dipole Array

Apparent resistivity in Dipole Dipole method is given by the following equation

$$\rho = \frac{V \Pi ban(n+1)(n+2)}{I}$$

2.7.2.3 Pole Pole

It is one of the most simplest array. Current and voltage electrodes are placed far away so that they can be considered as infinity. It is recommended to put the electrodes at practical distance. Pole Pole method can be used to conduct survey in a small area. Apparent resistivity is calculated by the following equation

$$\rho = \frac{V 2 \Pi a}{I}$$

Electrode configuration of Pole Pole array is shown in Figure 2.34.
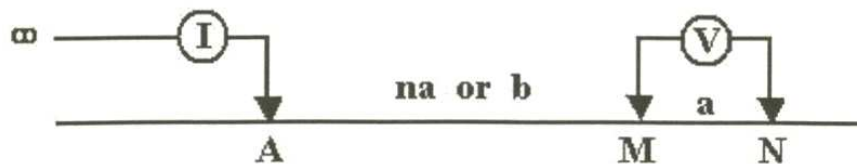
Figure 2.34: Electrodes Set up in Pole Pole Array

2.7.2.4 Pole Dipole

This method is frequently used for electrical resistivity survey. One of the current electrodes are placed at infinite distance in Pole Dipole array. If the spacing of voltage electrodes is

41

"a", then current electrodes are placed at distance "na" or b. The equation of apparent resistivity is either

$$\rho = \frac{V \Pi b (b + a)}{Ia} \quad or$$

$$\rho = \frac{V 2 \Pi n a (n + 1)}{I}$$

Schematic of Pole Dipole configuration is presented in Figure 2.35.
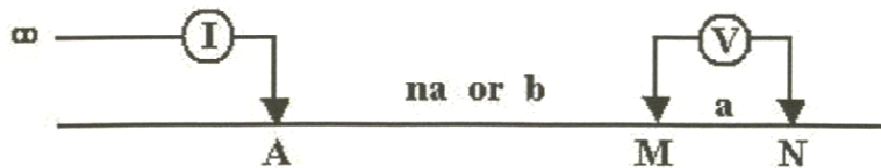
Figure 2.35: Electrodes Set up in Pole Dipole Array

2.7.2.5 Wenner

In Wenner array, current and voltage electrodes are placed symmetrically in same spacing as presented in Figure 2.36.
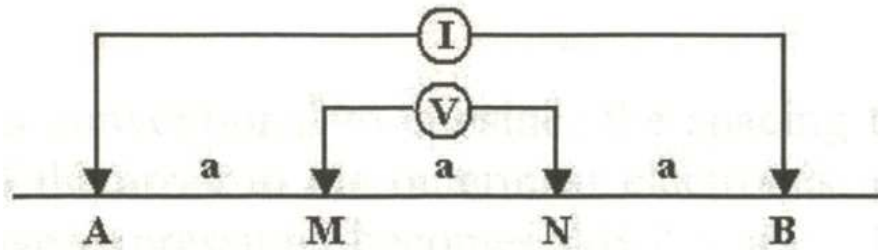
Figure 2.36: Electrodes Set up in Wenner Array

Apparent resistivity is calculated by the following equation

$$\rho = \frac{2 \Pi a V}{I}$$

CHAPTER 3

METHODOLOGY

3.1 Introduction

The objective of this study is to determine the relationship between geotechnical proper-ties of clayey soil with electrical resistivity. Soil samples were collected from the slope at highway US 287 and US 67. Laboratory testing on the collected samples were conducted to determine soil type, Index properties, optimum dry unit weight and moisture content and unconfined strength. Electrical resistivity was also measured in the laboratory to determine the correlation of geotech-nical properties with the soil resistivity. Moreover, high energy X-Ray fluorescence (XRF) and scanning electronic microscopic (SEM) tests were conducted to determine the percentage of dif-ferent ions present and to analyze fabric structure and pore space of the samples.

3.2 Sample Collection

Soil samples were collected from two sites of Midlothian, Ellis County, Texas. The sites were located along slopes of highway US 287 and US 67. Three soil test borings were conducted on each site. The locations of the sites are presented in Figure 3.1 and 3.2.

Figure 3.1: Location of Highway US 67

Figure 3.2: Location of Highway US 287

Soil test borings were conducted using truck mounted rig. The depth of test borings were ranged from 25 to 45 ft. Samples were collected at every 5 ft in each borehole. However, a total of six soil samples were selected to determine geotechnical and electrical properties in this study. Five of the samples were taken from US 287 location and one sample was taken from US 67 location. Boring operation and sample collection are presented in Figure 3.3.

(a)   (b)

(c)

Figure 3.3: Boring Operation and Sample Collection (a) Truck Mounted Rig (b) Boring Operation (c) Sample Collection

3.3 Test Methodology

An extensive laboratory experimental program was undertaken to achieve the objectives of the study. The collected soil samples were classified according to the Unified Soil Classification System (USCS) using sieve analysis, liquid limits and plastic limits test results. Moreover, ion composition of the soil samples and fabric structures were analyzed by XRF and SEM. After that, soil resistivity of the samples was determined at different condition. Summary of laboratory tests to identify geotechnical properties is presented in Table 3.1.

Table 3.1: Laboratory Tests for Geotechnical Properties of Soil Samples

Type of Test	Sample Location	No of Test
Sieve Analysis	US 287 and US 67	6
Liquid Limit	US 287 and US 67	6
Plastic Limits	US 287 and US 67	6
XRF	US 287 and US 67	6
SEM	US 287 and US 67	5
Compaction	US 287 and US 67	28
UCS	US 287 and US 67	29

The primary objective of the study was to investigate the resistivity response of soils for different geotechnical parameters. To achieve the objectives, resistivity tests were conducted for different conditions as presented in Table 3.2.

Table 3.2: Summary of Soil Resistivity Tests for Different Conditions

Soil Resistivity			
Fixed Parameters	Variable Parameters	Specimen Location	No of Tests
Moisture Content	Dry Unit Weight	US 287	20
Dry Unit Weight	Moisture Content	US 287	59
Compaction Level	Moisture Content and Dry Unit Weight	US 287 and US 67	29
Moisture Content and Dry Unit Weight	Fine Content and Atter-berg Limits	US 287 and US 67	5

46

3.3.1 Sieve Analysis

Particle size distribution is one of the most important characteristics of soil in engineering implications. This property indicates how the soil would interact with water. Moreover, plasticity, permeability and electric conductivity, consolidation, shear strength and chemical diffusion are dependent on particle size distribution. In this study, sieve analyses were conducted on the collected samples in the laboratory according to ASTM standard D422.

Sieve analysis was carried out using 65 gm of air dried samples to determine the particle size distribution Aggregation of the particles was broken by mortar and rubber covered pestle. The grain size distribution was conducted using a set of US standard sieves (No. 4, 10, 20, 40, 60, 100, 200 and pan). A lid was also placed at the top to provide cover of the sample. Weight of each sieve was determined before staking. Stack of sieves were shaken by mechanical sieve shaker. After 5 min the stack of sieves were removed. Combined weight of each sieve and sample was measured. Wet washing was conducted to prevent aggregation of large clumps of fine particles in soil samples retained on sieve No. 200. A bowl was placed under the sieve. Washing of sample was continued until clean water was coming out. Remaining sample was dried in the oven and weight was measured. Figure 3.4 showed the stake of sieves used in sieve analysis in geotechnical engineering laboratory of the UTA.

Figure 3.4: Stake of Sieves

3.3.2 Liquid limit and Plastic limit

To obtain Liquid limit and Plastic limit of the soil samples, ASTM standard D4318 method - A was adopted. Soil Samples passing through No. 40 sieve were used in the test. Moisture cans were labeled and their individual mass was recorded. Casagrande Liquid limit device and the grooving tool was cleaned as well as fall height (1 cm) of the cup was adjusted. Appropriately, 250 gm soil samples were taken in a bowl and mixed with water. Water content of 25% was considered in the first trial. After addition of water, the soil sample was chopped, stirred and kneaded repeatedly. A portion of the soil was placed in the device. A groove was cut at the center of the placed soil in the device. The cup of the device was lifted and dropped by a rate of 2 drops/second. The process was continued until the groove was closed around 13 mm. The test was repeated for three times to plot no of blow against moisture content. Liquid limit was the moisture content corresponding to 25 blows on the straight line. Followed procedure of liquid limit tests are presented in Figure3.5.
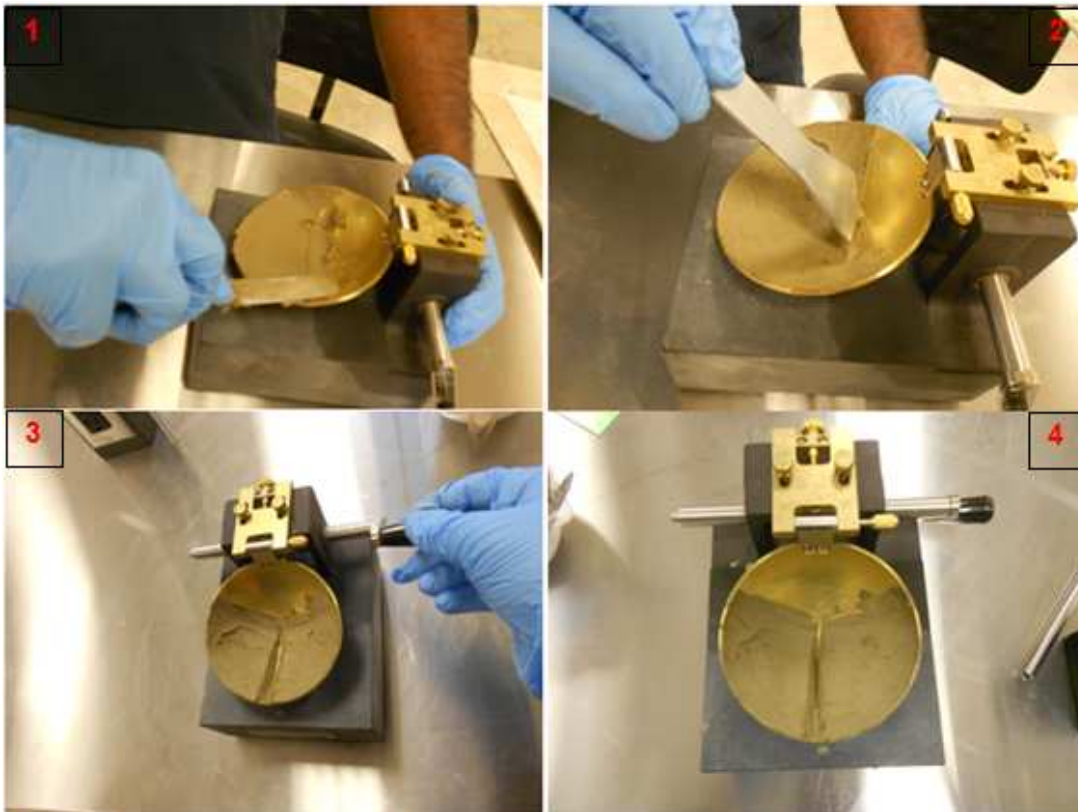
Figure 3.5: Step by Step Procedures followed in Liquid Limit Test

For Plastic limit, soil samples were separated in the plate. Ellipsoidal soil masses were formed by adding water. Soil masses were rolled in the glass plate until they became threads of about 3 mm. When the threads were broken at 3 mm diameter, they were taken in the moisture cans. Samples were dried in the oven and moisture contents were determined. Figure 3.6 shows two soil threads, one of which reached Plastic limit and another did not.

Figure 3.6: Plastic Limit Test

3.3.3 Energy Dispersive X-Ray Fluorescent

High energy dispersive X-Ray fluorescent was utilized to determine the percentage of cations present in the soil samples. When an X-Ray photon of sufficient energy strikes an atom, electron from that atom is dislodged. An electron from higher electron shell goes the lower shell to fill the vacant place. The electron that fills the void, loses some energy. As the electron drops to the lower state of energy, excess energy is emitted as X-Ray (Kaiser and Wright, 2008). The energy level is different for different element. Therefore, energy of X-Ray fluorescence peak can be correlated for a distinct element. High peaks are associated with the presence of high percentage of ions of an element. The working principle of XRF is presented in Figure 3.7.
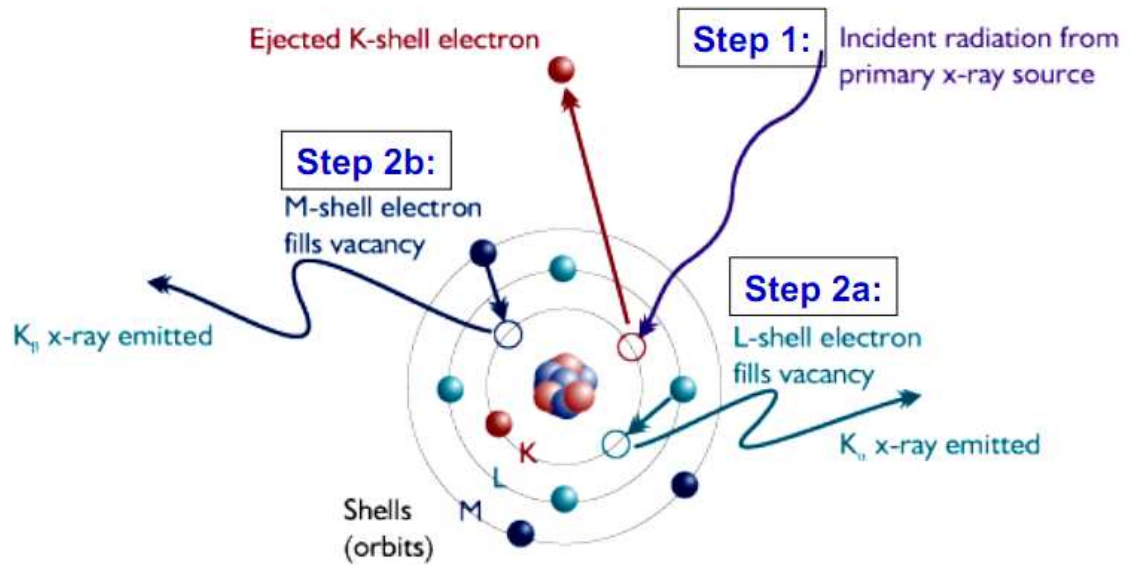
Figure 3.7: Working principle of XRF (http://www.nmai.si.edu)

Soil samples were oven dried, pulverized and pressed at 20 tons before XRF tests. Pressed pellets were analyzed by Bruker TRACER III-V handheld ED-XRF unit. Analyses were focused only to determine the percentage of cations. Samples were calibrated by using a suite of 91-mud rock reference material. The schematic of typical XRF test samples and handheld equipment are presented in Figure 3.8.

(a)   (b)

Figure 3.8: XRF test (a) Samples (b) Equipment (http://www.bruker-axs.com)

3.3.4 Scanning Electron Microscope

Scanning Electron Microscope (SEM) was utilized to observe clay structure and analyze pore space of five different samples. Scanned images of the soil samples were obtained in the magnification range of 1000 to 15000 times. In SEM, images are produced by scanning the sample with high energy beam of electrons. The electrons interact with the inherent electrons of the atoms. Due to this interaction, atoms of the samples produce signals. These signals contain information about the surface topography, composition and other properties. The SEM used in the study is presented in Figure 3.9.

Figure 3.9: Scanning Electron Microscope

Dry soil samples were used in the tests. A coating of silver was provided in each sample before testing. The objective of coating was to ensure a conductive media for electron beam of SEM. Soil samples were placed on the base plate. Then, sputtering system was utilized for application of vacuum and coating of silver on the samples. When silver coating on the samples were completed then they were put in the SEM. Images at different magnification and different particles were captured. Figure 3.10, 3.11, 3.12 show different steps of SEM imaging.

Figure 3.10: Sputtering Equipment

Figure 3.11: Samples before and after Silvering
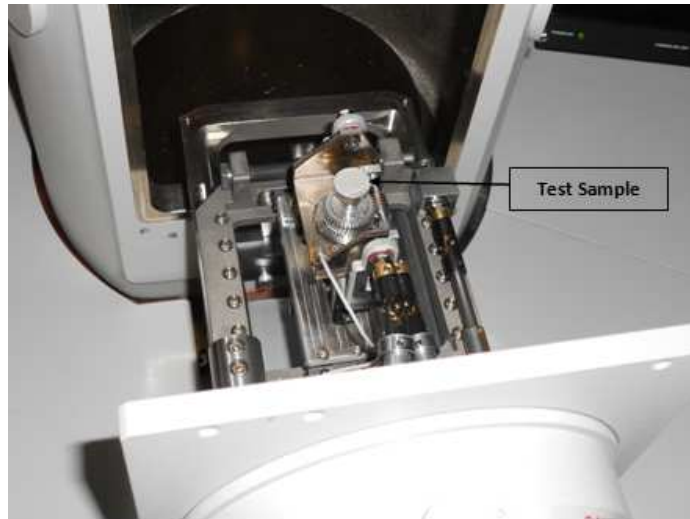
Figure 3.12: Placement of Prepared Sample in SEM

Scanning electron images were analyzed by Adobe Photoshop to differentiate between pore space and solid soil particle. Total area and pore area of the soil samples were determined by AutoCAD software.

3.3.5 Compaction

Compaction tests on the soil samples were conducted to observe soil resistivity at different compaction conditions. ASTM standard D698 procedure was followed for the test. Approximately, 3000 gm soil sample passing through No. 40 sieve was taken for each test. Required amount of water was added to produce five different compaction samples. Water was mixed thoroughly with the soil samples. Compaction mold and collar was placed appropriately. Inside of the mold, grease was applied to create a smooth surface. The weight of the mold was determined before compaction. The soil was compacted at three different layers with 25 blows at each layer. After completion of each layer, soil was grooved to ensure proper bonding between successive layers. The collar of the mold was took out and extra soil above the collar was removed. Mass of mold with soil was measured. A small piece of sample was brought from compacted soil for determination of moisture content. The process was repeated for five times to produce a compaction curve. The schematic of compaction is presented in Figure 3.13.

Figure 3.13: Standard Proctor Compaction Test

3.3.6 Unconfined Compression Test

The objective of unconfined compression tests were to identify relation between cohesive strength and resistivity of soil. Unconfined compression test was conducted according to ASTM standard D2166. Soil samples were prepared at same water content and unit weight of Standard Proctor compaction. The height and diameter of each specimen were 5.6 inches and 2.8 inches. The specimen was placed in the triaxial frame. The top platen was moved close to the top of the specimen. Initial readings of load cell and LVDT were recorded. Tests were conducted at strain rate of 1.27 mm/min. Sample was assumed to be failed when load displacement curve reached at peak and then dropped. However, tests were continued for sometimes after peak to ensure failure. Figure 3.14 shows the unconfined compression test cell and sample after failure.

(a)	(b)
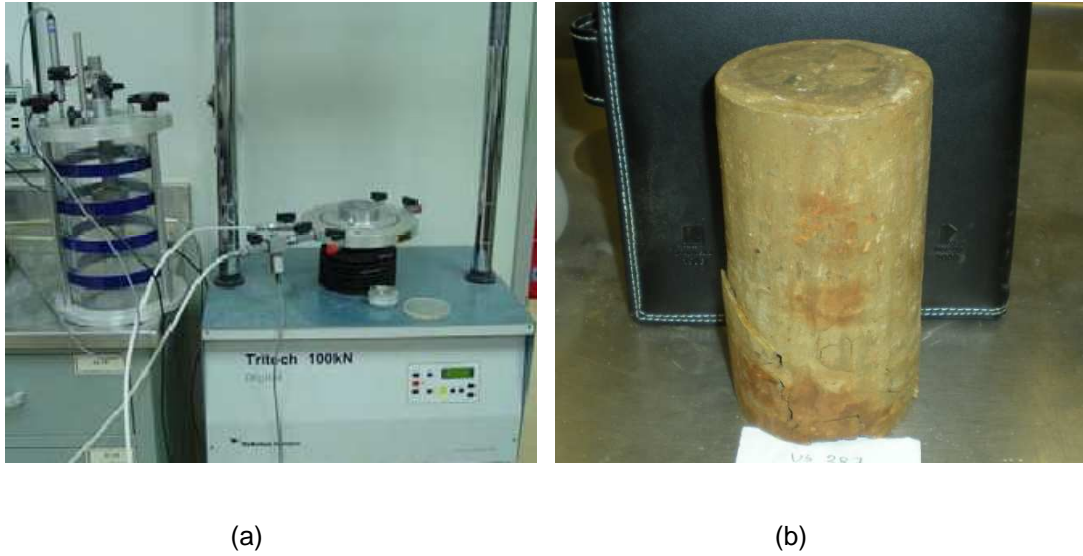
Figure 3.14: Unconfined Compression Test (a) Triaxial Set up (b) Schematic of Failed Sample

3.3.7 Calibration for Soil Resistivity

The calibration factor was determined before measurement of soil resistivity. To obtain calibration factor, resistivity of tap water was measured by Super Sting IP equipment (41.09 Ohm-m). Then conductivity of tap water was measured by bench top conductivity meter. Resistivity of tap water was calculated from the observed conductivity (346 micro-simens/cm). Calibration factor was determined by dividing the measured resistance from bench top conductivity meter with Super Sting IP. Determination of tap water conductivity by bench top conductivity meter is presented in Figure 3.15. A factor of 0.696 was obtained from calibration.

Figure 3.15: Measurement of Conductivity by Bench Top Conductivity Meter

3.3.8 Soil Resistivity

Soil resistivity of the collected samples were measured in the laboratory according to AASHTO T288-91. Soil sample was compacted in the resistivity box in a predetermined unit weight and moisture content. Two voltage electrodes were inserted in the soil sample through the holes in resistivity box. Cables were connected with current and the voltage electrodes. Then the box was connected with the Super Sting IP resistivity equipment. Electrical resistance of soil sample was recorded in manual mode of the equipment. Measured resistance was multiplied by calibration factor (0.696) and geometric dimension factor (1.01) to obtain resistivity of the sample. Step by step procedures of electrical resistivity measurement and Super Sting IP equipment are presented in Figure 3.16 and 3.17.

Figure 3.16: Resistivity Measurement

Figure 3.17: Super Sting IP Equipment

Soil resistivity tests were conducted at different conditions such as

- At fixed unit weight with different moisture content.

- At fixed moisture content with different unit weight.

- At unit weight and moisture content corresponding to Standard Proctor compaction.

- At fixed unit weight and moisture content.

Soil resistivity tests were conducted at fixed unit weight with different moisture condition. Moisture content was varied from 10% to 50%. Optimum dry unit weight was considered to calculate required weight of soil samples. The samples were compacted in the resistivity box after thorough mixing with moisture.

To obtain soil resistivity and unit weight correlation, dry unit weight was varied from 75 pcf to optimum in each sample. Test was repeated for three moisture conditions such as 18%, 24% and 30% in each sample. According to the dry unit weight, soil samples were weighed and compacted in the resistivity box at specific moisture content.

To identify the variation soil resistivity with compaction condition, six soil samples were utilized. The followed procedures can be summarized below

- Standard Proctor compaction test was conducted at different moisture contents and dry unit weights. From the test results, a compaction curve was generated for each sample.

- Unconfined compression strength was determined at moisture content and unit weight as that of Standard Proctor compaction.

- Soil resistivity was determined for the moisture condition and unit weight corresponding to Standard Proctor compaction.

- Therefore, soil resistivity was correlated with compaction condition and state of strength at that condition.

Soil resistivity tests were conducted at 85 pcf dry unit weight and 25% moisture to determine the effects of fine fraction, liquid limit, plastic limit on resistivity of the soil samples.

CHAPTER 4

RESULTS AND DISCUSSIONS

4.1 Introduction

Laboratory tests were conducted on the collected soil samples to determine the relation-ship between electrical resistivity and geotechnical properties. The purpose of this chapter is to present the results and analyses of the conducted laboratory tests.

The test results of sieve analyses, liquid limits, plastic limits, XRF, SEM, and variation of soil resistivity with various geotechnical properties are presented and discussed in the following subsections. Six soil samples are differentiated by site locations. Soil samples collected from highway US 287 and US 67 location are designated by "A" and "B". First letter in the designation is the location of the site, second letter and number are for borehole and third letter including the number denotes the depth of sample. The designation of the samples are presented in Table 4.1.

Table 4.1: Designation of the Samples

Designation of Soil sample	Location	Bore Hole	Depth (ft)
A-B2-D15	Highway US 287	2	15
A-B3-D10	Highway US 287	3	10
A-B3-D15	Highway US 287	3	15
A-B2-D20	Highway US 287	2	20
A-B3-D20	Highway US 287	3	20
B-B1-D15	Highway US 67	1	15

<u>4.2 Sieve Analysis</u>

Sieve Analysis on the collected soil samples showed that percent passing through No. 200 sieve was more than 82% for all the samples except A-B2-D20. Percent finer than No. 200 in soil sample A-B2-D20 was 66%. Particle size distribution obtained from sieve analysis of soil samples is shown in Figure 4.1. Calculation tables of sieve analyses are attached in Appendix A.
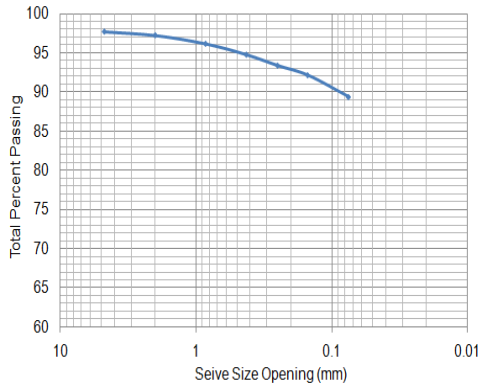
(a)
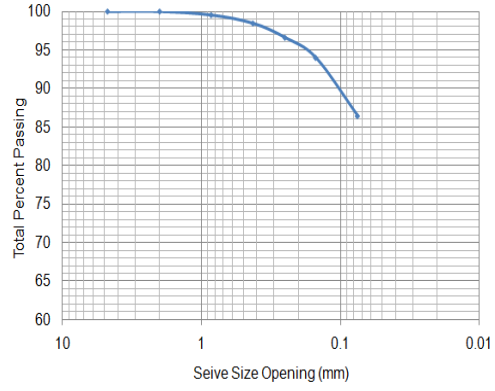
(b)
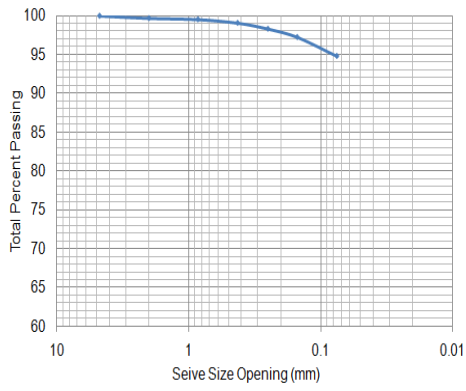
(b)
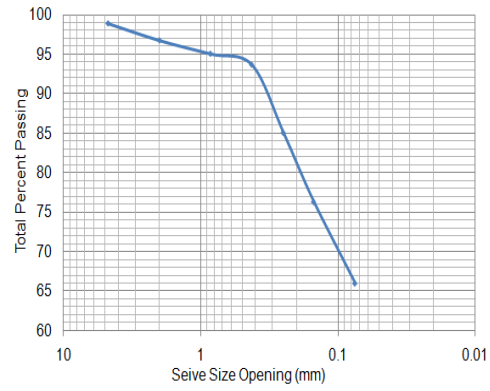
(d)
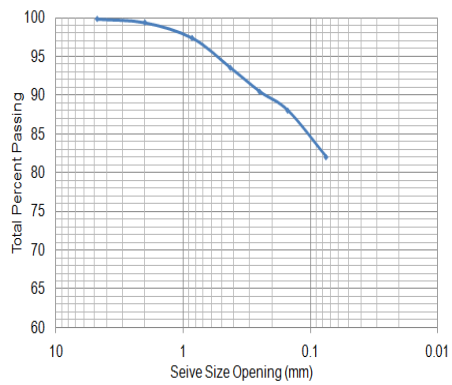
(e)
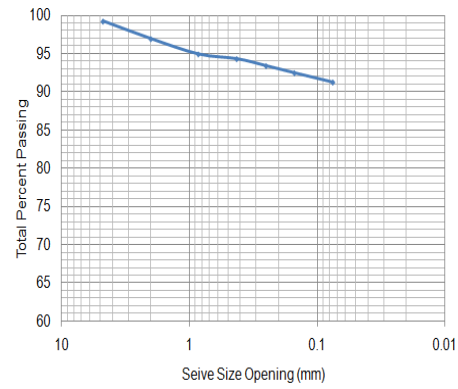
(f)

Figure 4.1: Particle Size Distibution of Soil Samples (a) A-B2-D15 (b) A-B3-D10 (c) A-B3-D15 (d) A-B2-D20 (e) A-B3-D20 (f) B-B1-D15

One of the objectives of the current study was to determine the relationship between fine fraction and soil resistivity. Therefore, percentage fine fraction in soil samples has specific importance in the current study. Fine content of the soil samples ranged from 66% to 94.78%. A summary of the fine fraction of collected soil samples is pesented in Table 4.2.

Table 4.2: Summary of Fine Fraction of the Soil Samples

Designation	Fine Fraction (%)
A-B2-D15	89.38
A-B3-D10	86.46
A-B3-D15	94.78
A-B2-D20	66
A-B3-D20	82
B-B1-D15	83.38

4.3 Liquid Limits and Plastic Limits

Liquid limits and plastic limits were determined for soil classification and identification their relationship with soil resistivity. Liquid limits of the soil samples ranged from 58 to 79. Observed plastic limits of the samples were in between 18 to 28. The liquid limit, plastic limit and plasticity index of the samples are presented in Table 4.3.

Table 4.3: Summary of Liquid limits, Plastic limits and Plasticity Index of the Soil Samples

Designation of Soil sample	Liquid Limit	Plastic Limit	Plasticity Index
A-B2-D15	73	28	45
A-B3-D10	61	27	34
A-B3-15	79	28	51
A-B2-D20	61	26	35
A-B3-D20	58	26	32
B-B1-D15	65	18	47

Figure 4.2 shows the liquid limits and plasticity index chart and the location of the data points.
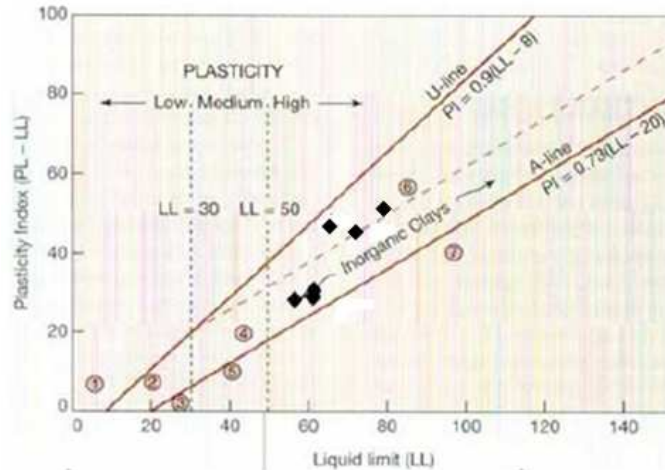
Figure 4.2: Location of the points in the Plasticity Chart

The soil samples are classified as highly plastic clay (CH) according to USCS from the laboratory investigation. Boring logs of the collected samples are attached in Appendix A.

In addition to soil classification, liquid limits and plastic limits can be used to determine the type of clay minerals. The correlations of clay minerals with liquid limits and plastic limits are presented in Table 4.4.

Table 4.4: Atterberg Limits of Different Clay Minerals (Mitchell and Soga, 2005)

Mineral	Liquid Limit (%)	Plastic Limit (%)
Montmorillonite	100-900	50-100
Illite	60-120	35-60
Kaolinite	30-110	25-40

Most of the samples used in the study were in the range of illite from the presented correlations (Table 4.4). Mitchell and Soga (2005) described the probable causes of variation of liquid limit and plastic limit in clay soils. Particle size, degree of crystallinity, adsorbed cations, presence of free electrolyte, and organic matter were reported as the contributing factors of variations.

Therefore, clay soil with similar mineralogy may provide different liquid limits and plastic limits due to the difference in degree of crystallinity and presence of organic matter and free electrolyte.

Liquid limits of clay soils are associated with the specific surface area. Clay soil with large surface area requires more water to reach the liquid limit (Mitchell and Soga, 2005). Specific surface area can be determined from liquid limit of soil sample with the following empirical equation.

$$LL=19+0.56A_s$$

where, As = Specific surface area in m^2/gm, LL= Liquid limit of the sample.

Calculated specific surface areas of the samples are presented in the Table 4.5.

Table 4.5: Specific Surface Area of the Samples

Samples	Liquid Limit	Specific Surface Area
A-B2-D15	73	96.4
A-B3-D10	61	75
A-B3-15	79	107.1
A-B2-D20	61	75
A-B3-D20	58	69.6
B-B1-D15	65	82.1

The ranges of specific surface area of kaolinite, montmorillonite and illite are about 10 to 20 m^2/gm, 50 to 120 m^2/gm and 65 to 100 m^2/gm (Mitchell and Soga, 2005). It should be noted that there are overlapping ranges of specific surface area for montmorillonite and illite. Thus, calculated specific surface areas indicated that further testing on ion composition and fabric structure are required to identify clay minerals.

4.4 X-Ray Fluorescence

The ionic compositions (weight percentage) of the samples were determined by high energy X-ray fluorescence (XRF). Tests were conducted to quantify the amount of cations. Typical anions in clay soil such as oxygen and hydrogen were not determined. Moreover, sodium ions

were not detected because the energy level of the equipment was below the level of detection. According to the test results, percentage of silicon and aluminum ions were high compare to other ions. Test results also showed that percentage of potassium ion was not significant (>2%). The amount of calcium ions ranged from 7% to 14%. It was observed that magnesium, manganese, sulphur, titanium and phosphorus were less than 1%. The XRF test results of the soil samples are presented in Table 4.6.

Table 4.6: Summary of Different Cations in Soil Samples

	A-B2-D15	A-B3-D10	A-B3-D15	A-B2-D20	A-B3-D20	B-B1-D15
	Percentage of Weight					
Mg	0.2	0.4	0.3	0.1	0.4	0.4
Al	6.1	5.5	6.0	6.0	5.6	7.5
Si	17.0	18.5	16.7	18.9	20.7	21.5
P	0.0	0.0	0.0	0.0	0.1	0.0
S	0.2	0.2	0.3	0.3	0.3	0.5
K	1.5	1.1	1.4	1.2	1.1	1.7
Ca	13.1	11.4	13.9	10.8	8.3	7.0
Ti	0.4	0.4	0.4	0.4	0.5	0.5
Mn	0.0	0.1	0.0	0.1	0.1	0.1
Fe	3.6	3.6	3.5	4.0	3.8	4.0

The schematics of different ions obtained from the tests are presented in Figure 4.3.
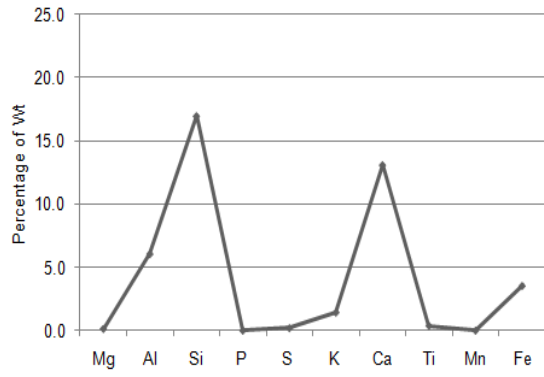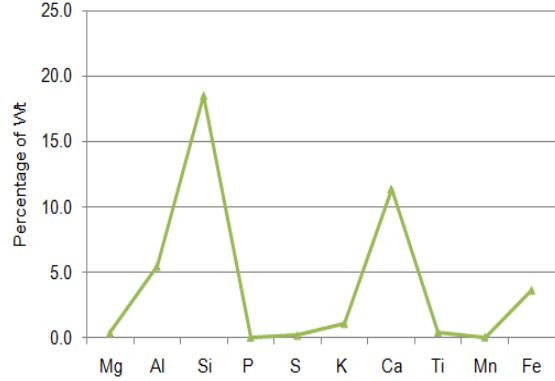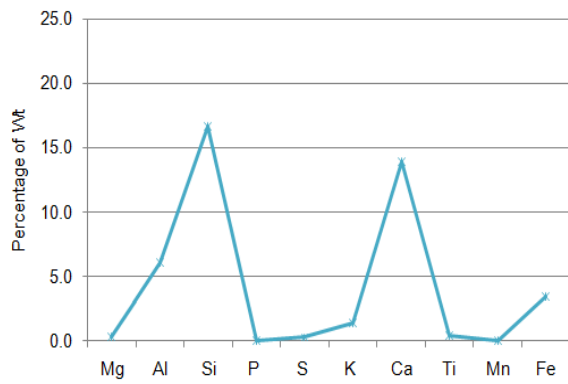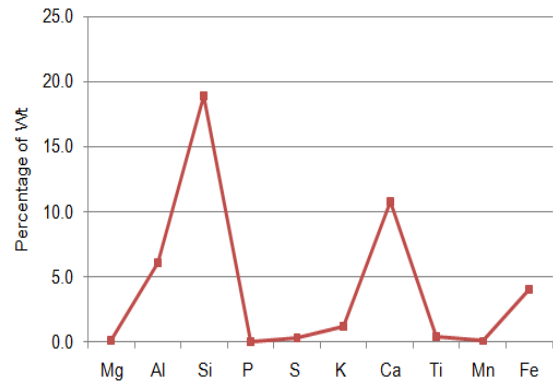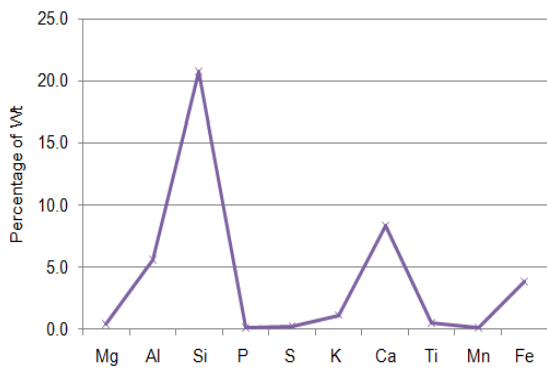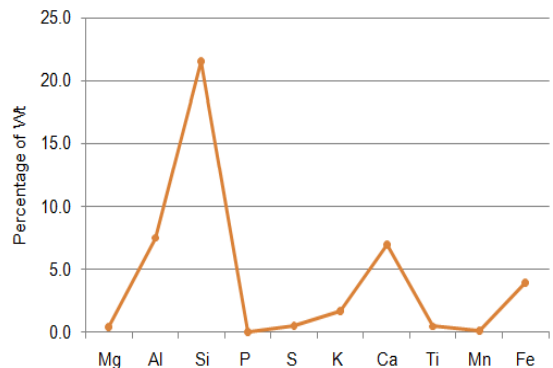
Figure 4.3: Cation Composition of Different Soil Samples (a) A-B2-D15 (b) A-B3-D10 (c) A-B3-D15 (d) A-B2-D20 (e) A-B3-D20 (f) B-B1-D15

Montmorillonite and illite both have 2:1 structure. One alumina sheet is sandwiched between two silica sheets. Alumina sheet is combined with the silica sheet by hydroxyl ion in montmorillonite. In illite, interlayers are bonded together by potassium ions. Therefore, percentage of potassium, ions should be high in illite. XRF test results showed that the percentage of potassium ions ranged from 1.1% to 1.7%. Moreover, the chemical formula of illite can be presented as $(K,H_3O)(Al,Mg,Fe)_2(Si,Al)_4O_{10}[(OH)_2,(H_2O)]$ (http://webmineral.com/data/Illite.shtml). Chemical formula shows that there is no calcium ion in the illite. However, high percentage of calcium ions was observed in the samples. In addition, the percentage of aluminum and silicon were expected to be high because they are basic elements in the clay structure.

According to the analysis of XRF test results, the samples were in the range of montmorillonite. The obtained results from XRF were in well agreement with the geological information of Ellis county provided by United States Geological Survey (USGS). According to USGS, geology of Ellis county consisted of Austin Chalk, Eagle ford shale, Ozan formation, Wolf city formation, Neylandville and Marlbrook Marls, alluvium and terrace deposits. Relative proportion of different formations in Ellis county are presented in Table 4.7.

Table 4.7: Geologic Units of Ellis County, Texas (http://tin.er.usgs.gov/geology/state/fips-unit.php?code=f48139)

Geologic Unit	Coverage Area
Austin Chalk	Approximately 35 %
Eagle Ford Formation	Approximately 11 %
Neylandville and Marlbrook Marls	Approximately 7.4 %
Ozan Formation	Approximately 25 %
Wolfe City Formation	Approximately 9.0 %
alluvium	Approximately 11 %
Terrace deposits	Approximately 1.2 %

Raney et al., (1987) conducted a study on the presence of clay minerals in different geologic units near Waco, TX. It was reported that Austin Chalk layer consisted of 94% montmorillonite and Neylandville Marl composed of 62% to 82% montmorillonite. The dominant clay mineral in Ozan formation was dioctahedral montmorillonite. Therefore, the dominant clay minerals in the soil samples might be montmorillonite.

<div align="center">4.5 Scanning Electron Microscope</div>

The magnified image of clay structure was obtained from Scanning Electron Microscope (SEM). The images were magnified up to 15000 times of original size. Tests were conducted on five samples, i.e. A-B3-D10, A-B3-15, A-B2-D20, A-B3-D20 and B-B1-D15. High resolution pictures of structure were captured when they were clearly viewed. Figure 4.4 shows SEM images of the samples.
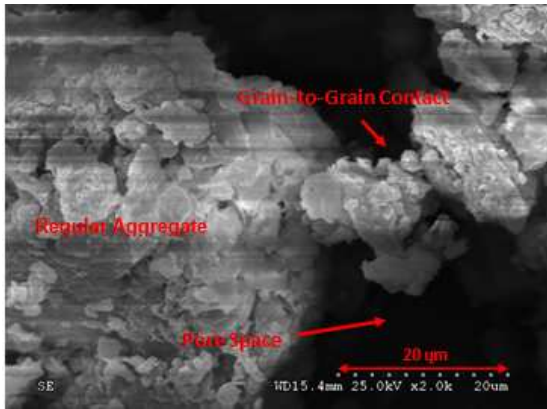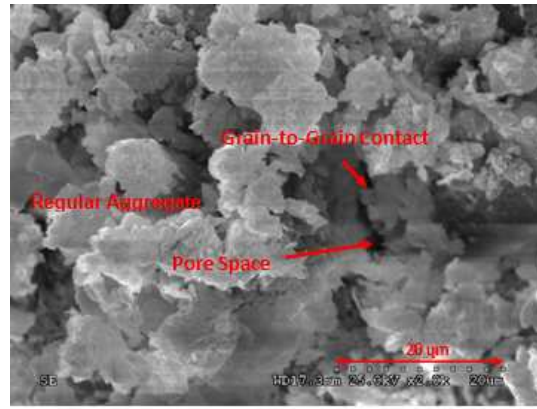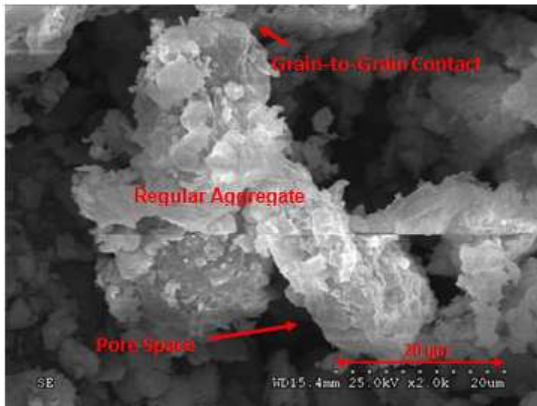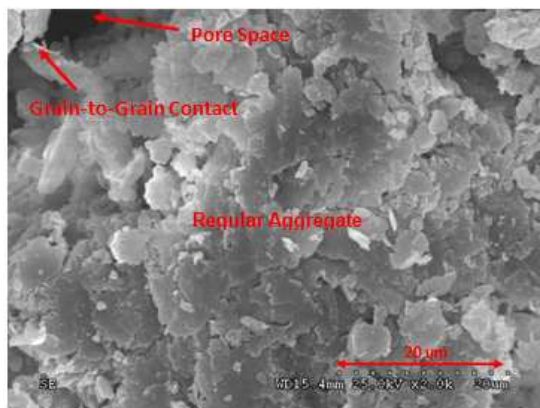
Figure 4.4: Scanning Electron Microscope Image of the Samples (a) A-B3-D10 (b) A-B3-D15 (c) A-B2-D20 (d) A-B3-D20 (e) B-B1-D15

Magnified images of sample A-B3-D20 are presented in Figure 4.5.
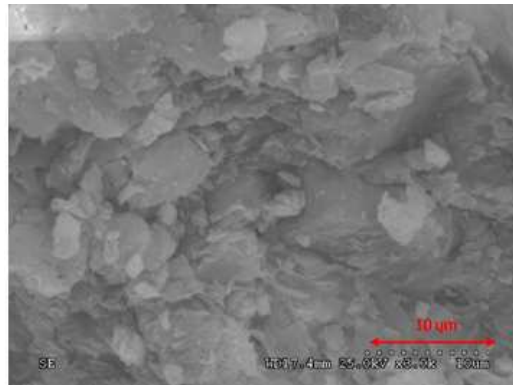
(a)
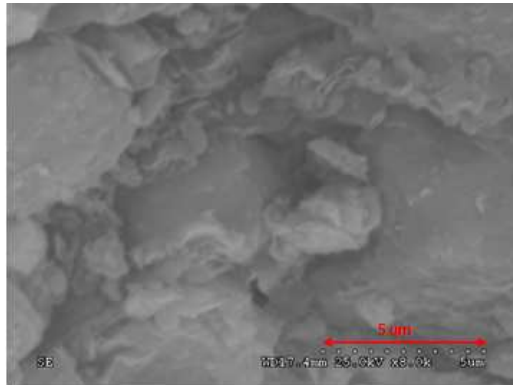
(b)
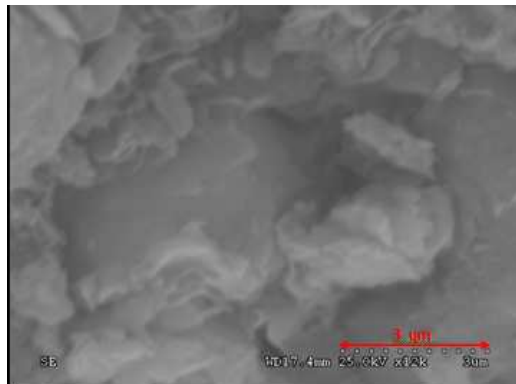
(c)

Figure 4.5: Magnified Image of Sample A-B3-D20 (a) 3000 times magnified (b) 8000 times magnified (c) 12000 times magnified

The SEM image of well crystallized particle of kaolinite look like six sided plate. Lateral dimensions of the plate are in the order of 0.1 to 0.4 micrometer and their thickness ranged from 0.05 to 2 micrometer (Mitchell and Soga, 2005). However, the hexagonal shape of poorly crystallized kaolinite is not distinct.

Montmorillionite looks like equidimensional flakes in scanning electron microscope. It appears like thin film (Mitchell and Soga, 2005). Montmorillonite appears as needle shaped when large amount of iron and magnesium substitute aluminum. Substitution of iron and magnesium cause directional strain in clay structure (Mitchell and Soga, 2005).

Illite is generally flaky particles. Well crystallized illite may consist hexagonal outline (Mitchell and Soga, 2005). Generally, illite consists of other clay and non clay material. Highly pure illite is rare.

The analysis on the SEM images of the sample showed that the fabrics were in horizontal layers when magnified by 2000 times. The horizontal layers might be attributed due to disturbance of the soil samples. Generally, aggregates of soil are aligned in horizontal layers under the application of load. According to Mitchell and Soga (2005) the main difficulties of SEM study is the preparation of surface replicas. Therefore, special attention is required to obtain undisturbed sample for SEM analysis. The authors also reported that the collapse of fabric under the application of load is possible to occur.

The presence of hexagonal shape or hexagonal outline was not observed in highly magnified images (Figure 4.5). Samples were appeared as flaky material at high magnification. Therefore, there is a good possibility of occurrence of montromorillonite in the samples. However, specific conclusions about the clay mineral might not be drawn only from SEM images because of the sample disturbance.

The analysis of previous study, XRF test results and SEM image indicated that montomorillonite might be the most dominant clay mineral of the soil samples.

Based on the SEM image representative percentage of pore space was determined from image analysis. The objective was to correlate the pore space with the electrical resistivity of soil. Percentage of pore space ranged from 1.91% to 39.01%. The analyses were conducted on the images magnified by 2000 times. The schematic of pore configurations is presented in Figure 4.6.

(a)   (b)

(c)   (d)

(e)
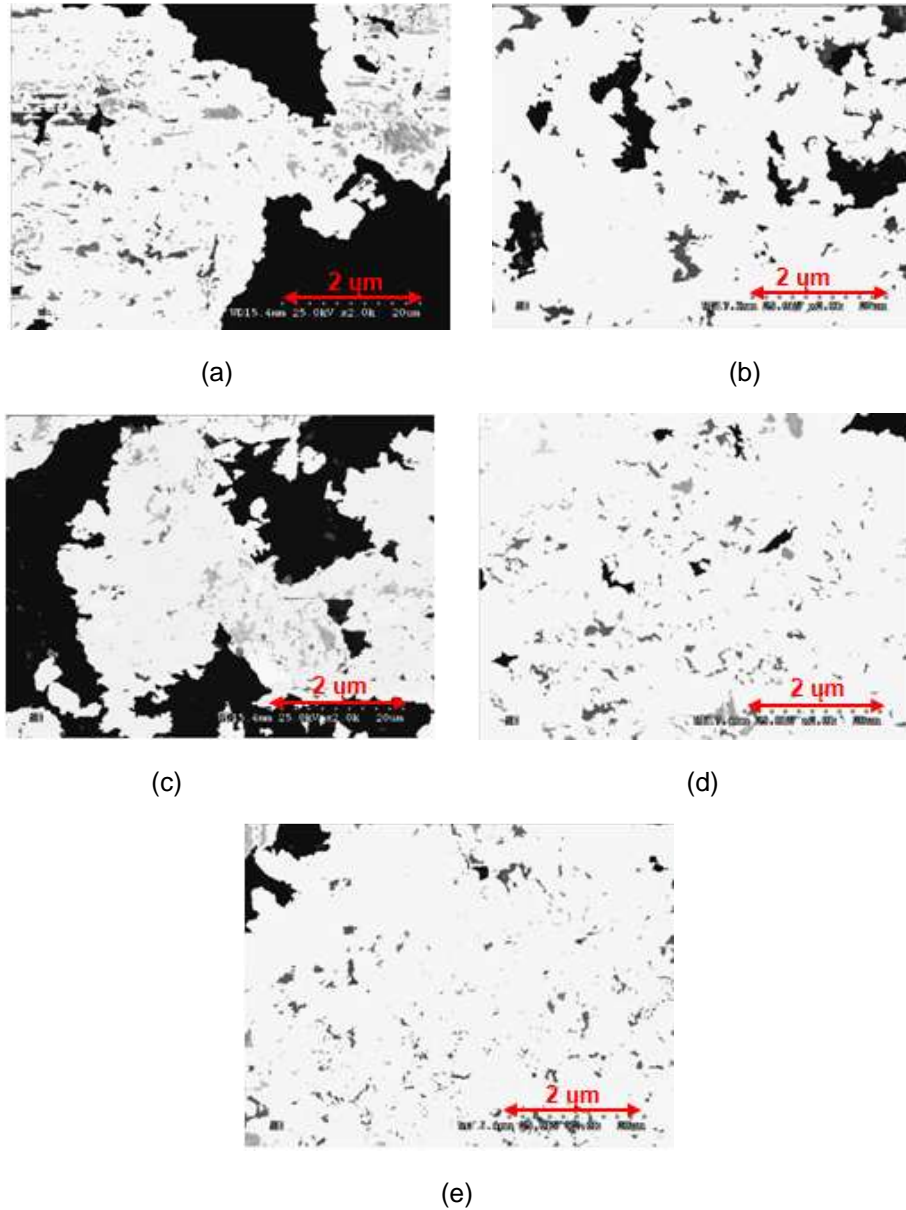
Figure 4.6: Pore Space Analysis of SEM Images (a) A-B3-D10 (b) A-B3-D15 (c) A-B2-D20 (d) A-B3-D20 (e) B-B1-D15 (Black portion is void and White portion is Soil)

Percentage of void in 2000 times magnified SEM image has been summarized in Table 4.8.

Table 4.8: Summary of Percentage of Pore Area in SEM Images

Designation of Sample	Percentage of Pore Area
A-B3-D10	27.39
A-B3-D15	10.56
A-B2-D20	39.01
A-B3-D20	1.91
B-B1-D15	2.45

4.6 Soil Resistivity

Sol resistivity tests were conducted at various moisture and unit weight condition to corre-late with different geotechnical parameters. The test results and discussions are presented in the following subsection.

4.6.1 Soil Resistivity with Moisture Content

One of the primary objectives of this study was to determine the variation of soil resistivity with gravimetric moisture content. To achieve this objective, soil resistivity tests were conducted at varied moisture content keeping the unit weight constant. Moisture contents were varied from 10% to 50% during tests. Soil samples were compacted at maximum dry unit weight in the soil resistivity box. Four samples were considered to determine the variation of resistivity with mois-ture content i.e. sample A-B2-D15, A-B3-D10, A-B3-D15 and A-B3-D20. It was observed that soil resistivity decreased almost linearly up to moisture content around 20% for all soil samples. The average rate of reduction in soil resistivity was 13.8 Ohm-m for the increase of moisture from 10% to 20%. Maximum variation was observed in soil sample A-B3-D10. Resistivity decreased from 21.1 Ohm-m to 3.3 Ohm-m for the increase of moisture content from 10% to 20% in sample A-B3-D10. Moreover, it was found that soil resistivity results were almost constant after 40% mois-ture content. The observed soil resistivity ranged from 2.1 to 2.42 ohm-m at 50% moisture con-

tent in the soil samples. The variations of resistivity with moisture content of soil samples are pre-sented in Figure 4.7. Calculation tables for resistivity measurement are attached in Appendix A.

(a)　　　　　　　　　　　　　　　　　　(b)

(c)　　　　　　　　　　　　　　　　　　(d)
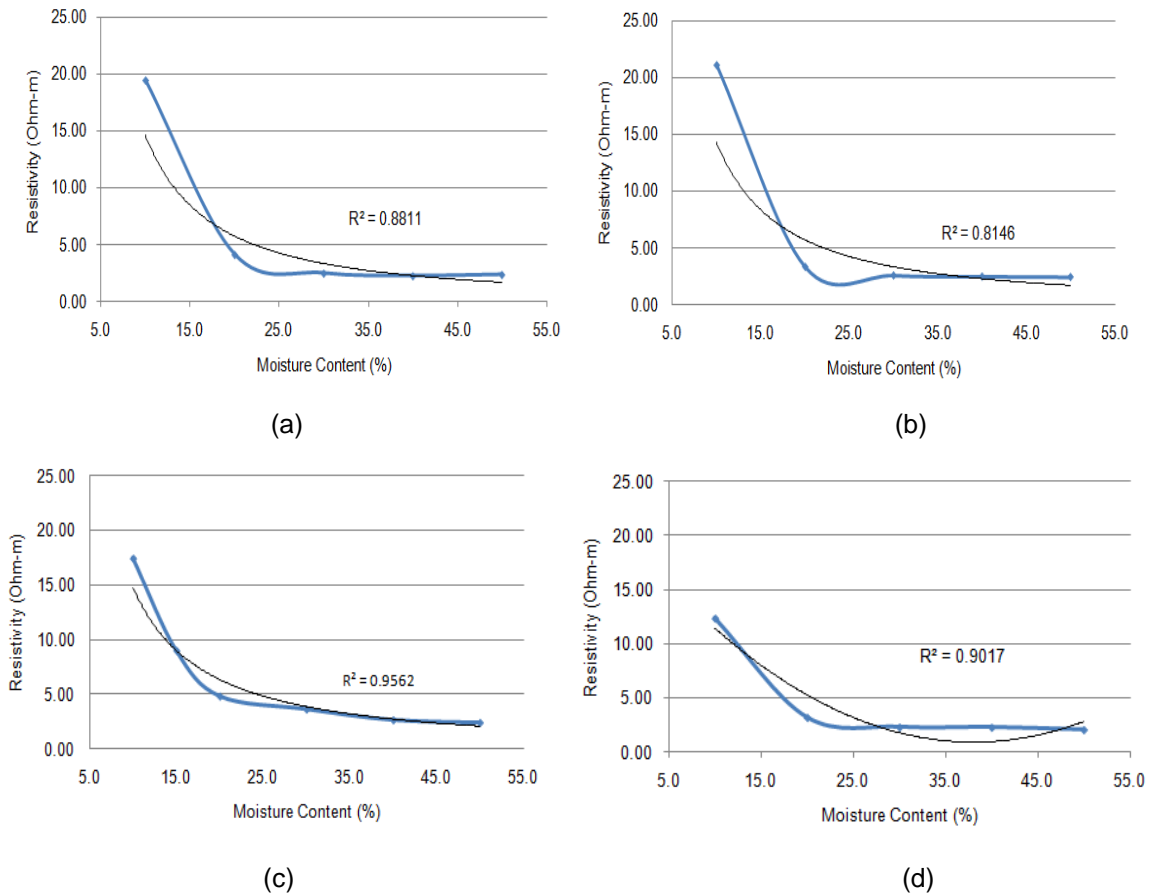
Figure 4.7: Variation of Soil Resistivity with Gravimetric Moisture Content (a) A-B2-D15 (b) A-B3-D10 (c) A-B3-D15 (d) A-B3-D20

　　　　Moreover, soil resistivity test was conducted in the dry state to identify the influence of surface charge of clay in the absence of moisture. It was observed that there was no flow of current through the soil in the dry state. Thus, test results indicated that soil samples behaved as a dielectric material in the absence of moisture.

　　　　Clay particle contains net negative charge due to isomorphous substitution and broken continuity of the structure (Das, 1983). They attract cations to balance the net negative charge. When water comes in to the clay soil, cations and anions float around the structure (Das, 1983).

Therefore, electrical conduction is enhanced in the presence of water in clay soil. As a result soil resistivity decreased with the increase of moisture content.

Pozdnyakov et al., (2006) described the interaction between soil and water under the application of electrical potential. Authors proposed that the mobility of electrical charge in soil is highly affected by water. Present electrical charge forms diffuse double layer in the surface of soil particle. When water is added from air dry to saturated condition, adsorbed charges are released in the solution. Therefore, mobility of electrical charges increases with the addition of water. Moreover, the mobility of charges is also affected by the mobility of hydroxyl (OH^-) and hydrogen ions (H^+) ions of water.

Water retained in the soil grain by the attraction of Van der Waals' force and molecular electrostatic force among water, solid molecules and solid surface (Pozdnynakov et al., 2006). At low moisture content water is attached to the soil surface by forming thin films. The dominant force is molecular attraction. At high water content, water retains in the soil by relatively weak capillary forces.

The pattern of change of soil resistivity with moisture content at fixed unit weight can be explained by Voronin (1986) molecular attraction concept. The variation curve of soil resistivity with water content is divided in to adsorbed, film, film-capillary, capillary and gravitational water zones in Voronin (1986) concept (Figure 2.8). Soil resistivity decreases abruptly with the increase of moisture from dry state in adsorption range. However, water molecules and solute in adsorption water zone are relatively immobile. The dipolar molecules of water create a conductive path that decreases resistivity rapidly. Soil resistivity decreased less significantly in the film water zone because presence of high Van der Waals' force. Van der Waals' and electrostatic force try to keep the water film stick to the soil grain. When a possible thickness of water film is achieved, water goes from film to fissure between the soil grains. In the capillary zone, combination of all molecular forces are very strong. Therefore, substantial reduction in soil resistivity does not occur in this zone. Soil resistivity curve is almost linear because the mobility of charges becomes inde-

75

pendent of moveable ions of water molecules in the gravitational water zone. The break point of different zones can be different, depending on the type of soils.

Figure 4.7 showed that initially soil resistivity decreased significantly up to 20% moisture content with an average rate of 13.8 Ohm-m/percent moisture content. Adsorption water zone might exist up to 20% moisture content in soil resistivity and moisture variation curve for the soil samples presented here. Soil resistivity varied from 2.1 to 2.4 Ohm-m after 40% moisture content. Therefore, beyond 40% moisture content gravitational water zone might exist. The existence of film water zone and capillary zone might be in between 20% to 40% moisture content in the soil resistivity and moisture variation curve.

4.6.2 Soil Resistivity with Unit Weight

To determine the correlation of soil resistivity with unit weight, resistivity tests were conducted at different dry unit weight condition while keeping gravimetric moisture content fixed. Tests were conducted on four soil samples i.e. sample A-B2-D15, A-B3-D10, A-B3-D15 and A-B3-D20. Moisture contents were varied from 18%, 24% and 30% in each soil sample. Dry unit weight for each sample was varied from 75 pcf to optimum for all soil samples. The variation of resistivity with unit weight at fixed moisture content of studied soil samples are presented in Figure 4.8, Figure 4.9 and Figure 4.10. It was found that soil resistivity decreased with the increase of unit weight for all soil samples. Soil resistivity decreased almost linearly with an average rate of 0.3 Ohm-m/pcf between moist unit weight 88.5 to 100 pcf at 18% moisture content. The changes in soil resistivity were significant up to moist unit weight of 100 pcf in soil samples A-B2-D15 and A-B3-D15 at 18% moisture content. Soil resistivity decreased from 14.2 to 7.7 Ohm-m for the increase of moist unit weight from 88.5 to 100 pcf in soil sample A-B3-D15 at 18% moisture content. The range of reduction in soil resistivity was from 10.7 to 6.6 Ohm-m in soil sample A-B2-D15 at similar condition. However, soil resistivity decreased with an average rate of 0.08 Ohm-m/pcf for further increase in moist unit weight in 18% moisture content. In addition, soil resistivity decreased from 5.7 Ohm-m to 3.2 Ohm-m at 24% moisture content with the increase of moist unit weight from 93 pcf to 117.7 pcf in an average. The average reduction in soil resistivity was 4.1 to

76

3 Ohm-m for the increase of moist unit weight from 97 to 122 pcf at 30% moisture content. There-fore, the variation in soil resistivity with unit weight was not substantial at high moisture content.
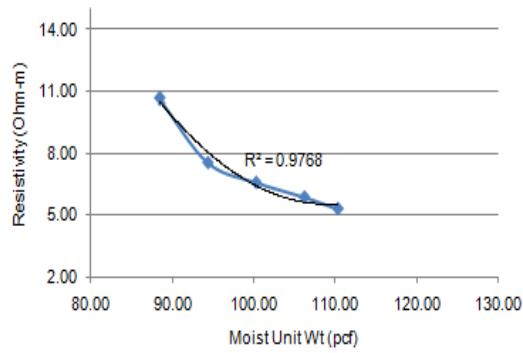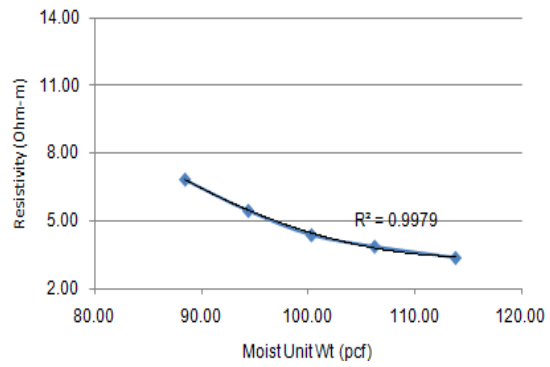
(a)   (b)
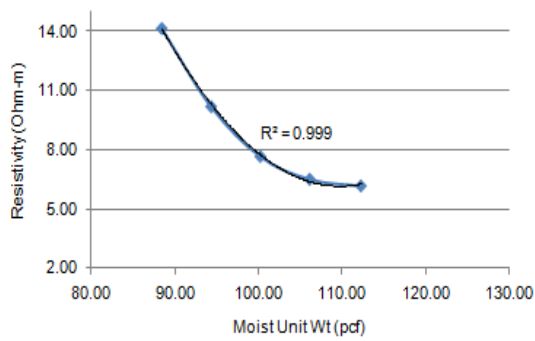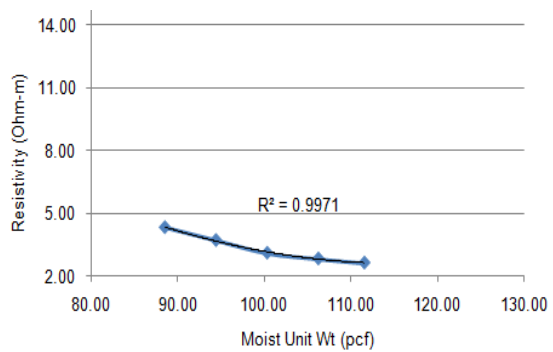
(c)   (d)

Figure 4.8: Variation of Resistivity with Moist Unit Weight at 18% Moisture Content (a) A-B2-D15 (b) A-B3-D10 (c) A-B3-D15 (d) A-B3-D20
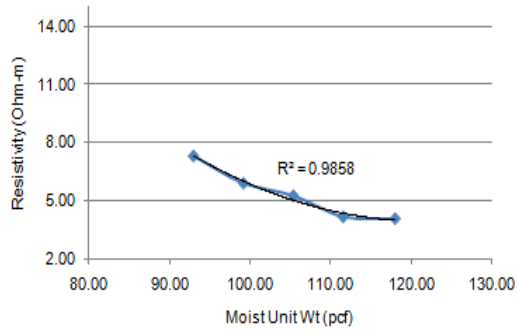
(a)
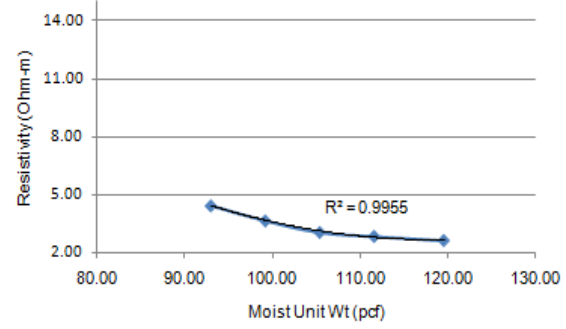
(b)
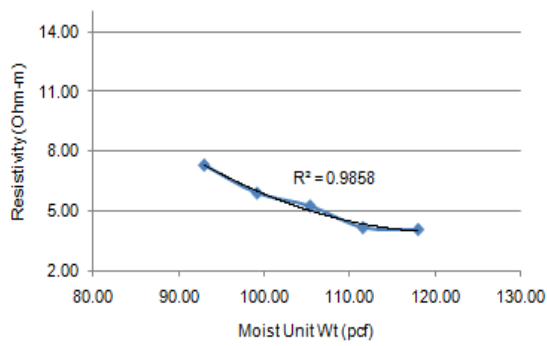
(c)
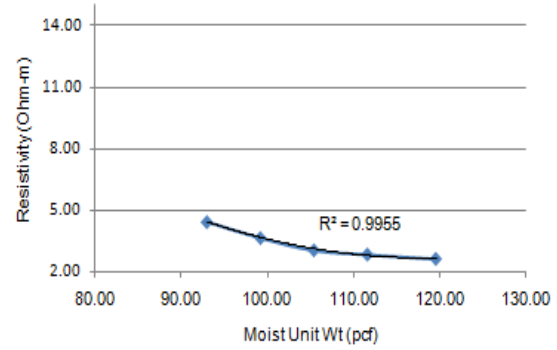
(d)

Figure 4.9: Variation of Resistivity with Moist Unit Weight at 24% Moisture Content (a) A-B2-D15 (b) A-B3-D10 (c) A-B3-D15 (d) A-B3-D20
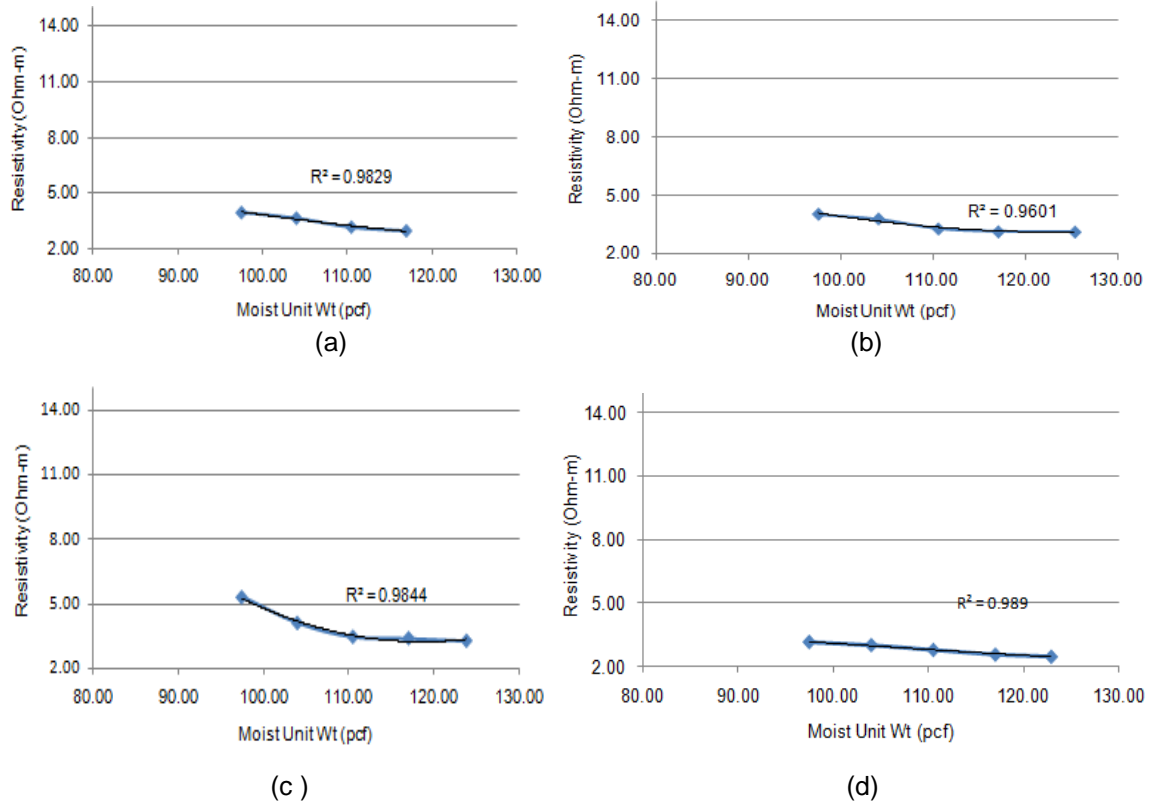
Figure 4.10: Variation of Resistivity with Moist Unit Weight at 30% Moisture Content (a) A-B2-D15 (b) A-B3-D10 (c) A-B3-D15 (d) A-B3-D20

Calculation tables for resistivity measurement are attached in Appendix A.

The variation of soil resistivity with unit weight can be explained by the study of Abu Hassanein et al., (1996). An increase in moist unit weight is associated with the increase in degree of saturation. More pronounce bridging occurs between the particles at high degree of saturation. In addition, increase of moist unit weight is associated with remolding of clay clods, elimination of interclod voids and reorientation of particle (Abu Hassanein, 1996). Therefore, soil resistivity decreases with the increase of moist unit weight.

According to Mitchell and Soga (2005), reduction in the large pores and breakdown in flocculated open fabric occur during remolding of clay soil. As a result, conduction path in soil reduced at high unit weight. Test results showed that resistivity did not changed significantly after 100 pcf. This phenomenon might be caused due to the breakdown of flocculated fabric at high unit weight condition and associated reduction in current flow path.

4.6.3 Comparison of Moisture Content and Unit Weight in Soil Resistivity

The effects of moisture content and unit weight are presented in subsection 4.6.1 and 4.6.2. It was observed that soil resistivity decreased with the increase of moisture content and unit weight. However, test results showed that soil resistivity was more sensitive to moisture content compare to unit weight. The comparison of their effects is presented in Figure 4.11.
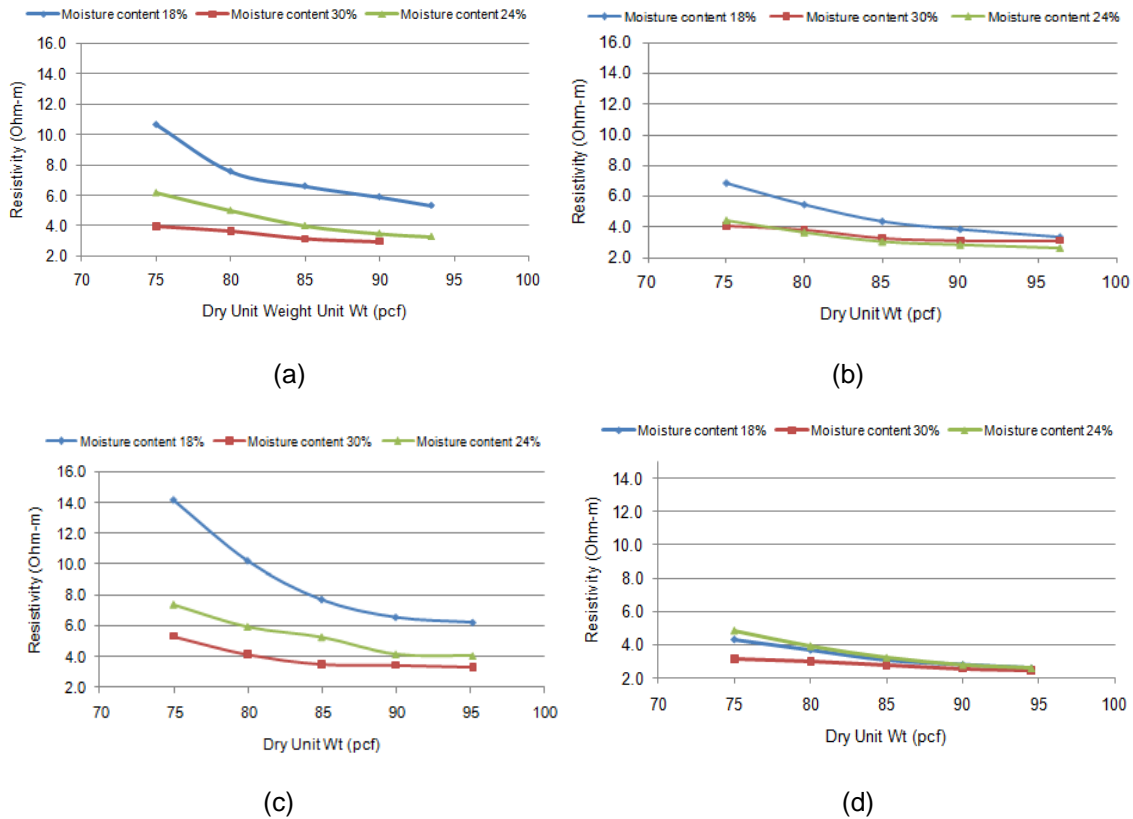
Figure 4.11: Comparison of the Effect of Moisture Content and Unit Weight with Soil Resistivity
(a) A-B2-D15 (b) A-B3-D10 (c) A-B3-D15 (d) A-B3-D20

According to Figure 4.11 soil resistivity decreased with the increase of moisture content and unit weight. However, soil resistivity ranged from 5.3 to 2.5 Ohm-m at 30% moisture content in soil samples presented here. Thus, the effect of unit weight was not prominent at 30% moisture content. The average rate of reduction in soil resistivity with the increase of dry unit weight from 75 to 95 pcf is presented in Table 4.9.

Table 4.9: Summary of Average Reduction Rate of Soil Resistivity

Moisture Content (%)	Reduction Rate of Resistivity (Ohm-m/pcf)
18	0.28
24	0.16
30	0.07

The rate of reduction was high at 18% moisture content and decreased with the increase of moisture content. Soil resistivity was sensitive to unit weight at low moisture content. However, rate of reduction decreased to 0.07 Ohm-m/pcf at 30% moisture content. Therefore, soil resistivity was more sensitive to moisture content compare to unit weight.

Electrical conduction in soil is mostly ionic in nature (Shah and Singh, 2005). The charges of clay soil are precipitated in water in the presence of moisture (Rinaldi and Cuestas. 2002). Under applied electrical field, conduction occurs through the pore space by water solution. Thus, electrical conduction in soil mainly depends on moisture content.

4.6.4 Soil Resistivity with Volumetric Moisture Content

Volumetric moisture content is correlated with dry unit weight of soil, unit weight of water and gravimetric moisture content. Obtained test results from subsection 4.6.1 and 4.6.2 are combined to correlate soil resistivity with volumetric moisture content. Variation of soil resistivity with volumetric moisture content is presented in Figure 4.12.
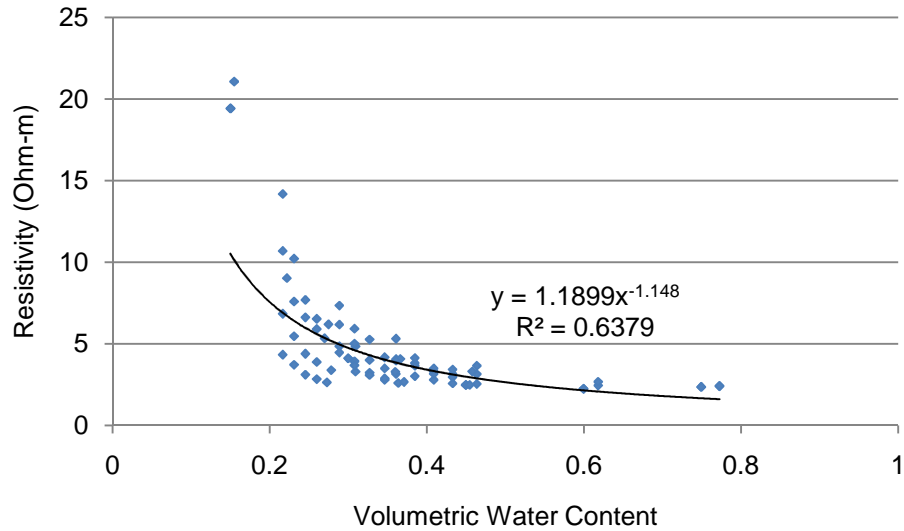
Figure 4.12: Variation of Soil Resistivity with Volumetric Water Content

It was observed that plotted data followed the trend of power function (R^2=0.64). The determined function is

$$\rho= 1.1899\, \theta^{-1.148}$$

where, ρ = Resistivity of the soil sample in Ohm-m, θ= Volumetric moisture content.

From the relationship of volumetric water content with dry unit weight of soil, unit weight of water and gravimetric water content the following equation is developed

$$\rho=136.89\, [\gamma_m.\, w/(1+w)]^{1.148}$$

where, ρ =Resistivity in Ohm-m, γ_m=Moist unit weight in pcf, w= gravimetric moisture content.

Three dimensional surface area was obtained from the equation using Mathematica software. The obtained surface is presented in Figure 4.13.
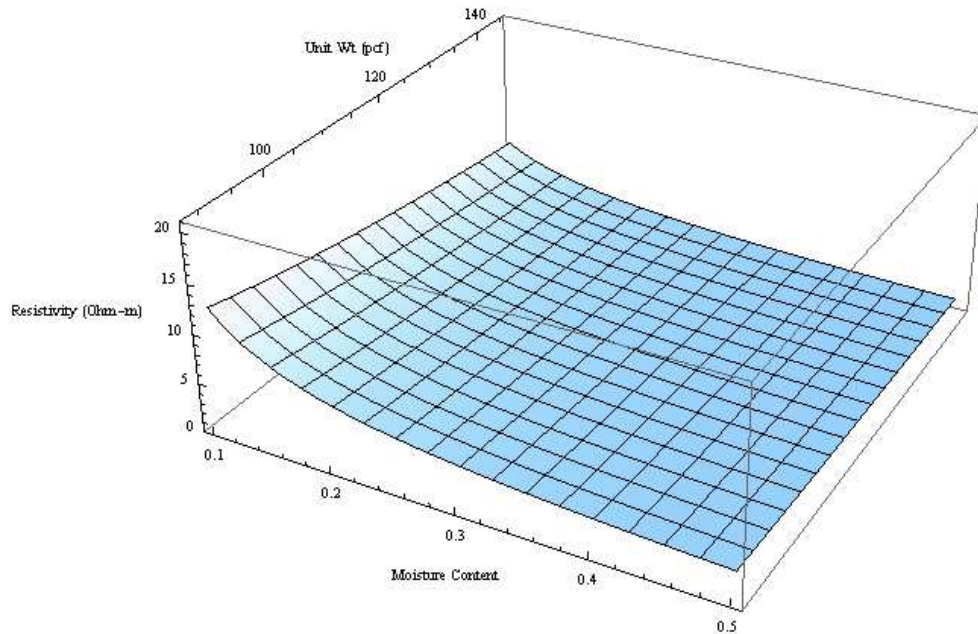
Figure 4.13: Three Dimensional Surface Area Combining Moist Unit Weight and Moisture Content with Resistivity

It is evident from the Figure 4.13 that the soil resistivity decreased with the increase of both moisture content and unit weight. At moisture content beyond 40%, the surface becomes almost parallel to the plane of moisture content and unit weight.

4.6.5 Soil Resistivity with Degree of Saturation

The water content and dry unit weight can be combined to a single geotechnical parameter called degree of saturation Degree of saturation increases with the increase of water content or dry unit weight (Abu Hassanein, 1996). The variation of soil resistivity with degree of saturation is presented in Figure 4.14 for soil samples A-B2-D15, A-B3-D10, A-B3-D15 and A-B3-D20. To obtain degree of saturation, specific gravity of 2.65 was assumed. It was observed that soil resistivity decreased with the increase of degree of saturation. Average soil resistivity was 6.7 Ohm-m at 40% degree of saturation. However, average soil resistivity decreased to 3.2 Ohm-m at 90% degree of saturation.

Increase in degree of saturation yields changes in clay clods, reduction in interclod macro voids and orientation of clay particles (Lambe, 1958). Therefore, soil resistivity decreased with the increase in degree of saturation as presented in Figure 4.14.

(a)

(b)

(b)

(d)
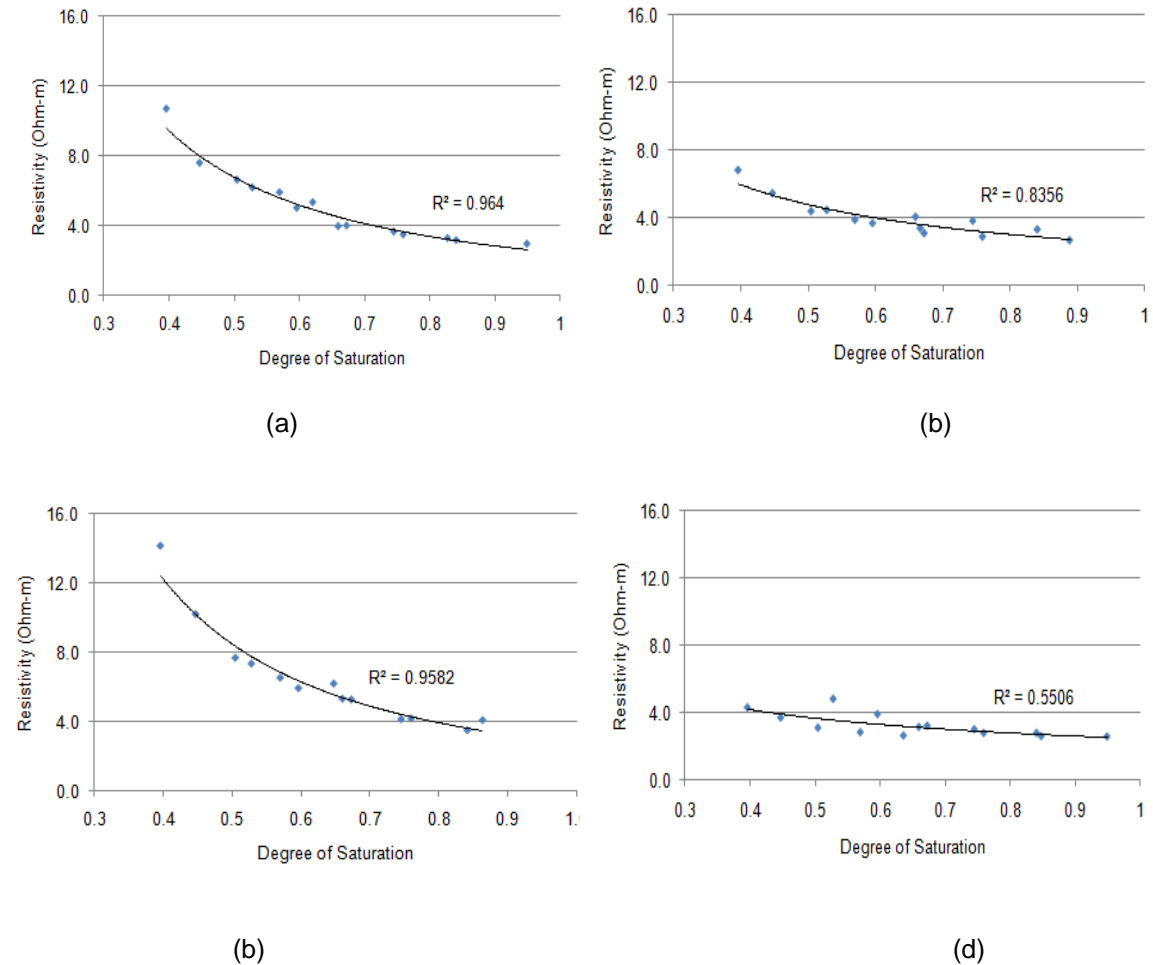
Figure 4.14: Variation of Soil Resistivity with the Degree of Saturation (a) A-B2-D15 (b) A-B3-D10 (c) A-B3-D15 (d) A-B3-D20

4.6.6 Soil Resistivity with Specific Surface Area

Specific surface area was calculated from liquid limits of the collected soil samples as presented in section 4.3. A summary of specific surface area of soil sample samples A-B3-D20, A-B3-D10, A-B2-D15 and A-B3-D15 is presented in Table 4.10.

Table 4.10: Summary of Specific Surface Area of Soil Samples

Designation	Specific Surface Area (m^2/gm)
A-B3-D20	69.6
A-B3-D10	75
A-B2-D15	96.4
A-B3-D15	107.1

Specific surface areas of samples were plotted against soil resistivity at different moisture content and dry unit weight. It was observed that soil resistivity increased with the increase of specific surface area. The increments were more pronounced at moisture content 18% and 24%. Soil resistivity increased from 4.3 to 14.2 Ohm-m for the increase of surface area from 69.6 to 107.1 m^2/gm at 18% moisture content and 75 pcf dry unit weight. However, soil resistivity increased from 3.2 to 5.3 Ohm-m at 30% moisture content and 75 pcf dry unit weight. Moreover, soil resistivity ranged from 2.8 to 3.2 Ohm-m at 30% moisture content and 90 pcf dry unit weight in all the soil samples. The variation of soil resistivity with specific surface area is presented in Figure 4.15.
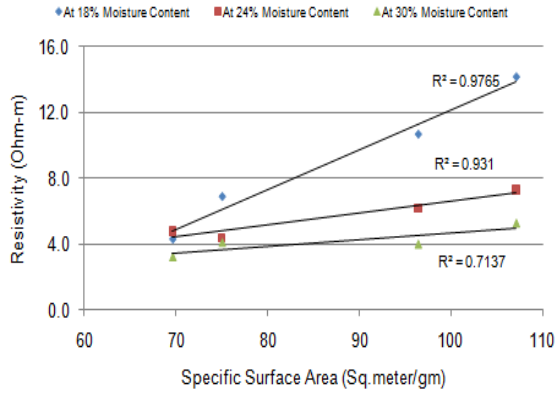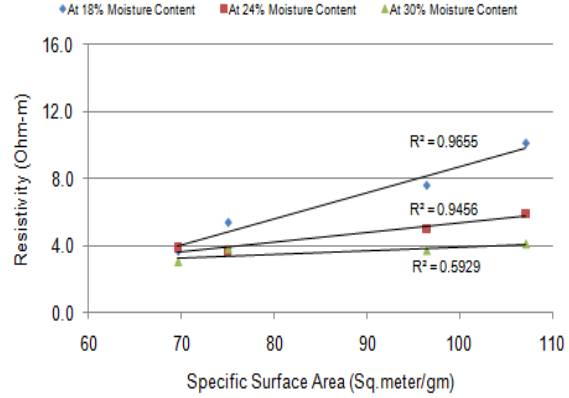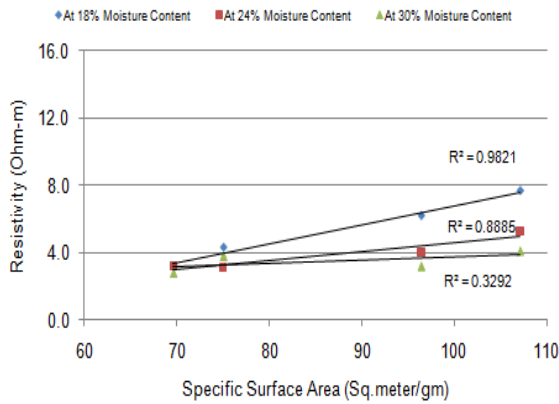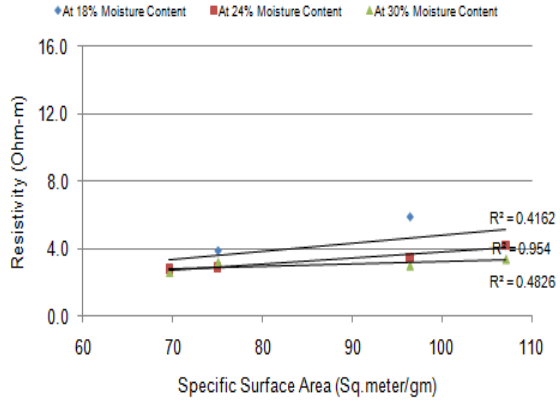
Figure 4.15: Variation of Soil Resistivity with Specific Surface Area at Dry Unit Weight (a) 75 pcf (b) 80 pcf (c) 85 pcf (d) 90 pcf

With the increase of surface area, more water is required for the formation of water film around fine particles. In the absence of water film, bridging between the soil particles is not possible to occur. In addition, ionic conduction does not take place without proper water bridging between soil particles. Therefore, lack of formation of water film around the particle due to large specific surface area might cause the observed variation at 18% water content as presented in Figure 4.15. With the increase of moisture, water bridging between the particles occurred. Therefore, the rate of variation was 0.08 Ohm-m/ (m^2/gm) at 24% moisture content and 0.04 Ohm-m/ (m^2/gm) in 30% moisture content at 75 pcf dry unit weight. At 30% moisture content and

90 pcf dry unit weight, soil resistivity was independent of surface area because of the formation of water film around particles in a compacted soil condition.

4.6.7 Soil Resistivity with Pore Space

Representative void spaces in soil samples were analyzed using 2000 times magnified SEM images (Figure 4.6). The porosity of the soil grain can be divided in to three groups such as macro porosity, meso porosity and micro porosity. Macro porosity refers to the pores having diameter more than 0.05 micrometer, meso porosity refers to the pores with diameter more than 0.002 micrometer and less than 0.05 micrometer. Micro porosity is associated with the pores with diameter less than 0.002 micrometer (http://en.wikipedia.org/wiki/Porosity). According to the scale, the observed pores in the images were in macro porosity level. A summary of pore space for soil samples A-B3-D10, A-B2-D15 and A-B3-D15 is presented in Table 4.11.

Table 4.11: Summary of Percentage Pore Space and Specific Surface Area

Designation	Percentage of Pore Space	Specific Surface Area (m^2/gm)
A-B3-D10	27.39	75
A-B3-D15	10.56	107.1
A-B3-D20	1.91	69.6

The objective of pore analysis was to identify the relationship of soil resistivity with porosity. The resistivity was plotted with the percentage of voids as presented in Figure 4.16.
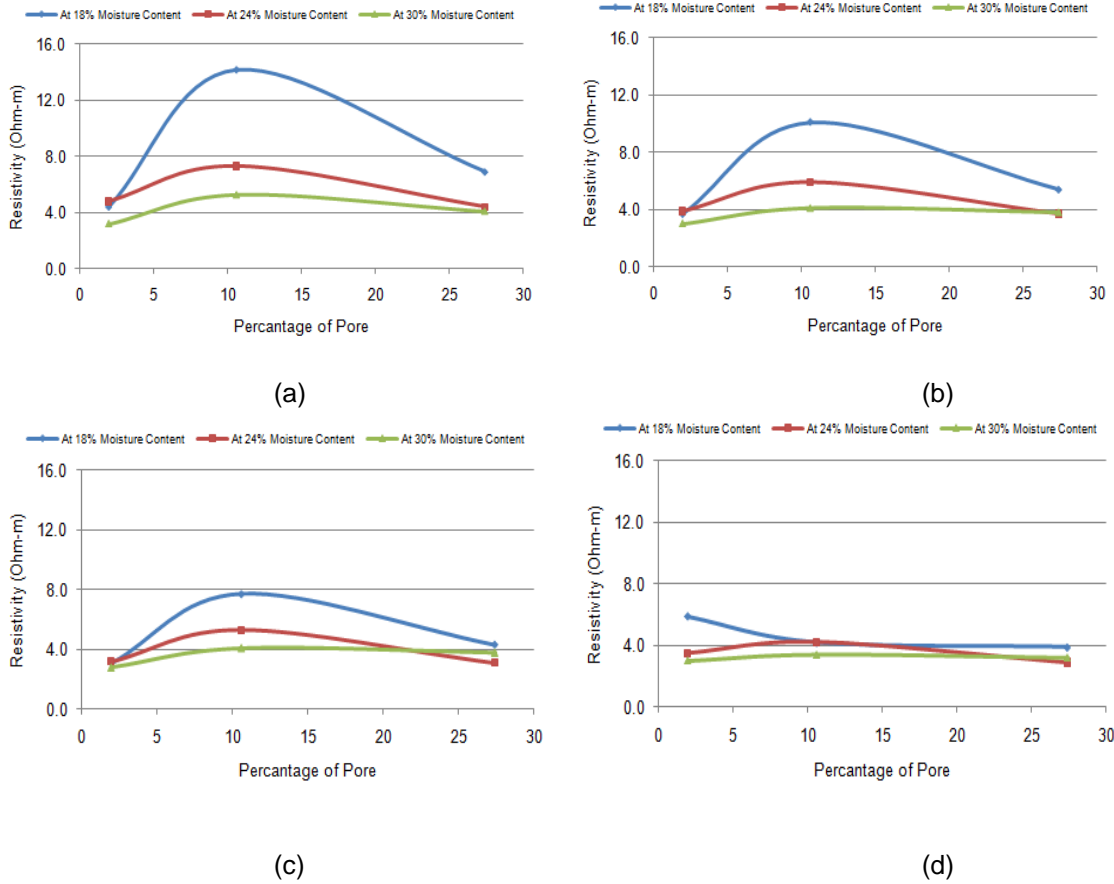
Figure 4.16: Variation of Resistivity with Obtained Pores from SEM Images at Dry Unit Weight (a) 75 pcf (b) 80 pcf (c) 85 pcf (d) 90 pcf

Figure 4.16 showed that soil resistivity increased with the increase of pore space initially and then decreased. The variation was more pronounced at 18% moisture content and 75 pcf dry unit weight. Soil resistivity increased from 4.4 to 14.2 Ohm-m for the increase of pore space from 1.91% to 10.56% at 18% moisture content and 75 pcf dry unit weight. However, resistivity decreased from 14.2 to 6.9 Ohm-m for the increase of pore space from 10.56% to 27.39%. The initial increase in soil resistivity at 18% moisture content (at dry unit weight 75 pcf, 80 pcf and 85 pcf) might be caused due to the presence of air voids. The reduction in resistivity for the increase of pore space from 10.56% to 27.39% might be attributed due to the specific surface area. The specific surface area of the sample A-B3-D10 was 75 m^2/gm and sample A-B3-D15 was 107.1 m^2/gm. Water film and moisture bridging between the particles might form more easily at 18% moisture content in the soils with small surface area. Therefore, soil resistivity decreased though there was an increase in pore space due to the pronounce moisture bridging between the par-

ticles. In addition, the comparison of soil resistivity with the moisture content and unit weight showed that soil resistivity was more sensitive to moisture. The variation in soil resistivity was not significant at 90 pcf unit weight due to the formation of water film around the particles and reduction in pore space.

4.6.8 Soil Resistivity with Ion Composition

The percentage of Mg, Mn, Fe, Ti, Al, Si, S, P and K ion composition were not significant (<2%) in the soil samples. Summary of calcium ion percentage and associated specific surface area in soil sample A-B3-D20, A-B3-D10, A-B2-D15 and A-B3-D15 is presented in Table 4.12.

Table 4.12: Summary of Calcium Ions and Specific Surface Area in Soil Samples

Designation	Calcium Ion (% Weight)	Specific Surface Area (m^2/gm)
A-B3-D20	8.3	69.6
A-B3-D10	11.4	75
A-B2-D15	13.1	96.4
A-B3-D15	13.9	107.1

It was observed that soil resistivity decreased with the increase of calcium ions at different moisture content as presented in Figure 4.17. The variations in soil resistivity with aluminum, iron, silicon and potassium ions are attached in Appendix A.
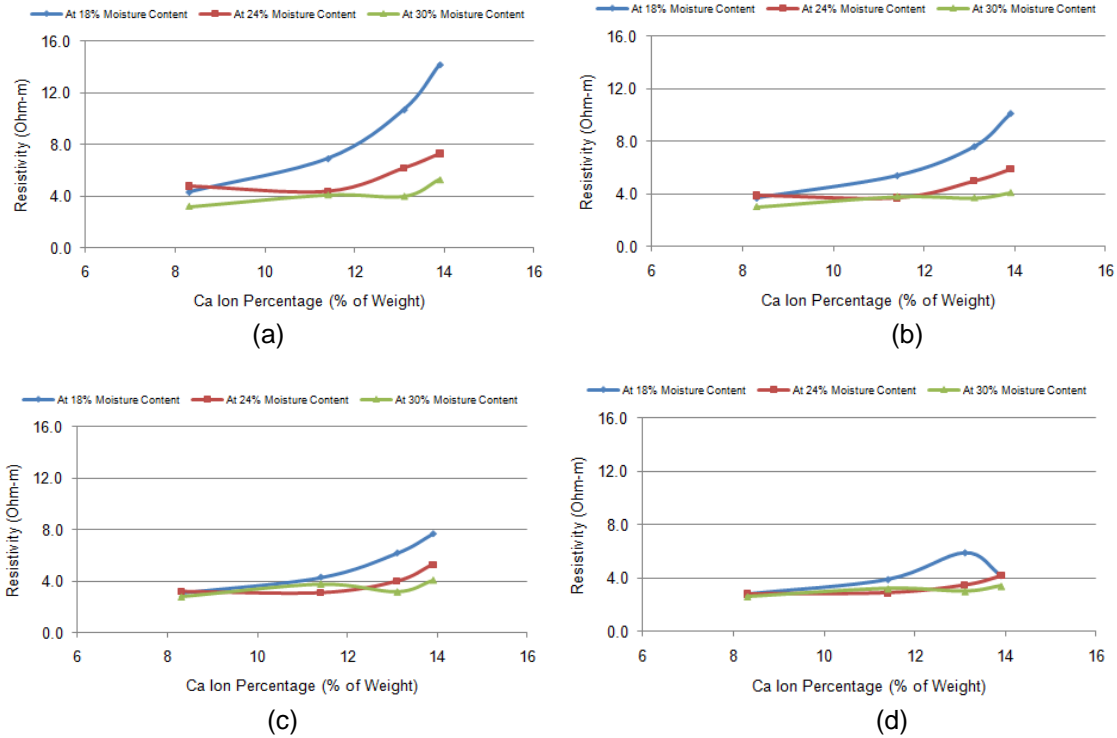
Figure 4.17: Percentage of Calcium Ions and their Variation with Resistivity at Dry Unit Weight (a) 75 pcf (b) 80 pcf (c) 85 pcf (d) 90 pcf

It was observed that there was no current flow through the clay soil in the absence of moisture. When moisture was added, resistivity of the soil samples decreased. This phenomenon indicated that the electrical conduction was mainly ionic in nature. Therefore, current flow can be defined by well known Ohm's law. Ohm's law is valid for ionic conduction in the absence of polarization and electrochemical diffusion (Rinaldi and Cuestas, 2002).

Test results showed that soil resistivity increased from 4.3 to 14.2 Ohm-m with the increase of calcium ion from 8.3% to 13.9% at 18% moisture content and 75 pcf dry unit weight. The rate of increase of soil resistivity decreased with the increase of moisture. At 30% moisture content and 75 pcf dry unit weight soil resistivity was in between 3.2 to 5.3 Ohm-m.

The variation might occur due to the lack of formation of water film around the particle with large specific surface area at low water content. Ionic conductor calcium might not be able to go in to the solution at low moisture content. Therefore, the effects of increase of calcium ion were not observed in the test results. With the increase of moisture content, dislocation of calcium

ion might occur and soil resistivity decreased. Ionic conduction was enhanced with the increase of moisture. However, soil resistivity was almost constant and independent of unit weight and calcium content at moisture content 30%. This phenomenon suggested that soil resistivity is very sensitive to moisture and the effect of moisture is higher that the effect of unit weight and ion concentration. Moreover, specific surface area has significant effect on soil resistivity.

4.6.9 Soil Resistivity with Compaction

Standard Proctor compaction tests were conducted to generate compaction curve. After that, resistivity of the soil samples were measured at corresponding moisture content and unit weight. It was observed that maximum dry unit weight of the samples ranged between 93.5 to 96.5 pcf. Zero void line was obtained assuming specific gravity of 2.65 for all the soil samples. Figure 4.18 showed the compaction curve of the soil samples. Calculation tables of Standard Proctor compaction is attached in Appendix A.

Optimum moisture content and dry unit weight of different soil samples are presented in Table 4.13.

Table 4.13: Optimum Moisture Condition and Dry Unit Weight of Soil samples

Designation of Soil Sample	Optimum Moisture Content (%)	Dry Unit Weight (pcf)
A-B2-D15	23	93.5
A-B3-D10	21.5	96.4
A-B3-D15	24.6	95.2
A-B2-D20	23.5	96.5
A-B3-D20	24	94.5
B-B1-D15	21.4	96
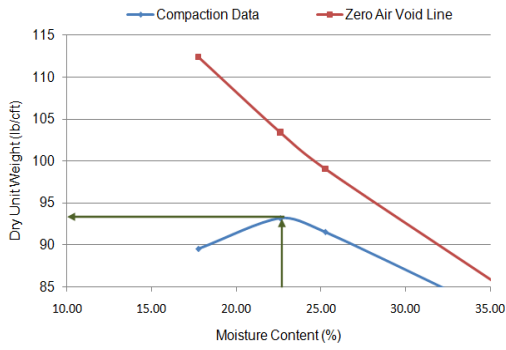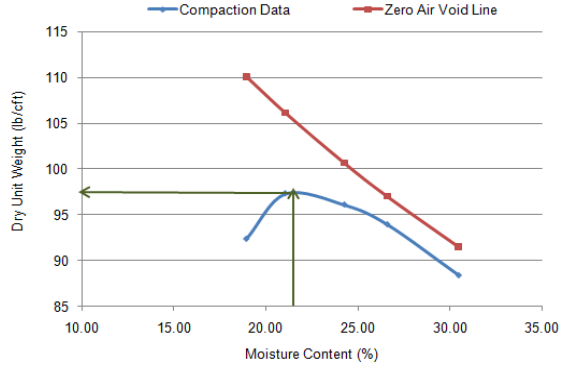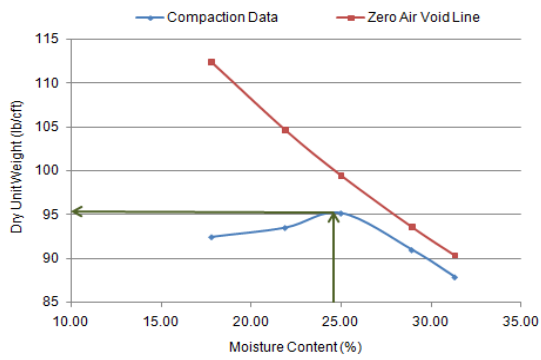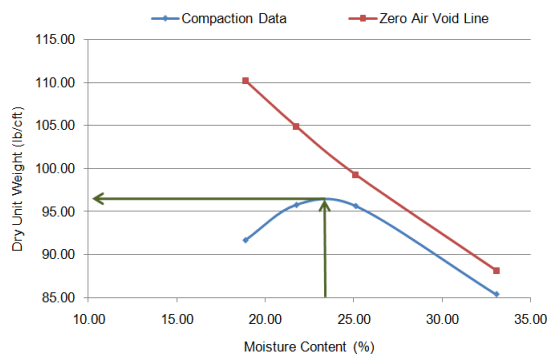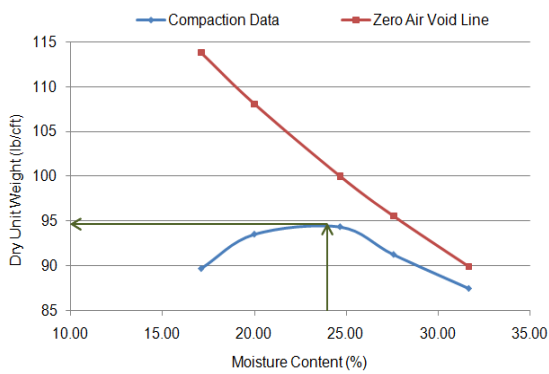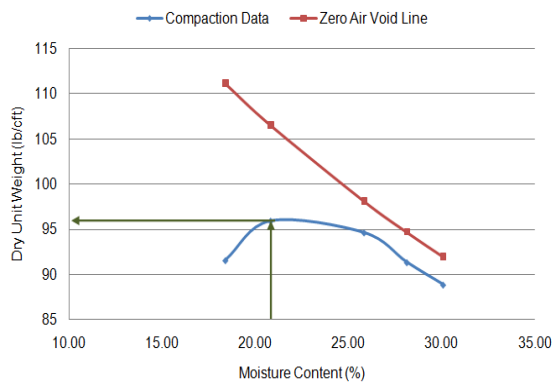
Figure 4.18: Generated Compaction Curve of Soil Samples (a) A-B2-D15 (b) A-B3-D10 (c) A-B3-D15 (d) A-B2-D20 (e) A-B3-D20 (f) B-B1-D15

Soil resistivity tests were conducted at moisture content and dry unit weight corresponding to compaction curve in each sample. Test results showed that resistivity was high when compacted at dry optimum. With the increase of moisture content and unit weight, resistivity decreased significantly. At wet side, soil resistivity was low. The schematic of the test results is presented in Figure 4.19.

According to Figure 4.19, soil resistivity decreased from 4.75 to 3.4 Ohm-m in an average when the sample was compacted at dry of optimum. However, the average soil resistivity was in between 2.2 to 2.6 Ohm-m in the wet of optimum. Therefore, soil resistivity was independent of molding water content and dry unit weight at wet of optimum.

The variation of soil resistivity with compaction condition can be discussed according to the structural change of soil during compaction. The clay clods are difficult to remold and interclod pores are large when compacted at dry of optimum (Benson and Daniel, 1990). The pores are filled with dielectric air at this condition. The contact between the particles is poor because of the presence of distinct clods at low dry unit weight. Therefore, resistivity was high at dry of optimum due to the presence of air filled voids and poor particle-to-particle contact compare to wet optimum.

According to the study of Benson and Daniel (1990), clay clods are remolded easily in the wet of optimum or high compactive effort. At wet of optimum, interclod pores are small and contain high percentage of water. Furthermore, particle-to-particle contact increases due to high dry unit weight and additional remolding of clods. High dry unit weight and near saturated pores increase electrical conductance (Abu Hassanein et al., 1996). Therefore, observed soil resistivity was as low as 1.8 Ohm-m (Soil Sample A-B3-D20) at wet of optimum.

(a)

(b)

(c)

(d)

(c)
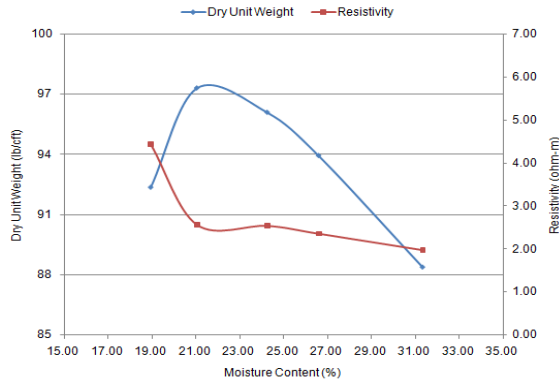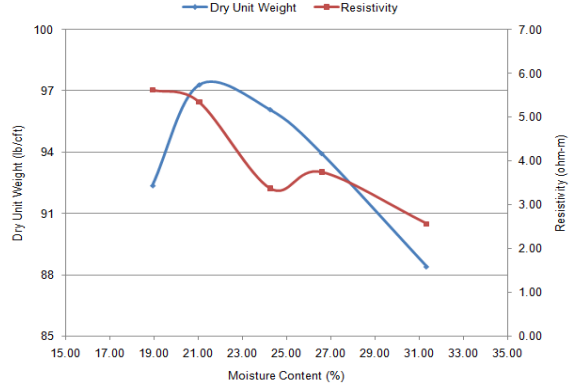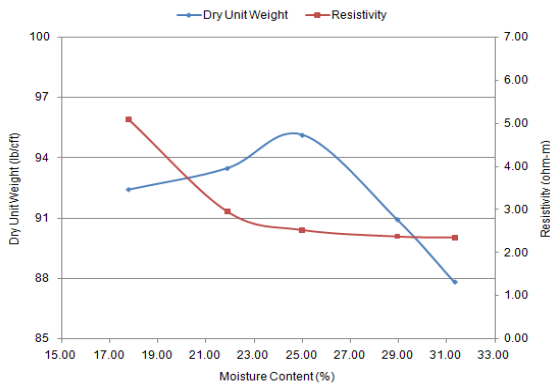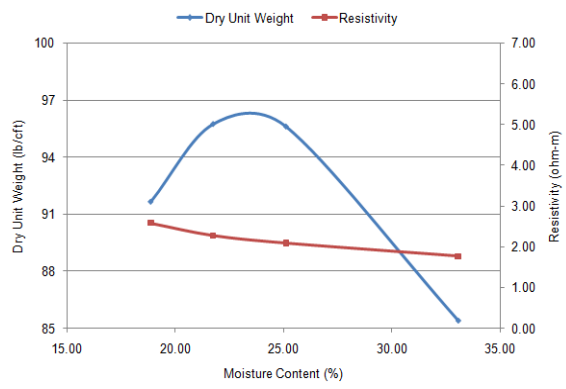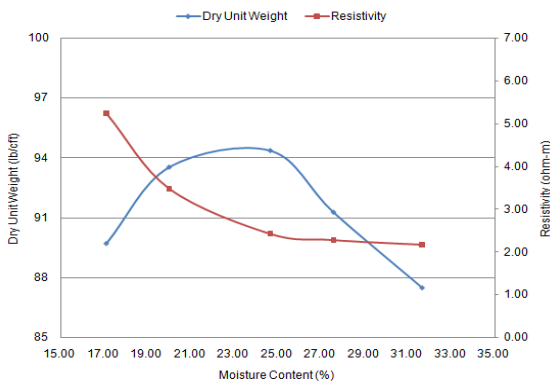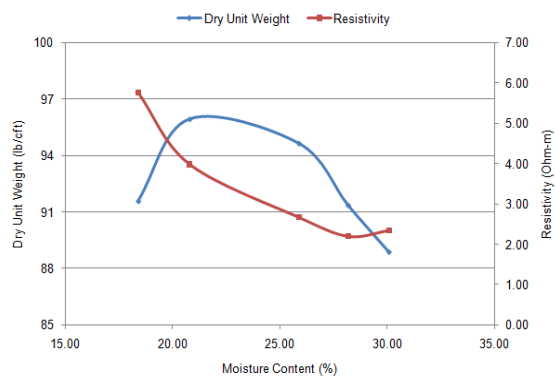
(f)

Figure 4.19: Comparison of Soil Resistivity at Different Compaction Condition Samples (a) A-B2-D15 (b) A-B3-D10 (c) A-B3-D15 (d) A-B2-D20 (e) A-B3-D20 (f) B-B1-D15

A three dimensional surface including dry unit weight and molding water content is presented in Figure 4.20.
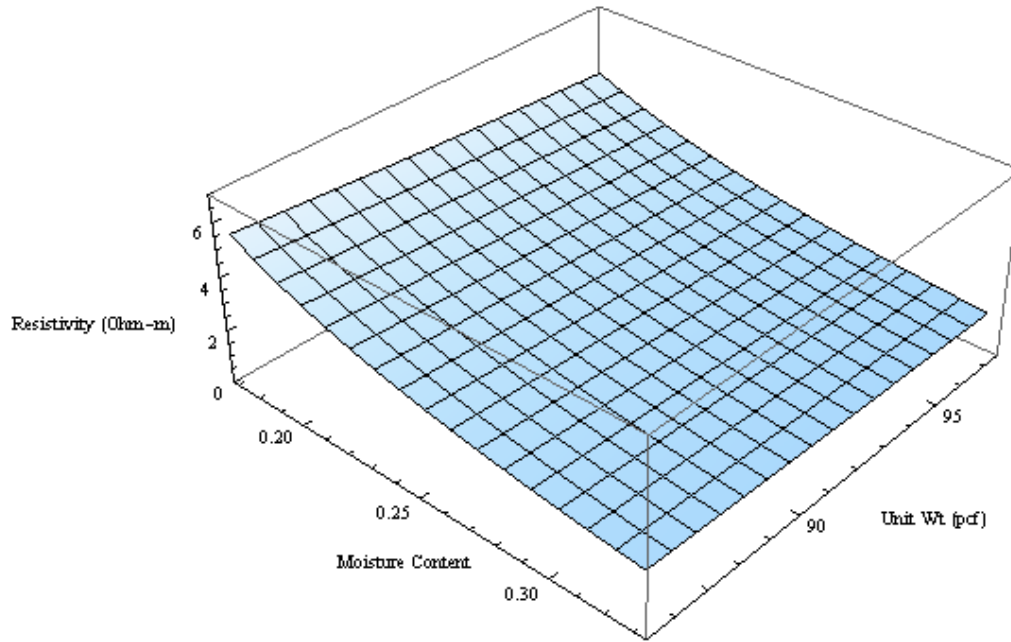
Figure 4.20: Three Dimensional Surface Showing the Variation of Soil Resistivity with Dry Unit weight and Moisture Content

4.6.10 Soil Resistivity with Unconfined Compression Strength

Soil samples were prepared at moisture condition and unit weight obtained from different points of compaction curve. Unconfined compression test results were plotted against the soil resistivity. It should be noted that soil resistivity test results presented in subsection 4.5.9 were used in this plot. It was observed that cohesion was high when moisture and unit weight of the samples close to optimum condition. The variation of soil resistivity with unconfined strength showed the similar trend as with different compaction condition. Figure 4.21 showed the variation of resistivity at various unconfined strength for different soil samples.
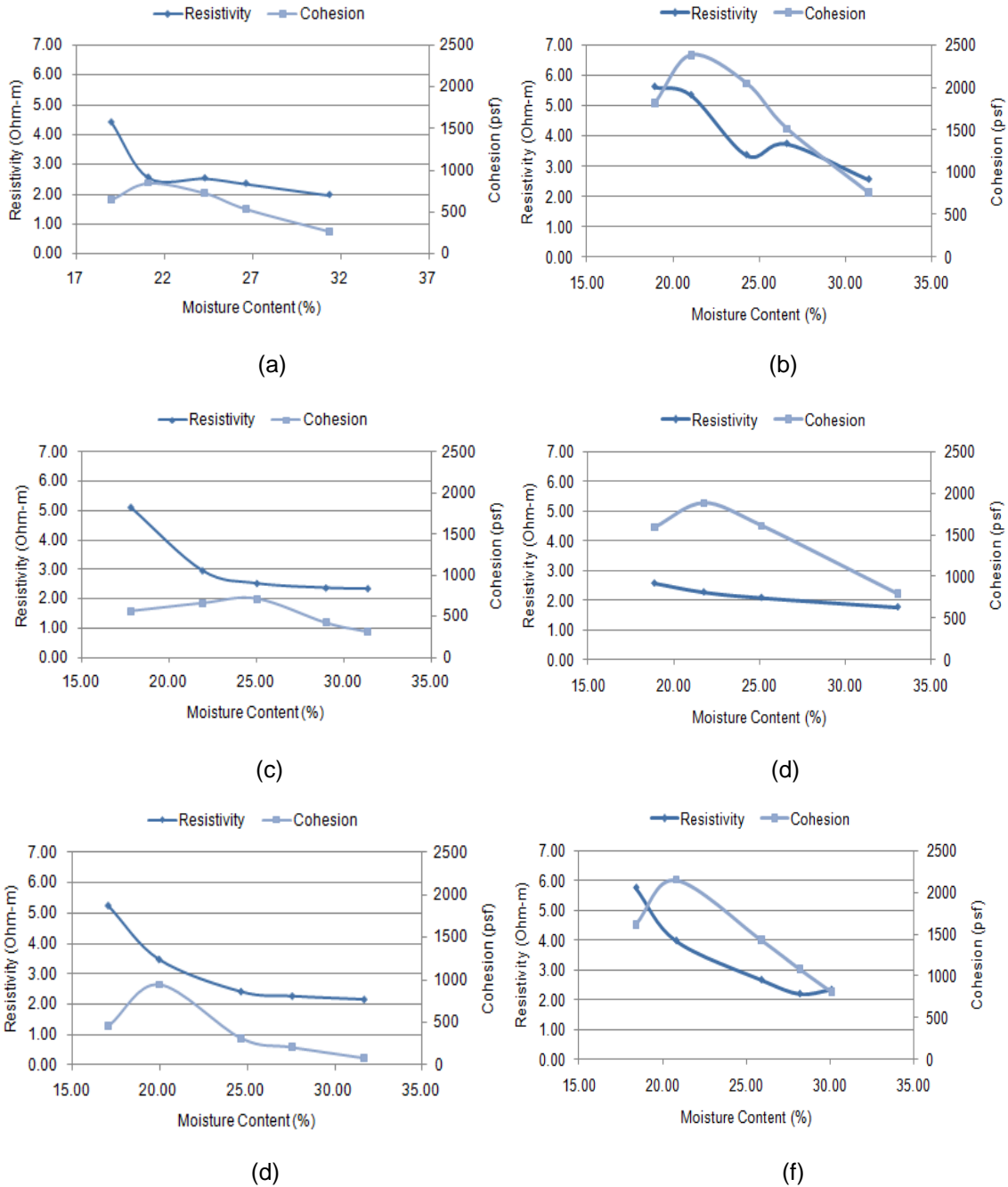
Figure 4.21: Variation of Resistivity at Different Unconfined Strength for Soil Sample (a) A-B2-D15 (b) A-B3-D10 (c) A-B3-D15 (d) A-B2-D20 (e) A-B3-D20 (f) B-B1-D15

It was observed that cohesion increased from 1115 to 1487 psf for the increase of moisture content 18.3% to 21.6% in an average. Corresponding increase in average dry unit of the samples was in between 91.7 and 95.8 pcf. Further increase of dry unit weight and moisture content resulted reduction in cohesion. Test results of soil resistivity with cohesion showed that aver-

age resistivity was in between 3.4 and 4.75 Ohm-m in soil samples with average cohesion 1115 to 1487 psf. Average cohesion of the soil samples were in between 506 to 1142 psf at wet of optimum. Corresponding average resistivity of soil ranged from 2.2 to 2.6 Ohm-m. The causes of variation can be explained by structural change of soil at different compaction condition. Due to the presence of large interclod pore and poor contact between particles, resistivity was high for the samples prepared at dry optimum. However, near saturated pore and better particle-to-particle contact resulted low electrical resistivity (Benson and Daniel, 1990) in the samples prepared at wet optimum. Test results indicated that compaction condition and corresponding unconfined compressive strength of remolded clay can be approximated by electrical resistivity.

4.6.11 Soil Resistivity with Sieve Analysis

Soil resistivity tests were conducted at 25% gravimetric moisture content and 85 pcf dry unit weight for five soil samples. The soil samples considered in the test were sample A-B2-D15, A-B3-D10, A-B3-D15, A-B2-D20 and B-B1-D15. The range of electrical resistivity of soil was in between 3.16 and 3.6 Ohm-m. Test results showed that soil resistivity was independent of fine fraction for the soil samples as presented in Figure 4.22. However, the data were not highly correlated (R^2=0.33).
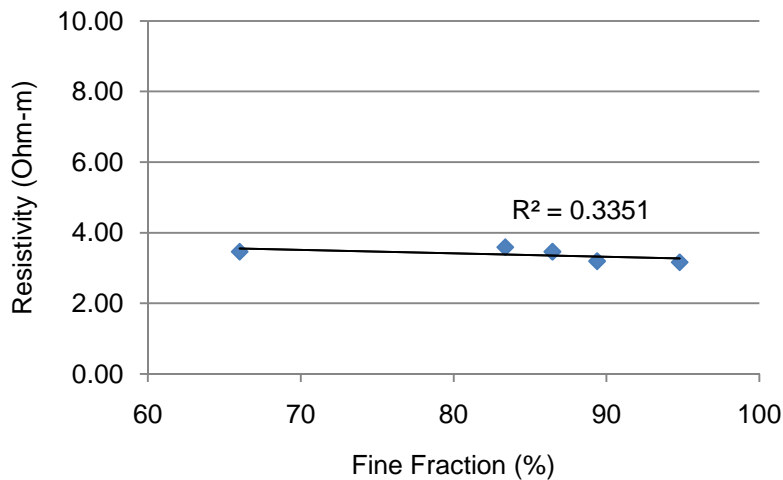
Figure 4.22: Variation of Resistivity with Fine Fraction of Soil Samples

Soils with high percentage of fine content often composed of more conductive clay particle (Abu Hassanein et al., 1996). Therefore, soil resistivity may decrease with the increase of fine content. However, the most influential factor in soil resistivity is moisture content and unit weight (McCarter, 1984). Test results showed that the range of resistivity were very close (3.16 to 3.6 Ohm-m) for the fine fraction range of 66% to 94.8%. All the soil samples were highly plastic clay and percentage of fines of the samples were very close to each other. Therefore, the obtained variation of soil resistivity with fine content was insignificant.

4.6.12 Soil Resistivity with Liquid Limits and plastic Limits

Soil resistivity results were plotted against liquid limits and plastic limits to identify their correlations. Soil resistivity results presented in the subsection 4.5.11 were utilized here. It was observed that the soil resistivity was almost same for different liquid limits of the soil samples. The correlation between the results was also satisfactory. It was also found that liquid limits of soil sample A-B3-D10 and A-B2-D20 were same (61). Soil resistivity test results indicated that resistivity of the both samples were also same (3.46 Ohm-m). The observed relationship between soil resistivity and liquid limits is presented in Figure 4.23.
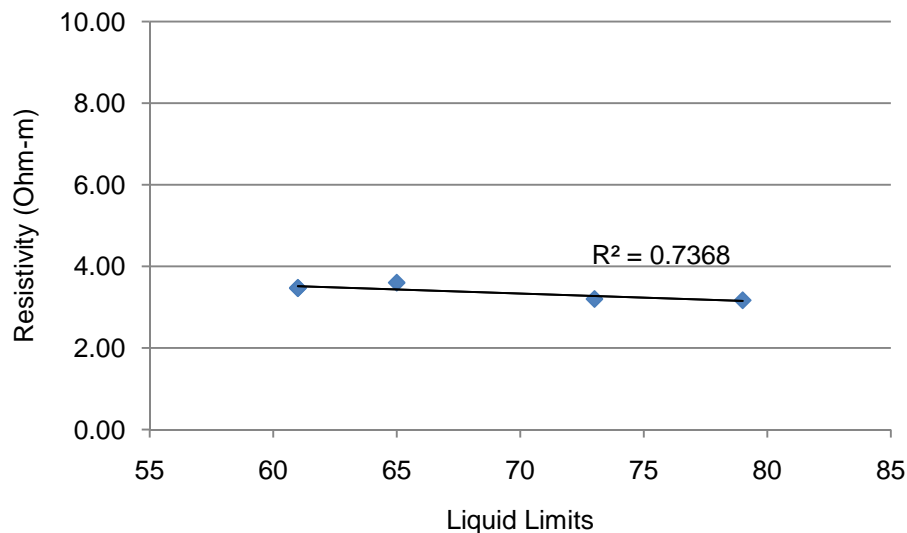
Figure 4.23: Relationship between Soil Resistivity and Liquid Limits

Soil resistivity varied from 3.16 to 3.6 Ohm-m for liquid limits range 61 to 79. Test results showed that the variation in soil resistivity was insignificant. All the soil samples were classified as highly plastic clay with high percentage of fines. Moreover, soil resistivity tests were conducted at fixed water content and unit weight. Thus, the obtained soil resistivity of the samples were close to each other and the effect of liquid limits on soil resistivity were not prominent.

The variation of soil resistivity with plasticity index of the soil samples showed that soil resistivity did not change notably with increase of plasticity index for different samples. However, the data were not highly correlated. The regression coefficient of the straight line was 0.22. Figure 4.24 shows the variation of soil resistivity with the plasticity index.
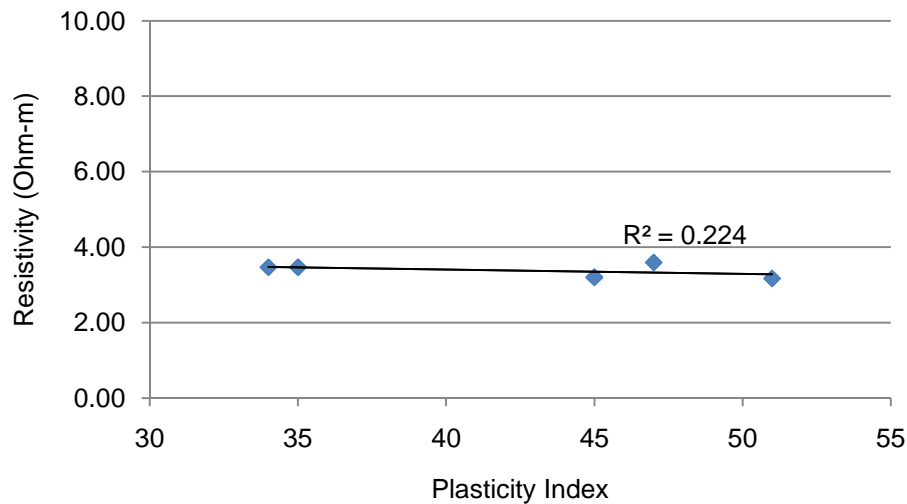
Figure 4.24: Relationship between Soil Resistivity and Plasticity Index of the Soil Samples

Figure 4.22, 4.23 and 4.24 indicated that variations in soil resistivity with fine faction and Index properties were insignificant in the same type of soil.

CHAPTER 5

CONCLUSIONS AND RECOMMENDATIONS

The relationship between soil resistivity and different geotechnical parameters has the potential to fill the gap between geotechnical and geophysical engineering site investigation. By developing the correlations of electrical resistivity of soil with geotechnical parameters, RI can be used extensively for geotechnical site investigation.

The objective of the study was to determine the relationship between different geotechnical properties of clay soils. Soil samples were collected from slopes along highway US 287 and US 67, Midlothian, Ellis County, Texas. Based on the laboratory investigation, soil samples were classified as highly plastic clay (CH) according to USCS. From XRF and SEM image analysis, it was found that the dominant clay mineral in samples might be montmorillonite. Soil resistivity tests were conducted at different condition to identify the relationship with fine fraction, coarse fraction, liquid limit, plastic limit, ion composition, compaction and unconfined strength condition, unit weight and moisture content. Finally, a relationship between volumetric water content with soil resistivity was developed.

5.1 Summary and Conclusions

The outcome of the study has been summarized below

1. Collected soil samples were highly plastic clay (CH) according USCS soil classification.

2. According to the liquid limit and plastic limit, specific information about clay minerals were not obtained. Therefore, clay mineralogy was determined based on XRF ion composition and SEM image analysis. The dominant clay mineralogy might be montmorillonite.

3. Soil resistivity decreased with the increase of moisture content. The average rate of reduction in soil resistivity was 13.8 Ohm-m/percent moisture content for the increase of moisture from 10% to 20%. It was observed that soil resistivity was almost independent

100

after 40% moisture content. Measured soil resistivity ranged from 2.1 to 2.42 ohm-m at 50% moisture content in the soil samples. Enhanced electrical conduction due to the presence of moisture might cause the reduction in soil resistivity with the increase of moisture.

4. Soil resistivity decreased almost linearly with an average rate of 0.3 Ohm-m/pcf between moist unit weight 88.5 to 100 pcf at 18% moisture content. However, soil resistivity decreased with an average rate of 0.08 Ohm-m/pcf for further increase in moist unit weight in same moisture content. Reduction of interclod pores and better particle-to-particle contact might cause reduction in soil resistivity with the increase of unit weight. Moreover, the effect of moisture content on soil resistivity was high compare to unit weight.

5. Soil resistivity decreased from 6.7 to 3.2 Ohm-m in an average with the increase of degree of saturation from 40% to 90% due to elimination of interclod macropores, reorientation of clay particle and remolding of clay clods. However, at low degree of saturation soil with high surface area showed high resistivity due to the lack of formation of water film.

6. Soil resistivity increased from 4.3 to 14.2 Ohm-m for the increase of surface area from 69.6 to 107.1 m^2/gm at 18% moisture content and 75 pcf dry unit weight. Soil with high surface area required more water for the formation of water film and bridging between the particles.

7. Soil resistivity increased from 4.4 to 14.2 Ohm-m for the increase of pore space from 1.91% to 10.56% at 18% moisture content and 75 pcf dry unit weight. However, resistivity decreased from 14.2 to 6.9 Ohm-m at 18% moisture and 75 pcf dry unit weight. The increase of soil resistivity at 18% moisture content might be caused due to the presence of air voids. The reduction in soil resistivity might be attributed due to the formation of water film around soil particle with small surface area.

8. Test results showed that soil resistivity increased from 4.3 to 14.2 Ohm-m with the increase of calcium ion from 8.3% to 13.9% at 18% moisture content and 75 pcf dry unit weight. The water content might not adequate for calcium ions to occur ionic conduction in soils with high surface area at 18% moisture content.

9. Soil resistivity tests were conducted at different compaction condition. It was obtained that the resistivity was high when the soil was compacted at dry optimum. Reduction in soil resistivity was observed when compacted at wet of optimum. At wet of optimum, more pronounced bridge between the particle occurred which caused reduction in resistivity. Moreover, soil resistivity and unconfined strength was low at wet of optimum.

10. Relationship between soil resistivity and fine fraction, liquid limits and plastic limits showed that soil resistivity was in between 3.16 to 3.6 Ohm-m at fine fraction range 66% to 94.8%, liquid limits range 58 to 79 and plastic limits range 32 to 51. The collected soil samples were highly plastic clay and percentage of fine content was close to each other. Therefore, significant variation in soil resistivity was not observed.

11. It can be concluded that specific surface area has significant effect on soil resistivity in addition to moisture, unit weight and ion compostion.

5.2 Recommendation for Future Study

To develop the reliable correlation between soil resistivity and geotechnical properties of soil, the presented work can be further extended as presented below

1. The developed relationship between soil resistivity and geotechnical parameters of soil are site specific. More research is required to develop relationship between soil resistivity with geotechnical properties that can be applicable for different place and type of soils.

2. Effects of anisotropy, temperature variation and dielectric permittivity can be observed because these two parameters have significant effect on soil resistivity.

3. The conducted tests can be repeated for undisturbed sample to obtain more reliable field representative results.

4. SEM image analysis can be done for undisturbed sample to obtain actual fabric structure of soil. Environmental scanning electron microscope analysis can be conducted to determine different moisture and compaction condition.

5. Ion composition analysis can be done to obtain both cations and anaions.

6. Correlation of soil moisture, strength and electrical resistivity can be determined by insitu testing and laboratory investigation on undisturbed sample.

7. Soil resistivity can be conducted at different phase of consolidation to determine the correlation of soil resistivity with consolidation.

8. More research can be conducted to identify the relationship between hydraulic conductivity and electrical resistivity of soil.

9. Statistical analysis can be done to introduce a model. The model of soil resistivity should incorporate all the factors affecting soil resistivity. Moreover, the model should be validated by RI results, insitu test results and laboratory test results.

APPENDIX A

LABORATORY TEST RESULTS

Borehole Log

Project: Slope Stabiliy Analysis	Log of Boring BH-2
Project Location: US 287 (North), Mansfield, TX.	Sheet 1 of 1
Project Number:	

Date(s) Drilled	10/28/10 - 10/28/10	Logged By	UTA	Checked By	UTA
Drilling Method		Drill Bit Size/Type		Total Depth of Borehole	25.0
Drill Rig Type	Hollow stem	Drilling Contractor		Surface Elevation	100.0
Groundwater Level(s)		Sampling Method(s)	Shelby Tube	Hammer Data	
Borehole Backfill	Cement Grout	Comments			

Figure A1: Borehole 2 at US 287 Location

Project: Slope Stabiliy Analysis	Log of Boring BH-3
Project Location: US 287 (North), Mansfield, TX.	
Project Number:	Sheet 1 of 1

Date(s) Drilled	10/28/10 - 10/28/10	Logged By	UTA	Checked By	UTA
Drilling Method		Drill Bit Size/Type		Total Depth of Borehole	25.0
Drill Rig Type Hollow stem		Drilling Contractor		Surface Elevation	100.0
Groundwater Level(s)		Sampling Method(s)	Shelby Tube	Hammer Data	
Borehole Backfill	Cement Grout	Comments			

Elevation feet	Depth, feet	SAMPLES Type	SAMPLES Number	Sampling Resistance, Blows / 6 in.	SPT N-Value Blows/ ft.	Pocket Penetrometer, tsf	Graphic Log	MATERIAL DESCRIPTION	Water Content, %	ATTERBERG LIMITS Liquid Limit	Plastic Limit	Plasticity Index	REMARKS/ OTHER TESTS
-100	0							Calcarious clay, Tan					
								CH, Dark tan	15.0				
-95	5		3+4			2			20.2	52	25	27	
								CH, Tan					
-90	10		3+3			1.5			29.9	62	27	35	
								CH, Dark Tan					
-85	15		4+5			2			33.3	79	28	51	
-80	20		7+8						28.7	58	26	32	
								CH, Dark brown					
-75	25		7+6						27.3	65	25	40	
-70	30												

UTA

Figure A2: Borehole 3 at US 287 Location

106

Project: Slope Stabiliy Analysis	Log of Boring BH-1
Project Location: US 67 (South), Mansfield, TX.	
Project Number:	Sheet 1 of 1

Date(s) Drilled	10/27/10 - 10/27/10	Logged By	UTA	Checked By	UTA
Drilling Method		Drill Bit Size/Type		Total Depth of Borehole	45.0
Drill Rig Type Hollow stem		Drilling Contractor		Surface Elevation	100.0
Groundwater Level(s)		Sampling Method(s)	Shelby Tube	Hammer Data	
Borehole Backfill	Inclinometer casing installed at the bore hole	Comments			

Elevation feet	Depth, feet	SAMPLES Type	Number	Sampling Resistance, Blows / 6 in.	SPT N-Value Blows/ ft.	Pocket Penetrometer, tsf	Graphic Log	MATERIAL DESCRIPTION	Water Content, %	ATTERBERG LIMITS Liquid Limit	Plastic Limit	Plasticity Index	REMARKS/ OTHER TESTS
-100	0							Fill					
-95	5		20+23						11.6				
-90	10		3+4			1.5		Clay, Tan & Gray	32.7				
-85	15		5+7			2			29.8				
-80	20		10+9			3.5			29.2				
-75	25		9+12			3.5		Clay, Tan & Brown					
-70	30		8+10			3.5			22.6				
-65	35		11+12			3.5			21.1				
-60	40		10+12			3.5		Clay, Tan & Gray	22.5				
-55	45												

UTA

Figure A3: Borehole 1 at US 67 Location

Sieve Analysis

Table A1: Calculation of Sieve Analysis (Sample A-B2-D15)

SI No.	Sieve No.	Opening Size	Sieve Mass	Sieve and Soil Mass	Retained Soil Mass	Retained on Sieve	Cumulative Retained	Cumulative Passing
-	-	mm	gm	gm	gm	%	%	%
1	4	4.75	800	801.5	1.5	2.31	2.31	97.69
2	10	2	494	494.3	0.3	0.46	2.77	97.23
3	20	0.85	426.3	427	0.7	1.08	3.85	96.15
4	40	0.425	384.7	385.6	0.9	1.38	5.23	94.77
5	60	0.25	366.4	367.3	0.9	1.38	6.62	93.38
6	100	0.15	352.4	353.2	0.8	1.23	7.85	92.15
7	200	0.075	274.1	275.9	1.8	2.77	10.62	89.38
8	pan	0			58.1	89.38	100.00	0.00

Table A2: Calculation of Sieve Analysis (Sample A-B3-D10)

SI No.	Sieve No.	Opening Size	Sieve Mass	Sieve and Soil Mass	Retained Soil Mass	Retained on Sieve	Cumulative Retained	Cumulative Passing
-	-	mm	gm	gm	gm	%	%	%
1	4	4.75	605	605	0	0.00	0.00	100.00
2	10	2	493.7	493.7	0	0.00	0.00	100.00
3	20	0.85	426.5	426.8	0.3	0.46	0.46	99.54
4	40	0.425	550	550.7	0.7	1.08	1.54	98.46
5	60	0.25	370	371.2	1.2	1.85	3.38	96.62
6	100	0.15	358.6	360.3	1.7	2.62	6.00	94.00
7	200	0.075	274.1	279	4.9	7.54	13.54	86.46
8	pan	0			56.2	86.46	100.00	0.00

Table A3: Calculation of Sieve Analysis (Sample A-B3-D15)

SI No.	Sieve No.	Opening Size	Sieve Mass	Sieve and Soil Mass	Retained Soil Mass	Retained on Sieve	Cumulative Retained	Cumulative Passing
-	-	mm	gm	gm	gm	%	%	%
1	4	4.75	605	605	0	0.00	0.00	100.00
2	10	2	493.7	493.9	0.2	0.31	0.31	99.69
3	20	0.85	426.5	426.6	0.1	0.15	0.46	99.54
4	40	0.425	550	550.3	0.3	0.46	0.92	99.08
5	60	0.25	370	370.5	0.5	0.77	1.69	98.31
6	100	0.15	358.6	359.3	0.7	1.08	2.77	97.23
7	200	0.075	274.1	275.7	1.6	2.46	5.23	94.77
8	pan	0			61.6	94.77	100.00	0.00

Table A4: Calculation of Sieve Analysis (Sample A-B2-D20)

SI No.	Sieve No.	Opening Size	Sieve Mass	Sieve and Soil Mass	Retained Soil Mass	Retained on Sieve	Cumulative Retained	Cumulative Passing
-	-	mm	gm	gm	gm	%	%	%
1	4	4.75	800	800.7	0.7	1.08	1.08	98.92
2	10	2	493.8	495.2	1.4	2.15	3.23	96.77
3	20	0.85	426.3	427.4	1.1	1.69	4.92	95.08
4	40	0.425	549.9	550.8	0.9	1.38	6.31	93.69
5	60	0.25	366.5	372.1	5.6	8.62	14.92	85.08
6	100	0.15	358.5	364.2	5.7	8.77	23.69	76.31
7	200	0.075	274.1	280.8	6.7	10.31	34.00	66.00
8	pan	0			42.9	66.00	100.00	0.00

Table A5: Calculation of Sieve Analysis (Sample A-B3-D20)

SI No.	Sieve No.	Opening Size	Sieve Mass	Sieve and Soil Mass	Retained Soil Mass	Retained on Sieve	Cumulative Retained	Cumulative Passing
-	-	mm	gm	gm	gm	%	%	%
1	4	4.75	605	605.1	0.1	0.15	0.15	99.85
2	10	2	493.7	494	0.3	0.46	0.62	99.38
3	20	0.85	426.5	427.8	1.3	2.00	2.62	97.38
4	40	0.425	550	552.5	2.5	3.85	6.46	93.54
5	60	0.25	370	372	2	3.08	9.54	90.46
6	100	0.15	358.6	360.2	1.6	2.46	12.00	88.00
7	200	0.075	274.1	278	3.9	6.00	18.00	82.00
8	pan	0			53.3	82.00	100.00	0.00

Table A6: Calculation of Sieve Analysis (Sample B-B1-D15)

SI No.	Sieve No.	Opening Size	Sieve Mass	Sieve and Soil Mass	Retained Soil Mass	Retained on Sieve	Cumulative Retained	Cumulative Passing
-	-	mm	gm	gm	gm	%	%	%
1	4	4.75	515.8	516.3	0.5	0.77	0.77	99.23
2	10	2	497.4	498.9	1.5	2.31	3.08	96.92
3	20	0.85	426.2	427.5	1.3	2.00	5.08	94.92
4	40	0.425	556	556.4	0.4	0.62	5.69	94.31
5	60	0.25	366.1	366.7	0.6	0.92	6.62	93.38
6	100	0.15	490.2	490.8	0.6	0.92	7.54	92.46
7	200	0.075	413.7	414.5	0.8	1.23	8.77	91.23
8	pan	0			59.3	91.23	100.00	0.00

Soil Resistivity at Varied moisture Condition with Fixed Unit Weight

Table A7: Soil Resistivity at varied moisture condition with fixed unit weight (Sample A-B2-D15)

unit weight 93.5 pcf (dry)						
SI NO	Moisture Content	Soil Unit Weight	Dry Unit Weight	Measured Resistance	Corrected Resistance	Resistivity
-	%	lb/cft	lb/cft	ohm	ohm	ohm-m
1	10.00	102.85	93.50	27.62	19.224	19.416
2	20.00	112.2	93.50	5.843	4.067	4.107
3	30.00	121.55	93.50	3.519	2.449	2.474
4	40.00	130.9	93.50	3.185	2.217	2.239
5	50.00	140.25	93.50	3.347	2.330	2.353

Table A8: Soil Resistivity at varied moisture condition with fixed unit weight (Sample A-B3-D10)

unit weight 96.4 pcf (dry)						
SI NO	Moisture Content	Soil Unit Weight	Dry Unit Weight	Measured Resistance	Corrected Resistance	Resistivity
-	%	lb/cft	lb/cft	ohm	ohm	ohm-m
1	10.00	106.04	96.40	29.96	20.85216	21.061
2	20.00	115.68	96.40	4.685	3.26076	3.293
3	30.00	125.32	96.40	3.607	2.510472	2.536
4	40.00	134.96	96.40	3.471	2.415816	2.440
5	50.00	144.6	96.40	3.406	2.370576	2.394

Table A9: Soil Resistivity at varied moisture condition with fixed unit weight (Sample A-B3-D15)

SI NO	Moisture Content	Soil Unit Weight	Dry Unit Weight	Measured Resistance	Corrected Resistance	Resistivity
			unit weight 95.2 pcf (dry)			
-	%	lb/cft	lb/cft	ohm	ohm	ohm-m
1	15.00	106.04	96.40	12.83	8.930	9.019
2	20.00	115.68	96.40	6.885	4.792	4.840
3	30.00	125.32	96.40	5.192	3.614	3.650
4	40.00	134.96	96.40	3.796	2.642	2.668
5	50.00	144.6	96.40	3.443	2.396	2.420

Table A10: Soil Resistivity at varied moisture condition with fixed unit weight (Sample A-B3-D20)

SI NO	Moisture Content	Soil Unit Weight	Dry Unit Weight	Measured Resistance	Corrected Resistance	Resistivity
			unit weight 94.5 pcf (dry)			
-	%	lb/cft	lb/cft	ohm	ohm	ohm-m
1	20.00	113.4	94.50	4.543	3.161928	3.194
2	30.00	122.85	94.50	3.286	2.287056	2.310
3	40.00	132.3	94.50	3.256	2.266176	2.289
4	50.00	141.75	94.50	2.94	2.04624	2.067

Soil Resistivity at Varied Unit Weight with Fixed Moisture Content

Table A11: Soil Resistivity at Varied Unit Weight (Sample A-B2-D15)

Moisture content 18%						
SI NO	Moisture Content	Dry Unit Weight	Moist Unit Weight	Measured Resistance	Corrected Resistance	Resistivity
-	%	lb/cft	lb/cft	ohm	ohm	ohm-m
1	18.00	75	88.50	15.2	10.579	10.685
2	18.00	80	94.40	10.79	7.510	7.585
3	18.00	85	100.30	9.411	6.550	6.616
4	18.00	90	106.20	8.393	5.842	5.900
5	18.00	93.5	110.30	7.581	5.276	5.329

Table A12: Soil Resistivity at Varied Unit Weight (Sample A-B2-D15)

Moisture content 24%						
SI NO	Moisture Content	Dry Unit Weight	Moist Unit Weight	Measured Resistance	Corrected Resistance	Resistivity
-	%	lb/cft	lb/cft	ohm	ohm	ohm-m
1	24.00	75	93.00	8.781	6.112	6.173
2	24.00	80	99.20	7.119	4.955	5.004
3	24.00	85	105.40	5.685	3.957	3.996
4	24.00	90	111.60	4.963	3.454	3.489
5	24.00	93.5	115.94	4.667	3.248	3.281

Table A13: Soil Resistivity at Varied Unit Weight (Sample A-B2-D15)

SI NO	Moisture Content	Dry Unit Weight	Moist Unit Weight	Measured Resistance	Corrected Resistance	Resistivity
-	%	lb/cft	lb/cft	ohm	ohm	ohm-m
1	30.00	75	97.50	5.634	3.921	3.960
2	30.00	80	104.00	5.193	3.614	3.650
3	30.00	85	110.50	4.494	3.128	3.159
4	30.00	90	117.00	4.199	2.923	2.952

Moisture content 30%

Table A14: Soil Resistivity at Varied Unit Weight (Sample A-B3-D10)

SI NO	Moisture Content	Dry Unit Weight	Moist Unit Weight	Measured Resistance	Corrected Resistance	Resistivity
-	%	lb/cft	lb/cft	ohm	ohm	ohm-m
1	18.00	75	88.50	9.726	6.769	6.837
2	18.00	80	94.40	7.768	5.407	5.461
3	18.00	85	100.30	6.24	4.343	4.386
4	18.00	90	106.20	5.519	3.841	3.880
5	18.00	96.4	113.75	4.812	3.349	3.383

Moisture content 18%

Table A15: Soil Resistivity at Varied Unit Weight (Sample A-B3-D10)

SI NO	Moisture Content	Dry Unit Weight	Moist Unit Weight	Measured Resistance	Corrected Resistance	Resistivity
-	%	lb/cft	lb/cft	ohm	ohm	ohm-m
1	24.00	75	93.00	6.343	4.415	4.459
2	24.00	80	99.20	5.232	3.641	3.678
3	24.00	85	105.40	4.379	3.048	3.078
4	24.00	90	111.60	4.088	2.845	2.874
5	24.00	96.4	119.54	3.782	2.632	2.659

Moisture content 24%

Table A16: Soil Resistivity at Varied Unit Weight (Sample A-B3-D10)

	Moisture content 30%					
SI NO	Moisture Content	Dry Unit Weight	Moist Unit Weight	Measured Resistance	Corrected Resistance	Resistivity
-	%	lb/cft	lb/cft	ohm	ohm	ohm-m
1	30.00	75	97.50	5.765	4.012	4.053
2	30.00	80	104.00	5.427	3.777	3.815
3	30.00	85	110.50	4.698	3.270	3.303
4	30.00	90	117.00	4.486	3.122	3.153
5	30.00	96.4	125.32	4.47	3.111	3.142

Table A17: Soil Resistivity at Varied Unit Weight (Sample A-B3-D15)

	Moisture content 18%					
SI NO	Moisture Content	Dry Unit Weight	Moist Unit Weight	Measured Resistance	Corrected Resistance	Resistivity
-	%	lb/cft	lb/cft	ohm	ohm	ohm-m
1	18.00	75	88.50	20.16	14.031	14.172
2	18.00	80	94.40	14.53	10.113	10.214
3	18.00	85	100.30	10.93	7.607	7.683
4	18.00	90	106.20	9.282	6.460	6.525
5	18.00	95.2	112.34	8.803	6.127	6.188

Table A18: Soil Resistivity at Varied Unit Weight (Sample A-B3-D15)

	Moisture content 24%					
SI NO	Moisture Content	Dry Unit Weight	Moist Unit Weight	Measured Resistance	Corrected Resistance	Resistivity
-	%	lb/cft	lb/cft	ohm	ohm	ohm-m
1	24.00	75	93.00	10.44	7.266	7.339
2	24.00	80	99.20	8.42	5.860	5.919
3	24.00	85	105.40	7.485	5.210	5.262
4	24.00	90	111.60	5.932	4.129	4.170
5	24.00	95.2	118.05	5.787	4.028	4.068

Table A19: Soil Resistivity at Varied Unit Weight (Sample A-B3-D15)

SI NO	Moisture Content	Dry Unit Weight	Moist Unit Weight	Measured Resistance	Corrected Resistance	Resistivity
Moisture content 30%						
-	%	lb/cft	lb/cft	ohm	ohm	ohm-m
1	30.00	75	97.50	7.553	5.257	5.309
2	30.00	80	104.00	5.868	4.084	4.125
3	30.00	85	110.50	4.96	3.452	3.487
4	30.00	90	117.00	4.865	3.386	3.420
5	30.00	95.2	123.76	4.695	3.268	3.300

Table A20: Soil Resistivity at Varied Unit Weight (Sample A-B3-D20)

SI NO	Moisture Content	Moist Unit Weight	Dry Unit Weight	Measured Resistance	Corrected Resistance	Resistivity
Moisture content 18%						
-	%	lb/cft	lb/cft	ohm	ohm	ohm-m
1	18.00	88.5	75.00	6.157	4.285272	4.328
2	18.00	94.4	80.00	5.282	3.676272	3.713
3	18.00	100.3	85.00	4.416	3.073536	3.104
4	18.00	106.2	90.00	4.028	2.803488	2.832
5	18.00	111.51	94.50	3.7433	2.6053368	2.631

Table A21: Soil Resistivity at Varied Unit Weight (Sample A-B3-D20)

SI NO	Moisture Content	Moist Unit Weight	Dry Unit Weight	Measured Resistance	Corrected Resistance	Resistivity
Moisture content 24%						
-	%	lb/cft	lb/cft	ohm	ohm	ohm-m
1	24.00	93	75.00	6.893	4.797528	4.846
2	24.00	99.2	80.00	5.581	3.884376	3.923
3	24.00	105.4	85.00	4.588	3.193248	3.225
4	24.00	111.6	90.00	3.965	2.75964	2.787
5	24.00	117.18	94.50	3.69	2.56824	2.594

Table A22: Soil Resistivity at Varied Unit Weight (Sample A-B3-D20)

SI NO	Moisture Content	Moist Unit Weight	Dry Unit Weight	Measured Resistance	Corrected Resistance	Resistivity
					Moisture content 30%	

SI NO	Moisture Content	Moist Unit Weight	Dry Unit Weight	Measured Resistance	Corrected Resistance	Resistivity
-	%	lb/cft	lb/cft	ohm	ohm	ohm-m
1	30.00	97.5	75.00	4.483	3.120168	3.151
2	30.00	104	80.00	4.282	2.980272	3.010
3	30.00	110.5	85.00	3.963	2.758248	2.786
4	30.00	117	90.00	3.655	2.54388	2.569
5	30.00	122.85	94.50	3.522	2.451312	2.476

Variation of Soil Resistivity with Ion Composition
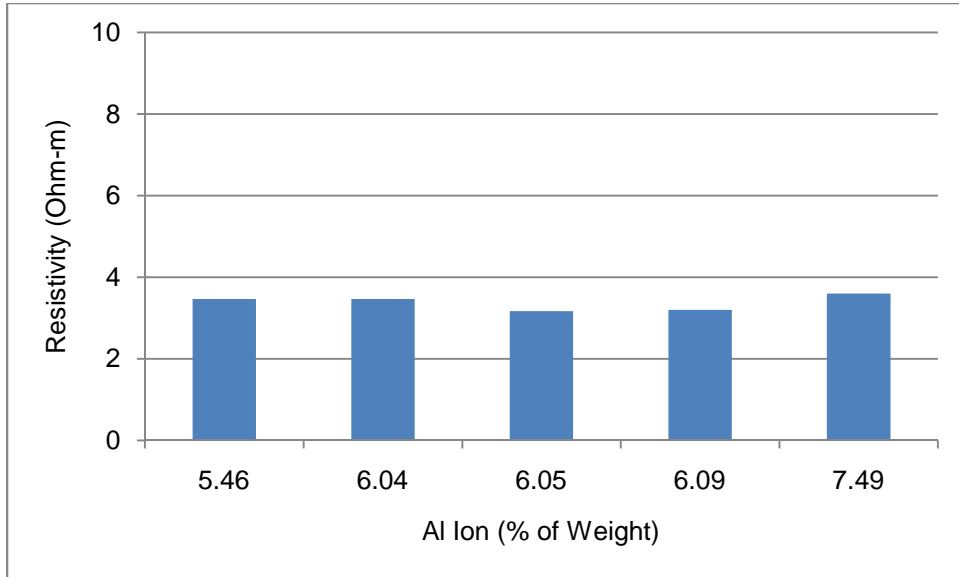
Figure A4: Soil Resistivity with Aluminum Ion
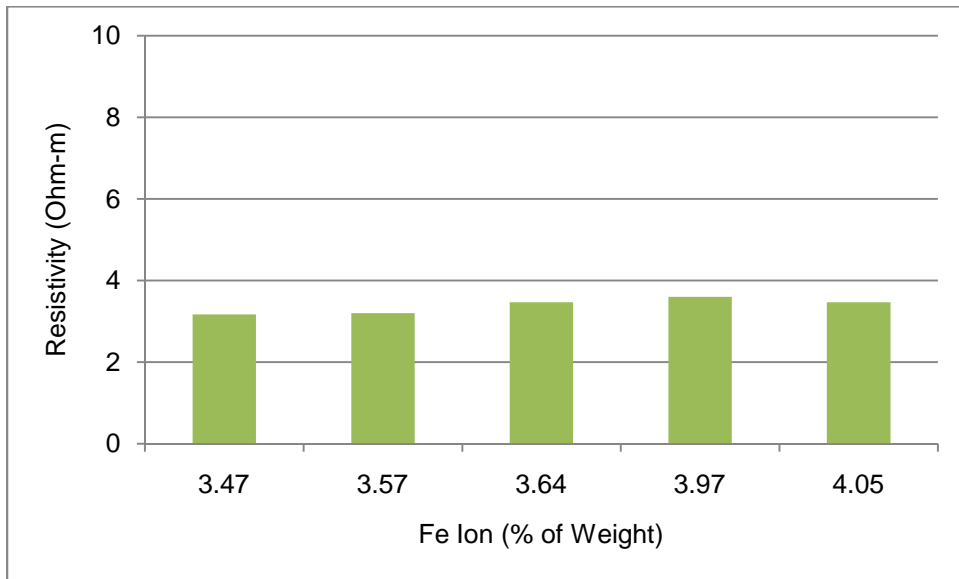
Figure A5: Soil Resistivity with Iron Ion
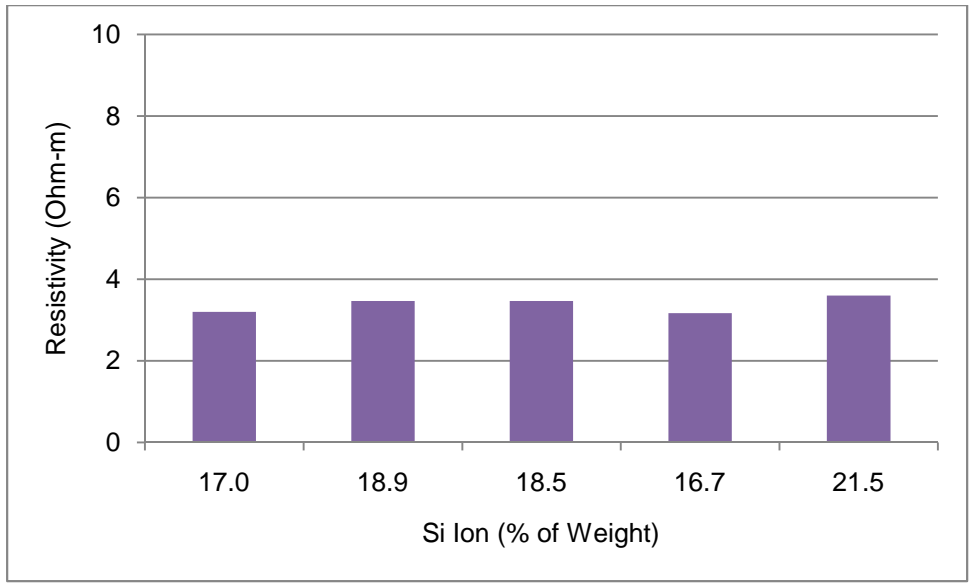
Figure A6: Soil Resistivity with Silicon Ion
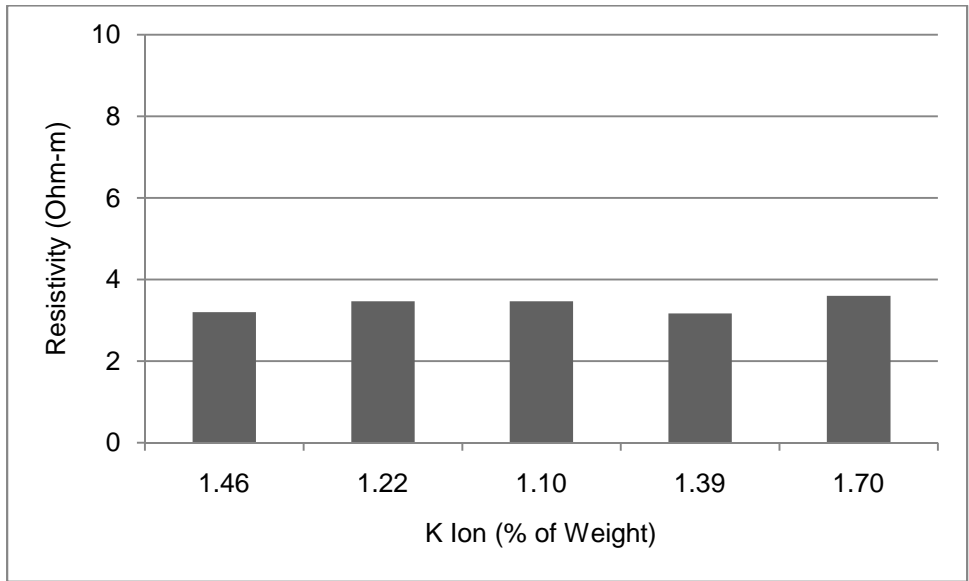
Figure A7: Soil Resistivity with Potassium Ion

Standard Proctor Compaction

Table A23: Compaction test (Sample A-B2-D15)

SI No.	Target Moisture Content	Weight of Can	Weight of Can + Wet Soil	Weight of Can + Dry Soil	Weight of Dry Soil	Weight of Water	Obtained Moisture Content
-	%	gm	gm	gm	gm	gm	%
1	18	28.7	64.5	59.1	30.4	5.4	17.76
2	24	28.4	64.2	57.6	29.2	6.6	22.60
3	28	32.5	70.2	62.6	30.1	7.6	25.25
4	35	92.4	171.6	150.9	58.5	20.7	35.38
UNIT WEIGHT							
Moisture Content	Weight of Mold	Weight of Mold + Sample	Weight of Sample	Soil Unit Weight	Dry Unit Weight	Specfic Gravity	Zero Air Void
%	lb	lb	lb	lb/cft	lb/cft	-	lb/cft
17.76	4.484	7.998	3.514	105.42	89.52	2.65	112.43
22.60	4.484	8.292	3.808	114.24	93.18	2.65	103.42
25.25	4.484	8.306	3.822	114.66	91.55	2.65	99.07
35.38	4.484	8.176	3.692	110.76	81.81	2.65	85.34

Table A24: Compaction test (Sample A-B3-D10)

SI No.	Target Moisture Content	Weight of Can	Weight of Can + Wet Soil	Weight of Can + Dry Soil	Weight of Dry Soil	Weight of Water	Obtained Moisture Content
-	%	gm	gm	gm	gm	gm	%
1	18	47.4	70	66.4	19	3.6	18.95
2	21	46.8	85.9	79.1	32.3	6.8	21.05
3	24	45.7	79.5	72.9	27.2	6.6	24.26
4	27	46.1	81.8	74.3	28.2	7.5	26.60
5	30	49	85.4	76.9	27.9	8.5	30.47
UNIT WEIGHT							
Moisture Content	Weight of Mold	Weight of Mold + Sample	Weight of Sample	Soil Unit Weight	Dry Unit Weight	Specific Gravity	Zero Air Void
%	lb	lb	lb	lb/cft	lb/cft	-	lb/cft
18.95	4.484	8.146	3.662	109.86	92.36	2.65	110.09
21.05	4.484	8.41	3.926	117.78	97.30	2.65	106.14
24.26	4.484	8.464	3.98	119.4	96.09	2.65	100.64
26.60	4.484	8.448	3.964	118.92	93.94	2.65	97.00
30.47	4.484	8.328	3.844	115.32	88.39	2.65	91.49

Table A25: Compaction test (Sample A-B3-D15)

SI No.	Target Moisture Content	Weight of Can	Weight of Can + Wet Soil	Weight of Can + Dry Soil	Weight of Dry Soil	Weight of Water	Obtained Moisture Content
-	%	gm	gm	gm	gm	gm	%
1	18	49	76.8	72.6	23.6	4.2	17.80
2	21	24.5	49	44.6	20.1	4.4	21.89
3	24	46.8	79.3	72.8	26	6.5	25.00
4	30	46.1	70.6	65.1	19	5.5	28.95
5	32	45.6	82.9	74	28.4	8.9	31.34
UNIT WEIGHT							
Moisture Content	Weight of Mold	Weight of Mold + Sample	Weight of Sample	Soil Unit Weight	Dry Unit Weight	Specific Gravity	Zero Air Void
%	lb	lb	lb	lb/cft	lb/cft	-	lb/cft
17.80	4.484	8.113	3.629	108.87	92.42	2.65	112.37
21.89	4.484	8.282	3.798	113.94	93.48	2.65	104.65
25.00	4.484	8.448	3.964	118.92	95.14	2.65	99.46
28.95	4.484	8.392	3.908	117.24	90.92	2.65	93.58
31.34	4.484	8.328	3.844	115.32	87.80	2.65	90.34

Table A26: Compaction test (Sample B-B1-D15)

SI No.	Target Moisture Content	Weight of Can	Weight of Can + Wet Soil	Weight of Can + Dry Soil	Weight of Dry Soil	Weight of Water	Obtained Moisture Content
-	%	gm	gm	gm	gm	gm	%
1	18	46.5	80.6	75.3	28.8	5.3	18.40
2	22	47.1	90.6	83.1	36	7.5	20.83
3	26	46.8	109.6	96.7	49.9	12.9	25.85
4	28	47.3	108.3	94.9	47.6	13.4	28.15
5	30	46.4	85.3	76.3	29.9	9	30.10
UNIT WEIGHT							
Moisture Content	Weight of Mold	Weight of Mold + Sample	Weight of Sample	Soil Unit Weight	Dry Unit Weight	Specific Gravity	Zero Air Void
%	lb	lb	lb	lb/cft	lb/cft	-	lb/cft
18.40	4.484	8.098	3.614	108.42	91.57	2.65	111.15
20.83	4.484	8.348	3.864	115.92	95.93	2.65	106.54
25.85	4.484	8.454	3.97	119.1	94.64	2.65	98.13
28.15	4.484	8.386	3.902	117.06	91.35	2.65	94.71
30.10	4.484	8.338	3.854	115.62	88.87	2.65	91.99

Table A27: Compaction test (Sample A-B2-D20)

SI No.	Target Moisture Content	Weight of Can	Weight of Can + Wet Soil	Weight of Can + Dry Soil	Weight of Dry Soil	Weight of Water	Obtained Moisture Content
-	%	gm	gm	gm	gm	gm	%
1	18	32.4	80.5	74.4	42	6.1	14.52
2	22	28.4	68.7	62.3	33.9	6.4	18.88
3	26	28.7	81.3	71.9	43.2	9.4	21.76
4	30	28.2	82.5	71.6	43.4	10.9	25.12
5	36	28.1	95.7	78.9	50.8	16.8	33.07
UNIT WEIGHT							
Moisture Content	Weight of Mold	Weight of Mold + Sample	Weight of Sample	Soil Unit Weight	Dry Unit Weight	Specfic Gravity	Zero Air Void
%	lb	lb	lb	lb/cft	lb/cft	-	lb/cft
18.88	4.484	8.116	3.632	108.96	91.66	2.65	110.22
21.76	4.484	8.37	3.886	116.58	95.75	2.65	104.88
25.12	4.484	8.472	3.988	119.64	95.62	2.65	99.28
33.07	4.484	8.272	3.788	113.64	85.40	2.65	88.13

Table A28: Compaction test (Sample A-B3-D20)

SI No.	Target Moisture Content	Weight of Can	Weight of Can + Wet Soil	Weight of Can + Dry Soil	Weight of Dry Soil	Weight of Water	Obtained Moisture Content
-	%	gm	gm	gm	gm	gm	%
1	18	23.2	49.9	46	22.8	3.9	17.11
2	21	46.7	95.3	87.2	40.5	8.1	20.00
3	24	46.8	83.7	76.4	29.6	7.3	24.66
4	27	46.2	88.3	79.2	33	9.1	27.58
5	30	105.2	160.5	147.2	42	13.3	31.67
UNIT WEIGHT							
Moisture Content	Weight of Mold	Weight of Mold + Sample	Weight of Sample	Soil Unit Weight	Dry Unit Weight	Specfic Gravity	Zero Air Void
%	lb	lb	lb	lb/cft	lb/cft	-	lb/cft
17.11	4.484	7.986	3.502	105.06	89.71	2.65	113.78
20.00	4.484	8.226	3.742	112.26	93.55	2.65	108.08
24.66	4.484	8.406	3.922	117.66	94.38	2.65	100.00
27.58	4.484	8.366	3.882	116.46	91.29	2.65	95.54
31.67	4.484	8.324	3.84	115.2	87.49	2.65	89.91

REFERENCES

Abu-Hassanein, Z. S., and Benson, C. H. (1996). "Electrical resistivity of compacted clays." *J. Geotech. Eng.,* 122 (5), 397-406.

A. D. Voronin, "The Bases of Soil Physics." *Mosk. Gos. Univ.*, Moscow, 1986.

Aizebeokhai, A. P. (2010). "2D and 3D geoelectrical resistivity imaging: Theory and field design." *Scientific Research and Essays,* 5(23), 3592-3605.

Archie, G. (1991). "The electrical resistivity log as an aid in determining some reservoir characteristics." *Petroleum Technology, T.P. 1422*, Shell Oil Co. Houston, TX.

Benson, C. H. and Daniel, D. (1990). "Influence of clods on the hydraulic conductivity of compacted clay." *J. Geotech. Eng.,* 116 (8), 1231-1248.

Barthelmy, D. (1997). "Minerology Database", <http://webmineral.com > (May 25, 2011)

Braga, A. C. O., Dourado, J. C., and Chang, H. K. (1999). "Correlation of Electrical Resistivity and Induced Polarization Data with Geotechnical Survey Standard Penetration Test Measurements." *J. Environ. Eng. Geophys.,* 4 (2), 123-130.

Braja, M. "Das, 1983." Advanced Soil Mechanics*.",Hemishepre Publishing Corporation, McGraw Hill,* NY*.*

Brunet, P., Clément, R., and Bouvier, C. (2010). "Monitoring soil water content and deficit using Electrical Resistivity Tomography (ERT)-A case study in the Cevennes area, France." *J. Hydrol.,* 380(1-2), 146-153.

Bryson, L. S. (2005). "Evaluation of geotechnical parameters using electrical resistivity measurements." *Proc., Earthquake Engineering and Soil Dynamics, GSP 133, Geo-Frontiers 2005,* ASCE, Reston, VA.

Campbell, R., Bower, C., and Richards, L. (1948). "Change of electrical conductivity with temperature and the relation of osmotic pressure to electrical conductivity and ion concentration for soil extracts." *Proc. Soil Sci. Soc. Am. 13,* 66-69.

Croney, D., Coleman, J., and Currer, E. (1951). "The electrical resistance method of measuring soil moisture." *Br. J. App. Phys.,* 2 (4), 85-91.

Ekwue, E., and Bartholomew, J. (2010). "Electrical conductivity of some soils in Trinidad as affected by density, water and peat content." *Biosystems Eng.,* 108 (2), 95-103*.*

Giao, P., Chung, S., Kim, D., and Tanaka, H. (2003). "Electric imaging and laboratory resistivity testing for geotechnical investigation of Pusan clay deposits." *J.Appl.Geophys.,* 52(4), 157-175.

Holtz, R. D., and Kovacs, W. D. (1981). "An introduction to geotechnical engineering." *Prentice-Hall, Inc.*, Englewood Cliffs, NJ.

Jay A. Raney, J. A., Allen, P. M., Reaser, D. F., and Collins, E. W. (1987). "Geologic Review of Proposed Dallas Fort Worth Area Site for the Superconducting Super Collider SSC." *Presented at the meeting of the Underground Tunnelling Advisory Panel, April 30*, *1989* at the SSC Laboratory at Lawrence Berkeley Laboratory.

Jakosky, J. J. (1950). "Exploration geophysics*." Trija Pub. Co*, Los Angeles, 119.

Kaiser, B., and Wright, A. (2008). "Draft BRUKER XRF Spectroscopy User Guide: Spectral Interpretation Sources of Interference." BRUKER, Madison, WI.

Kalinski, R., and Kelly, W. (1993). "Estimating water content of soils from electrical resistivity." *GTJ. ASTM,* 16(3), 323-329.

Keller, G. V., Frischknecht, F. C., and Cullen, A. (1966). "Electrical methods in geophysical prospecting." *Pergamon press,* Oxford, UK.

Kim, J. H., Yoon, H. K., and Lee, J. S. (2011). "Void Ratio Estimation of Soft Soils Using Electrical Resistivity Cone Probe." *J. Geotech. Geoenviron. Eng.,* 137 (1), 86-93.

Lambe, T. (1958). "The Structure of Compacted Clays." *J. Soil Mech. Found. Div*., 84(2), 2-34.

McCarter, W. (1984). "The electrical resistivity characteristics of compacted clays." *Geotechnique,* 34(2), 263.

McCarter, W. J., and Desmazes, P.. "Soil characterization using electrical measurements." *Geotechnique*, 47 (1)*,* 179-183.

Mitchell, J., and Soga, K. (2005). "Fundamentals of soil behavior." *John Wiley and Sons, Inc.,* Hoboken, NJ.

Ozcep, F., Tezel, O., and Asci, M. (2009). "Correlation between electrical resistivity and soil-water content: Istanbul and Golcuk." *Int. J. of Phys. Sci.,* 4(6), 362-365.

Pozdnyakov, A., Pozdnyakova, L., and Karpachevskii, L. (2006). "Relationship between water tension and electrical resistivity in soils." *Eurasian Soil Sci.,* 39 (1), 78-83.

Rinaldi, V. A., and Cuestas, G. A. (2002). "Ohmic conductivity of a compacted silty clay." *J. Geotech. Geoenviron. Eng.,* 128 (10), 824-835.

Robain, H., Descloitres, M., Ritz, M., and Atangana, Q. Y. (1996). "A multiscale electrical survey of a lateritic soil system in the rain forest of Cameroon." *J. Appl. Geophys.,* 34(4), 237-253.

Saarenketo, T. (1998). "Electrical properties of water in clay and silty soils." *J. Appl. Geophys.,* 40(1-3), 73-88.

Samouëlian, A., Cousin, I., Tabbagh, A., Bruand, A., and Richard, G. (2005). "Electrical resistivity survey in soil science: a review." *Soil Tillage Res.,* 83(2), 173-193.

Schwartz, B. F., Schreiber, M. E., and Yan, T. (2008). "Quantifying field-scale soil moisture using electrical resistivity imaging." *J. Hydrol.,* 362(3-4), 234-246.

Shah, P., and Singh, D. (2005). "Generalized Archie's law for estimation of soil electrical conductivity." *JAI.,* 2(5),.1-19.

Sudha, K., Israil, M., Mittal, S., and Rai, J. (2009). "Soil characterization using electrical resistivity tomography and geotechnical investigations." *J. Appl. Geophys.,* 67(1), 74-79.

U.S. Geological Survey (2010). "Geologic units in a given geographic area."

<http://tin.er.usgs.gov/geology/state/fips-unit.php?code=f48139)> (May 25, 2011)

Van Nostrand, R. G., and Cook, K. L. (1966). "Interpretation of resistivity data." *Geological Survey Professional paper; 499.* U.S. Govt. Print. Off., Washington*,* 310*.*

Wikimedia Foundation. Inc (2011). "Porosity in Earth Science and Construction."
<http://en.wikipedia.org/wiki/Porosity> (May 25, 2011).

Yang, J. S. (2002). " Three Dimensional Complex Resistivity Analysis for Clay Characterization in Hydrogeologic Study." *Ph.D. thesis*, University of California, Berkeley.

BIOGRAPHICAL INFORMATION

Golam Kibria was born in Khulna, Bangladesh on December 26, 1986. He graduated with a Bachelor of Science in Civil Engineering from Bangladesh University of Engineering and Technology in March 2009. He started his career as a Junior Engineer in the Institute of Water Modeling, Dhaka in May 2009. He served in the Coast, Port and Estuary Management Division of the institute till December 2009. The author joined the University of Texas at Arlington in spring 2010 for graduate studies. He had the opportunity to work as graduate research assistant under Dr. Sahadat Hossain of Civil Engineering Department. The author's research interest include electrical resistivity of soil, Mechanically Stabilized Earth (MSE) wall, slope stability analysis and remediation, application of geosynthetics, aspects of numerical modeling in geotechnical engineering, non-destructive testing in unknown foundation and geotechnical aspects of municipal solid waste (MSW).